WT-1451

AEC Catagory: HEALTH AND SAFETY
Military Catagory: 32

OPERATION PLUMB BOB

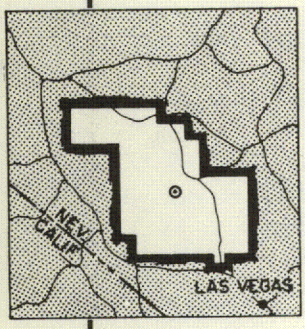

NEVADA TEST SITE
MAY-OCTOBER 1957

Project 30.4

RESPONSE OF PROTECTIVE VAULTS TO BLAST LOADING

Issuance Date: May 28, 1962

CIVIL EFFECTS TEST GROUP

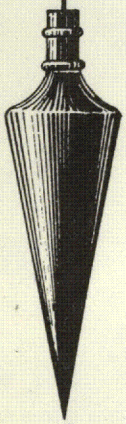

NOTICE

This report is published in the interest of providing information which may prove of value to the reader in his study of effects data derived principally from nuclear weapons tests.

This document is based on information available at the time of preparation which may have subsequently been expanded and re-evaluated. Also, in preparing this report for publication, some classified material may have been removed. Users are cautioned to avoid interpretations and conclusions based on unknown or incomplete data.

PRINTED IN USA
Price $2.00 Available from the Office of
Technical Services, Department of Commerce,
Washington 25, D. C.

USAEC Division of Technical Information Extension, Oak Ridge, Tennessee

Report to the Test Director

RESPONSE OF PROTECTIVE VAULTS TO BLAST LOADING

By

E. Cohen
E. Laing
A. Bottenhofer

Approved by: H. J. JENNINGS
Director Program 30

Approved by: R. L. CORSBIE
Director Civil Effects Group

Ammann & Whitney
New York
April 1961

ABSTRACT

A reinforced-concrete steel-plate-lined vault and steel vault door were exposed to a nuclear detonation (shot Priscilla, about 37 kt, balloon suspended, at 700 ft) at the predicted 75-psi peak incident pressure level (1150 ft from Ground Zero). The vault was designed by the ultimate-strength theory to utilize the additional strain energy available in the elastoplastic and plastic ranges. Flexural and thrust capacities were determined, and shear capacity was computed.

It was established that above-ground structures can be designed and constructed to survive the pressure levels experienced by this structure. The vault and door provided adequate blast and thermal protection for normal usage, and the structure was adequate to resist overturning and excessive sliding under conditions of the test.

ACKNOWLEDGMENTS

The authors wish to express sincere appreciation to the following individuals for their cooperation in behalf of this project:

R. L. Corsbie, Director, Civil Effects Test Group, U. S. Atomic Energy Commission

E. R. Saunders, Assistant to the Director, Civil Effects Test Group, Office of Civil and Defense Mobilization

H. J. Jennings, Director, Program 30, Office of Civil and Defense Mobilization

L. J. Vortman, Director, Program 34, Sandia Corporation

Management and Staff of the Mosler Safe and Vault Co.

Management and Staff of Ammann & Whitney

CONTENTS

CONTENTS (Continued)

ILLUSTRATIONS

ILLUSTRATIONS (Continued)

TABLES

Chapter 1

INTRODUCTION

1.1 OBJECTIVES

The primary objective of Project 30.4 was to evaluate the effectiveness of a reinforced-concrete steel-plate-lined vault and steel vault door in providing protection against the effects of a nuclear detonation. Secondary objectives were: (1) to obtain additional information regarding the effects of a nonideal shock wave on blast loading and (2) to verify the assumptions used in the design procedure.

1.2 BACKGROUND

The Mosler Safe Company contracted with Ammann & Whitney, Consulting Engineers, to design a selected type vault and to modify a standard vault door for exposure to a nuclear blast. The vault was included in the protective-structure tests sponsored by the Office of Civil and Defense Mobilization (OCDM), formerly the Federal Civil Defense Administration, and was tested in shot Priscilla of Operation Plumbbob. The vault was located at the predicted 75-psi overpressure level.

1.3 TEST-STRUCTURE DESCRIPTION

The test vault was a rectangular structure with an interior floor area of 102 sq ft (12 ft $7\frac{1}{2}$ in. by 8 ft $\frac{3}{4}$ in.) and a clear height of 8 ft. The longitudinal axis of the structure was radial to Ground Zero (GZ). Figure A.1 shows the architectural layout of the test structure.

The original plan was to have two identical structures in the test program, one at the 100-psi level and one at the 75-psi level, to cover the possible errors in predicted pressure, diffraction pattern, structural response, and strength. However, because of the high estimated cost, it was decided to reduce the scope to one structure at the predicted 75-psi level.

The walls and roof slab were 18-in. reinforced concrete lined with a $\frac{1}{2}$-in.-thick steel plate. The plate and concrete developed composite action by means of shear clips that were welded to the plate and embedded in the concrete. The vault was anchored into a large mat foundation from 2 to 6 ft thick to prevent it from overturning. The mat was 23 ft $1\frac{3}{4}$ in. by 33 ft 9 in.

The door was a standard 10-in.-thick vault door (Century-10, manufactured by the Mosler Safe Co.) modified to resist high-intensity loads. The $7\frac{1}{2}$-ton door was mounted on a steel-plate box frame weighing $14\frac{1}{2}$ tons and was placed facing GZ. The vault with the door closed was essentially gastight. The structure was oriented with its longitudinal center line radial to GZ. Figure 1.1 indicates the orientation of the structure, main blast line, goal post, and stake line with respect to GZ.

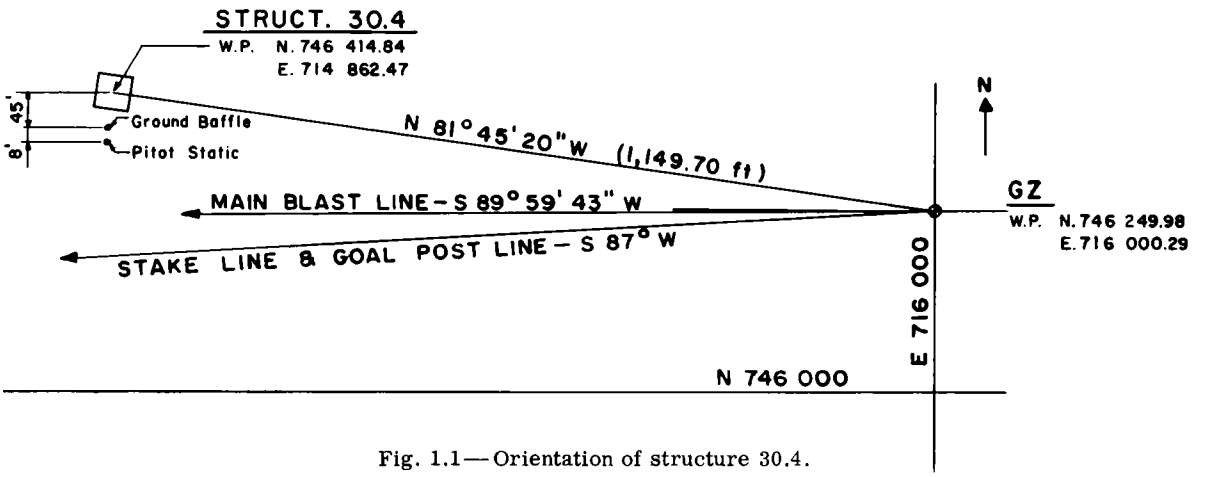

Fig. 1.1—Orientation of structure 30.4.

Design drawings for the test structure are included in Appendix A. The history of vault construction, with photographs, is included as Appendix B.

1.4 THEORY

The roof slab, side walls, and rear wall of the test vault were designed for dynamic behavior assuming an ideal 100-psi incident shock loading and a megaton-range weapon.

The steel-plate box frame and the vault door, both located radial to GZ, were originally designed for dynamic behavior using the theoretical reflected pressures[1] consistent with the 100-psi incident shock; the peak reflected pressure was computed[1] to be 495 psi. Because of the nonideal shock and the predicted high dynamic, q, pressures at the test structures, it was decided to locate the vault at the 75-psi level. The predicted q pressure at the 75-psi level was 300 psi, and the estimated peak front-face pressure was between 320 and 530 psi.

The maximum bearing capacity to be used for the foundation design was specified by OCDM to be approximately 10 tsf.

The vault was designed by the ultimate-strength theory to utilize the additional strain energy available in the elastoplastic and plastic ranges.[1–5]

The static material strengths used for the design of the vault were:

Concrete	4,000 psi (ultimate)
Reinforcing steel (intermediate grade)	47,500 psi (yield)
Structural steel	38,000 psi (yield)

The above stresses were increased[1,3] to compensate for the rapid strain rates.

Flexural and thrust capacities were determined from the data of Ref. 4; the shear capacity was computed from Ref. 1 and checked by recent laboratory data.

REFERENCES

1. Principles of Atomic Weapon Resistant Construction, Department of Civil and Sanitary Engineering, Massachusetts Institute of Technology, 1954. (Classified)
2. Design of Structures to Resist Atomic Blast, Ammann & Whitney, Consulting Engineers, New York, January 1954.
3. C. S. Whitney et al., Design of Blast-resistant Construction for Atomic Explosions, J. Am. Concrete Inst., 20(7): 589-683(March 1955).
4. C. S. Whitney and E. Cohen, Guide for Ultimate-strength Design of Reinforced Concrete, J. Am. Concrete Inst., 28(5): 455-490(November 1956).
5. C. S. Whitney, Plastic Theory of Reinforced-concrete Design, Trans. Am. Soc. Civil Engrs., 107: 251-282(1942).

Chapter 2

PROCEDURE

2.1 SOIL INVESTIGATIONS

Soil investigations were made by the International Testing Corporation under the direction of Holmes & Narver, Inc., at the request of Ammann & Whitney. One 16-in.-diameter boring 40 ft deep and one 48-in.-diameter shaft 40 ft deep were drilled at the site of the test vault (Fig. 2.1). Three 16-in.-diameter borings and one 48-in.-diameter shaft were drilled at the site[1] of the nearby underground parking garage and personnel shelter, Project 30.2. The large-diameter shaft was used to obtain undisturbed samples.

The following tests were made:

1. Field density.
2. Liquid and plastic limit.
3. Sieve analysis.
4. Unconfined compression tests.
5. Consolidation tests to determine the natural vertical state of stress.
6. Triaxial tests.

The soil encountered was unusual in character and possessed remarkable properties. It consisted of many thinly stratified layers cemented together. These layers were very fine grained (more than 95 per cent passing No. 200 sieve) and were nonplastic or slightly plastic in character ($0 \leq$ plasticity index ≤ 10). There was little variation in soil material, but variations in density occurred from layer to layer or in small pockets. There were pronounced horizontal planes of weakness. The cementing agent is thought to be calcium carbonate, which exists in some beds in pieces $\frac{1}{8}$ in. in diameter.

Analysis of the consolidation and triaxial test data from undisturbed samples of soil removed from the 48-in.-diameter shafts at the test vault and the nearby garage structure indicated that, within the significant depth region, the soil possesses a natural prestress of about 10 tsf. (Table 2.1 contains selected values from the test results.) The high triaxial stresses and small strains at failure are especially noted as a peculiar characteristic of this soil in its natural state.

A description of the sampling methods, testing procedures, and test results is contained in Appendix C. Additional information is available as a result of the soil-testing program of the Waterways Experiment Station, Vicksburg, Miss., and is reported[2] in the Project 3.8 report, WT-1427.

2.2 SURVEYS

Preshot and postshot high-order field surveys of the horizontal and vertical coordinates of the structure were requested to determine the absolute and relative lateral and vertical displacement of the structure during the blast. The survey points are shown in Fig. 2.2.

TABLE 2.1—STRESS–STRAIN RELATIONS, FAILURE-STRESS CONDITIONS, AND SHEARING STRENGTH OF SOILS BY TRIAXIAL TESTS AT A DEPTH OF 17 FT IN THE PROJECT 30.2, 48-IN. BORING[1]

Lateral stress (P3)		Triaxial failure stress		Strain at failure,	Max. shearing
Psi	Tsf	Psi	Tsf	in./in.	strength, tsf
20	1.44	154		0.06	
		140/147	10.6	0.04	5.3
40	2.88	217		0.02	
		238/228	16.4	0.06	8.2
50	3.6	276	19.8	0.07	9.9
61	4.1	197	14.2	0.08	7.1
80	5.8	303*	21.6	0.08	10.8

* No failure.

2.3 INSTRUMENTATION

2.3.1 Pressure and Structural Response

Blast instrumentation was provided by the Sandia Corporation and is described[3] in detail in the Project 34.1 report, WT-1472. The blast instrumentation of the structure proper consisted of seven variable-reluctance Bourdon-tube air-pressure gauges manufactured by the Wiancko Engineering Corp. One gauge was located in the foundation slab, flush with the ground surface, two were on the front face of the vault and vault door, and two each in the roof slab and the rear wall.

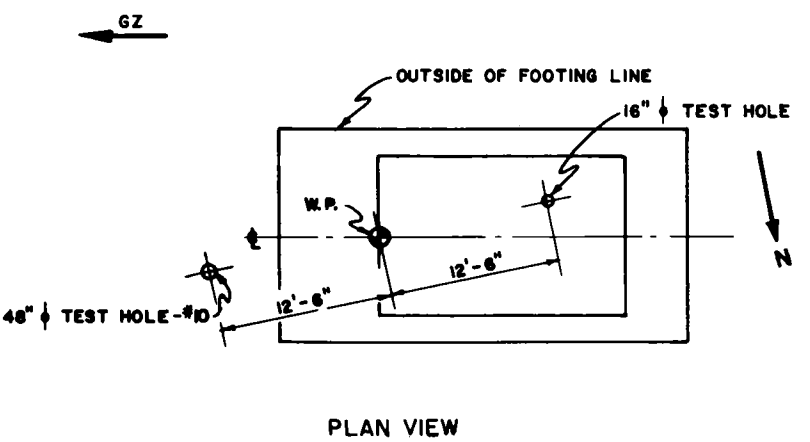

Fig. 2.1—Test holes for structure 30.4.

Free-field incident-overpressure data were supplied by a single Wiancko gauge located in a ground baffle 45 ft south of the vault and at the same radial distance as the vault. A single Pitot-static dynamic-pressure gauge was also located at this GZ distance (53 ft south of the vault) on a 3-ft-high tower (see Fig. 1.1).

In addition to the free-field pressure instrumentation supplied by Project 34.1, blast-line instrumentation between 350 and 6,000 ft from GZ was supplied[4] by Project 1.1. A total of 37 self-recording gauges was installed at 16 stations along the main blast line to obtain the desired data for shot Priscilla. Table 2.2 indicates the station numbers, the distances, the number of gauges used, and the type of gauge used. The P-t gauges are Ballistic Research Laboratories self-recording pressure-time gauges and the q gauges are the self-recording dynamic-pressure–time gauges.

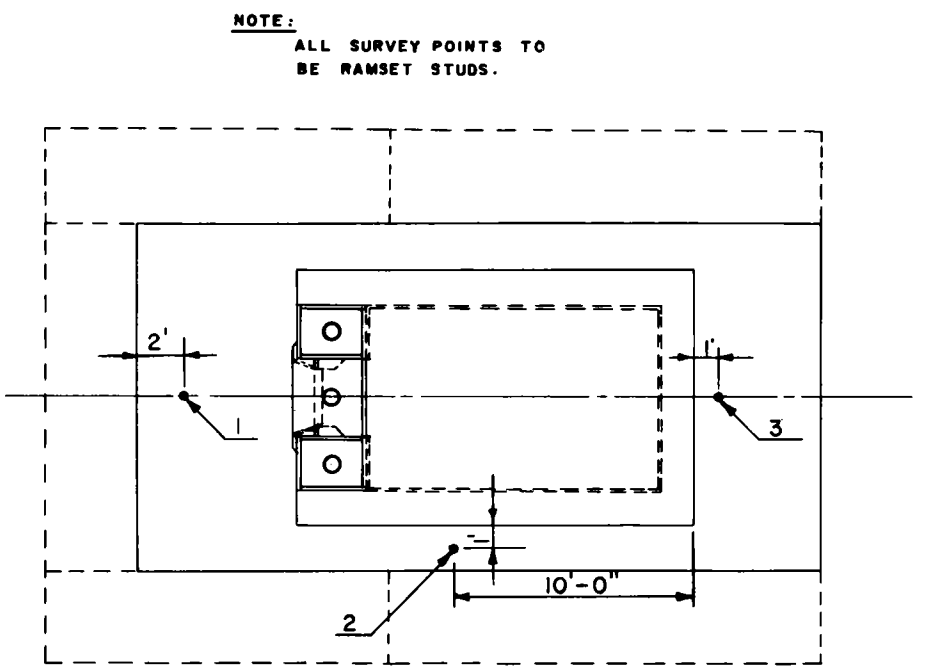

Fig. 2.2—Survey points for structure 30.4.

With the exception of data provided by two scratch gauges used to record the maximum inward deflection of the steel-plate box frame, the structural response of the vault was not recorded.

The locations of all gauges on or within the vault are shown in Fig. A.4.

TABLE 2.2—SUMMARY OF MAIN BLAST-LINE GAUGE INSTALLATION

Station No.	Ground range, ft	No. of gauges	
		P-t	q*
F1.1-9039.01	350	2	
F1.1-9039.02	450	2	
F1.1-9039.03	650	2	
F1.1-9040.01	850	2	1
F1.1-9040.02	1050	2	1
F1.1-9041.00	1350	2	2
F1.1-9042.01	1650	1	1
F1.1-9042.02	2000	1	1
F1.1-9042.05	2250	1	1
F1.1-9042.06	2500	1	2
F1.1-9042.07	3000	1	2
F1.1-9042.03	3500	1	1
F1.1-9042.08	4000	1	2
F1.1-9042.04	4500	1	1
F1.1-9043.01	5000	1	
F1.1-9043.02	6000	1	

* Where two q gauges are listed for one station, the second q gauge was a new design undergoing proof testing.

2.3.2 Radiation Instrumentation

Radiation measurements in the structure, as well as along the main blast line, were made with film dosimeters and gamma-radiation differential chemical dosimeters. These dosimeters were supplied and installed[5,6] by Projects 39.1a and 39.1, respectively. The locations of the radiation detectors on or in the structure are shown in Fig. 2.3.

The interior film dosimeters were placed on June 19; the three exterior film dosimeters and the one interior gamma-radiation chemical dosimeter were placed on June 22. The exact date of placement of the blast-line dosimetry is not known but is presumed to have been D−3 day.

2.3.3 Thermal

Thermal instrumentation consisted of a thermocouple on the outside surface of the door, two heavy-duty clinical type thermometers, and a 24-hr temperature recorder inside the vault. The thermocouple was used to indicate the temperature−time record of the outside surface of the door and was connected to a Leeds & Northrup Co. Speedomax stylus recorder potentiometer inside the vault. This was set for a temperature range from 0 to 2400°F and was activated by a time signal 1 min before the blast. The recorder operated on a 12-volt battery, and the chart ran for 20 min at a speed of 1.3 in./sec.

The 24-hr temperature recorder, a spring-wound stylus American temperature recorder with a range of 100 to 400°F, was wound and set at H−6 hr to give a temperature−time record of the air within the vault to H+18 hr.

The locations of the thermal instruments are shown in Fig. A.4.

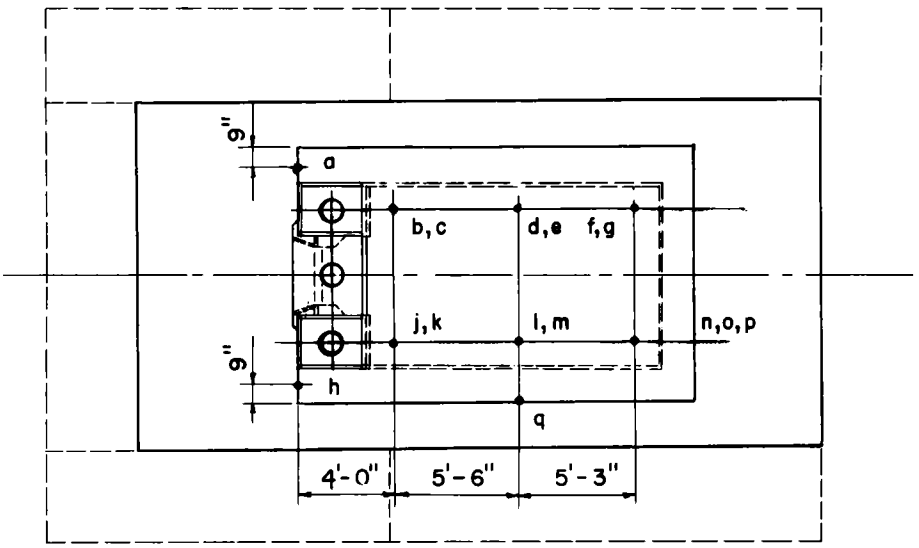

ROOF PLAN

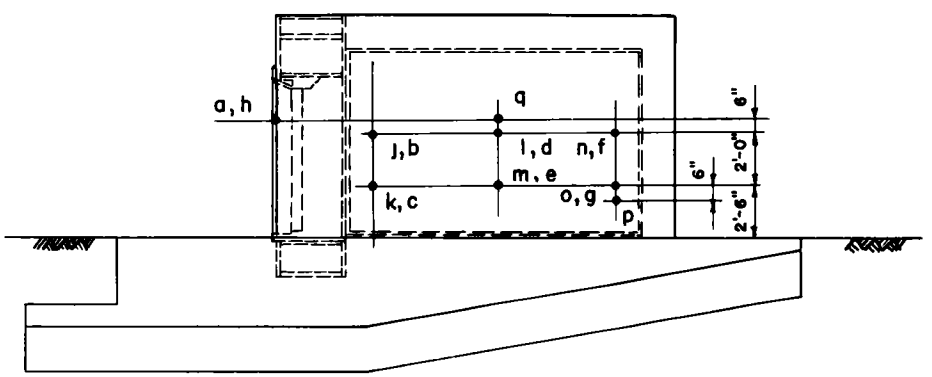

SIDE ELEVATION

NOTE:
ALL POINTS ARE FILM DOSIMETERS EXCEPT POINT P WHICH IS A CHEMICAL DOSIMETER.

Fig. 2.3—Locations of dosimeters for structure 30.4.

2.4 AIR TEST

The test vault was designed so that it would be essentially airtight both before and after the blast. The procedure for the air test was as follows:

Conduit covers for the pressure gauges were removed, and the threads were coated with a sealing compound. The covers were then screwed tightly into the conduits. The steel box in the center of the floor, used for bringing the instrumentation cables into a vault, was sealed with a rubber gasket, and a steel cover was screwed onto the box. An air compressor forced air into the vault through a pipe running through the left leg of the steel-box door frame. The air line contained one closing valve, a bleed-off valve, and a pressure gauge. The air pressure in the vault was increased 3 psi, and a pressure–time record was started.

Leaks were found by coating the seams with a thick soap solution. The vault was then observed for the formation of bubbles. Leaks that were found were sealed. The results of the final air test were:

Pressure, psi	Time, hr
3	0
2.3	1¾
0.3	19½

REFERENCES

1. E. Cohen et al., Response of Dual-purpose Reinforced-concrete Mass Shelter, Project 30.2, Operation Plumbbob Report, WT-1449, in preparation.
2. T. B. Goode et al., Soil Survey and Backfill Control in Frenchman Flat, Project 3.8, Operation Plumbbob Report, WT-1427, October 1959.
3. J. R. Banister and L. J. Vortman, Effects of a Precursor Shock Wave on Blast Loading of a Structure, Project 34.1, Operation Plumbbob Report, WT-1472, August 1961.
4. E. J. Bryant et al., Basic Air-blast Phenomena, Part I, Project 1.1, Operation Plumbbob Report, ITR-1401, October 1957. (Classified)
5. Nucleonics Department, Edgerton, Germeshausen & Grier, Inc., Gamma Dosimetry by Film-badge Techniques, Project 39.1a, Operation Plumbbob Report, WT-1466, July 1959. (Classified)
6. S. Sigoloff et al., Gamma Measurements Utilizing the USAF Chemical Dosimeter, Project 39.1, Operation Plumbbob Report, WT-1500, January 1960. (Classified)

Chapter 3

BLAST RESULTS

3.1 STRUCTURAL

Along the sides of the door box frame, the concrete wall was stripped off, both the inside-face and outside-face reinforcements were torn out and bent, and the first row of Z clips on the interior plate lining and a small section of the interior plate lining of the vault were partially exposed (Figs. 3.1 and 3.2).

One piece of the concrete wall approximately 6 ft by 3 ft 3 in. by 1 ft 6 in. was found 80 ft to the right rear (WNW) of the structure (Fig. 3.3), and a similar piece was found 85 ft to the left rear (WSW) of the structure.

The exposed fractured section of the remaining concrete wall showed full-height vertical cracks along the planes of the reinforcement separating the walls into three slices (Fig. 3.4). There were few, if any, breaks through the aggregate. The majority of the $\frac{3}{8}$-in.-diameter form ties welded to the sides of the door box frame were bent but were not torn off. The outer layers of wall reinforcing bars were torn out for approximately two-thirds of the vault length. Although the damage to the side walls was extensive, the vault interior was well protected.

There was no damage to the roof slab or rear wall of the vault.

The vault foundation showed no visual evidence of translation or rotation relative to the general ground level. There was a crack across the entire width of the footing slab on a line along the front edge of the door box frame. The crack was approximately $\frac{1}{8}$ in. wide along the steel-plate box frame. It narrowed toward the edges of the slab and continued vertically downward on the faces for about 22 in. on the left face and 12 in. on the right face.

The vault door withstood the blast without structural damage. The front face of the vault was partially blackened by the thermal radiation (Fig. 3.5). The light-gauge stainless-steel finish plates were warped and in some cases torn off (Fig. 3.6). The operating hardware on the surface of the pressure-system box was blown off, apparently in a downward direction. The hardware included two combination-lock dials, a pressure-system handwheel, and a throw-bolt handle. The hardware, except for the cast-iron pressure-system handwheel, which was fractured into several pieces, was found within a 10-ft radius from the door. The housing of the emergency combination dial, which was attached by means of three $\frac{1}{2}$-in.-diameter bolts, was blown off as a unit. The pressure housing, attached to the door by twelve 1-in.-diameter bolts, had a slight downward shift. The top $\frac{1}{2}$-in. plate of the pressure-system housing was deflected, but a similar plate below the housing was not damaged.

A visual inspection of the door hinge and door frame showed no apparent damage except for minor surface pitting. The original fit was apparently maintained, the door remaining parallel to its frame in all planes, thus indicating a tight fit at the seal between the door and striker. Although it was not practical to perform an air test prior to opening the door, it did not appear that the airtight and watertight condition of the door was affected by the blast.

The postshot opening of the door presented no major problems; it was opened without difficulty in about 10 min. A temporary dial, oriented by the combination-lock spindle end, was

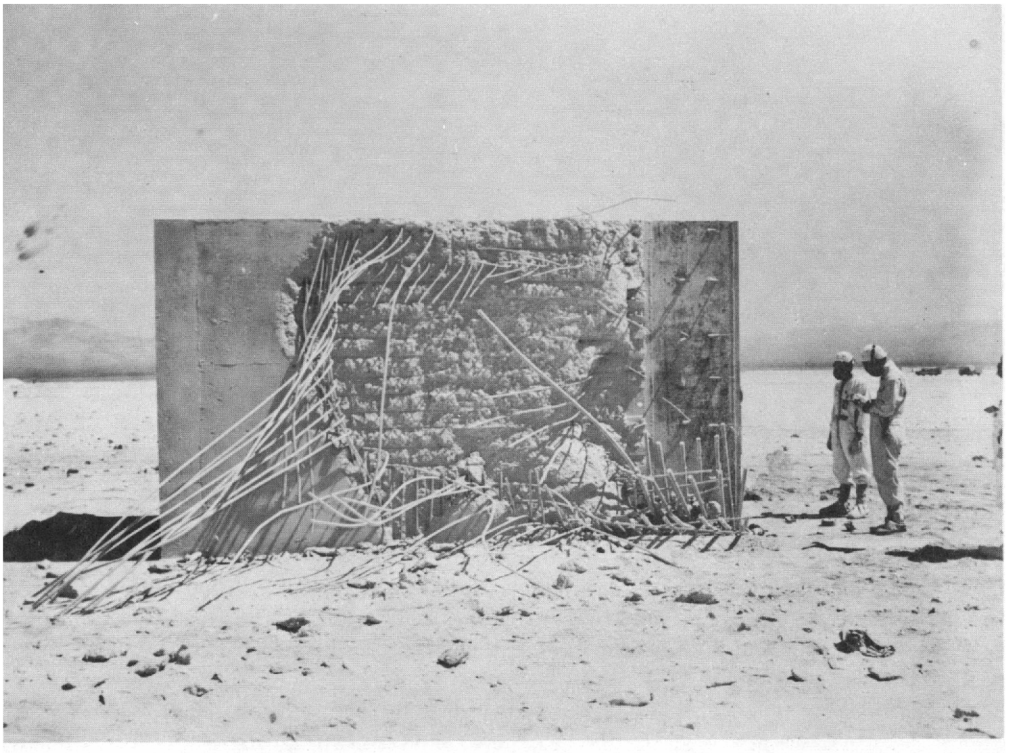

Fig. 3.1—Postshot, south face of vault.

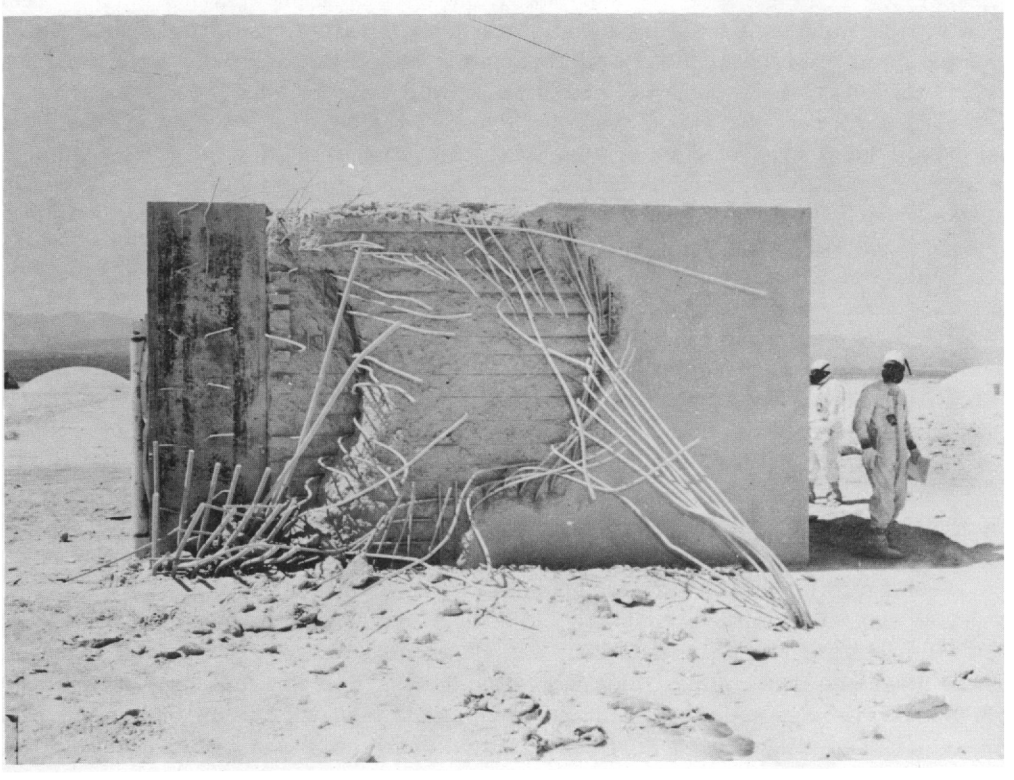

Fig. 3.2—Postshot, north face of vault.

Fig. 3.3—Postshot, piece of concrete debris found 80 ft from vault.

Fig. 3.4—Postshot, north face close-up showing separation of concrete along planes of reinforcement.

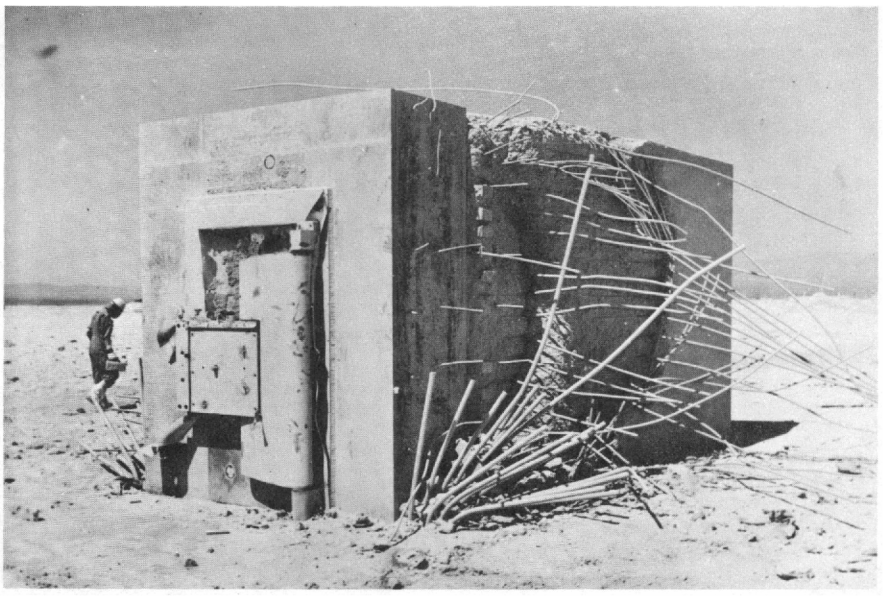

Fig. 3.5—Postshot, front and north faces of vault.

Fig. 3.6—Postshot, close-up view of front face from south showing damage to light-gauge finish plates and hardware.

placed on the lower-right spindle, and the combination was run off. The bolt-locking mechanism operated normally. The throw-bolt handle arbor was then turned with a pipe wrench, and the bolts were thrown open. The pressure system was operated by the same temporary handle, and the door was drawn out and easily opened by hand. The hinge and all other operating parts functioned smoothly and showed no apparent damage. Warped finish plates pressing against the door edge caused some rubbing of the door as it was drawn. Examination of the interior of the door, including the Lucite back plate, showed it to be in perfect condition (Fig. 3.7). The Neoprene seal was intact and was fully resilient along its entire periphery. The striker and its gussets, the door box-frame plates, and the joint where the plates joined the interior lining showed no damage, cracks, or weld failure. However, a careful inspection by a representative of the Mosler Safe Co. indicated that the door had been displaced downward by the blast. This displacement prevented the door from being fully closed after the initial opening. After the door-hinge pins were adjusted to raise the door approximately $\frac{1}{64}$ to $\frac{1}{32}$ in., the pressure system was easily operated to fully close the door. The boltwork was then thrown closed without difficulty.

The $\frac{1}{2}$-in. steel-plate lining of the vault was undamaged except for the wall lining directly behind the vertical sections of the door box frame, where the plate was dished inward (Fig. 3.8). A joint between the door box frame and the frontmost Z-clip batten plate of the vault lining was partially exposed when the side-wall concrete was torn off, allowing the blast pressure to infiltrate and build up in the $\frac{1}{2}$-in. space between the door box frame and the vault lining.

The wall plate behind the left side of the door box frame (looking into the vault) was dished inward a maximum of $\frac{3}{4}$ in., and the plate behind the right side of the door frame was dished inward a maximum of $3\frac{1}{2}$ in. Both maximum deflections occurred 12 in. from the side walls. Even with the seemingly large deformations, these plates still provided complete protection. There was no apparent fracture of the $\frac{1}{2}$-in. plate welds.

3.2 PRESSURE INSTRUMENTATION

The results from records obtained from the Project 34.1 instrumentation[1] are summarized in Table 3.1. This table also gives the location of the gauges, the calibration (anticipated) pressure, the times of arrival, the peak pressures and the times they occurred, the positive-phase duration, and the positive-phase impulse. The records from the two free-field gauges are shown in Fig. 3.9, and the records from the seven gauges on the structure are shown in Figs. 3.10 and 3.11.

Project 34.1 (WT-1472) indicated that the records of some of the gauges had to be modified to correct for dust filling, induced electrical signal, and low gauge signal. However, these modified gauge records must still be viewed with some skepticism.

The free-field dynamic-pressure gauge and the two gauges on the front face of the vault were dust filled, and, although an estimate has been made of their impulses, no suitable modification has been found to correct the records. A smoothed plot of the record from gauge P2 and a corrected plot for the record from gauge P3 are presented in Fig. 3.12 as the adjusted front-wall gauge records.

Gauge P6 (rear wall, top) picked up an induced 60-cycle signal from electrical equipment installed as another phase of Project 30.4. The effect of the 60-cycle signal (based on the average amplitude of the signal before and after the shock signal) was arithmetically filtered out, and the pressure-time curve shown in Fig. 3.13 resulted.

As shown in Figs. 3.10 and 3.11, the amplitude of gauge P7 was less than one-fourth that of gauge P6. Both gauges were located on the back wall of the structure. Impulses from gauges on the back of a 6- by 6- by 20-ft structure[1] showed considerable scatter but gave no conclusive evidence of an impulse gradient with height above the ground, even though there was an appreciable gradient on the front. It has been assumed that the same holds true for the test vault. Although no mechanical or electrical error could be found, one was suspected, and the amplitude of P7 has been arbitrarily increased by a multiplication factor of 4.7 to make its positive-phase impulse equal to P6. The results, when compared with the record from P6

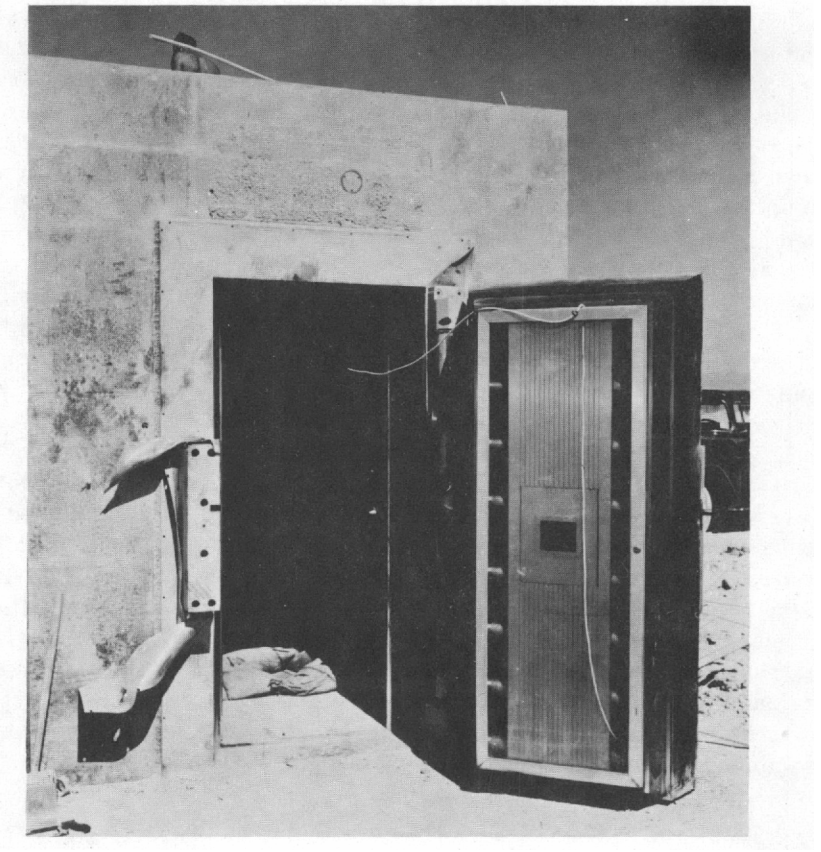

Fig. 3.7—Postshot, front face of vault, door open.

Fig. 3.8—Postshot, interior view looking toward door.

TABLE 3.1—SUMMARY OF VAULT GAUGE RESULTS

Gauge	Location	Calibration pressure, psi	Time of arrival, msec	First peak overpressure, psi	Time of arrival of first peak, msec	Second peak overpressure, psi	Time of arrival of second peak, msec	Positive-phase duration, msec	Positive-phase impulse, psi-sec	Remarks
Pressure	Ground baffle	75	222	17	268	87	312	462	8.14	Free field
Pitot-static	3 ft	375	223	518	305					Free field, total pressure
P1	Footing	600	219	277	309					Failed at 333 msec
P2	Front	600	222	410	313				24.0*	Dust filled
P3	Front	600	221	668	300				42.3*	Dust filled
P4	Top	75	225	20	270	66	316	400	5.43	
P5	Top	75	227	15.5	252	60	319	342	4.97	
P6	Back	66	227	18	259	39	345	363	4.36	
P7	Back	66	231	4.6 (21.3)*	250	6.2 (28.8)*	356	334	0.92 (4.32)*	

* Estimated by correction.

TABLE 3.2—MEASURED IMPULSES ON TEST VAULT

	Psi-sec	Ratio
Incident	8.14	
Front	33.15	
Front/incident		4.07
Top	5.20	
Top/incident		0.64
Back	4.34	
Back/incident		0.53
Net translational	28.81	
Net/incident		3.54

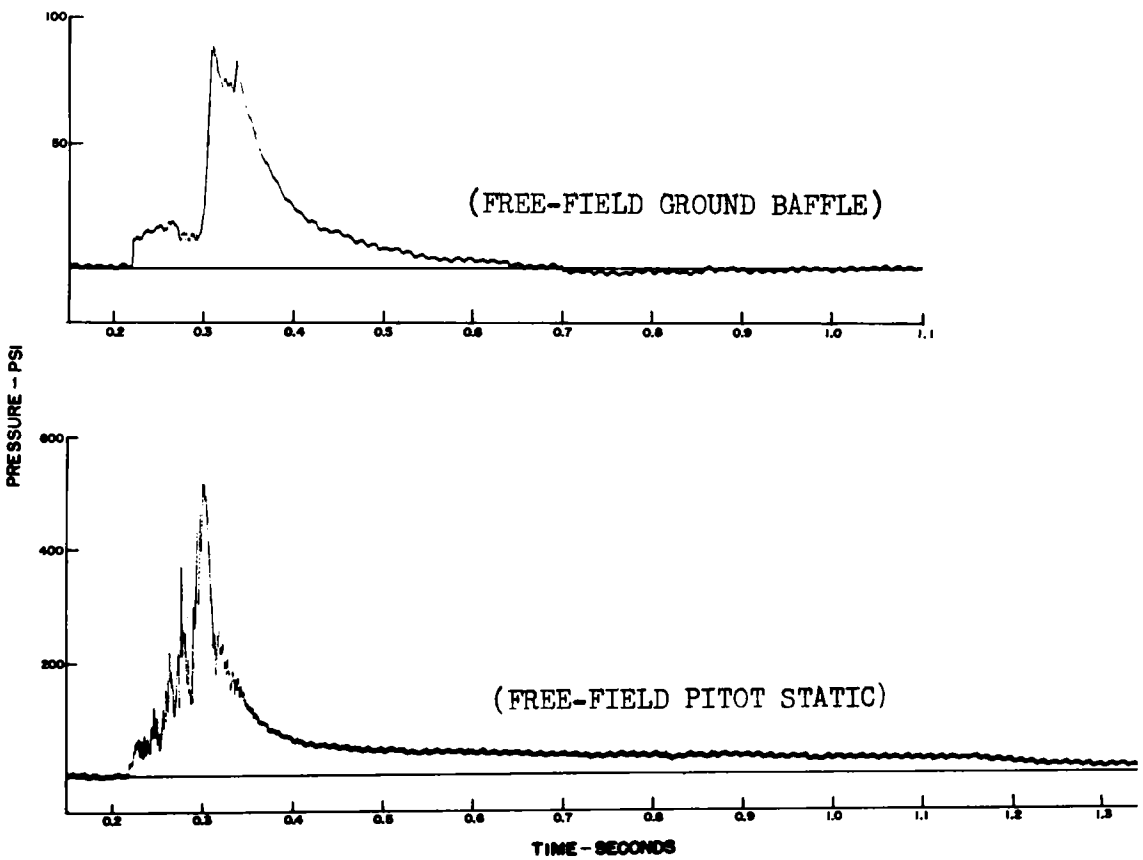

Fig. 3.9—Free-field gauge pressure–time records.

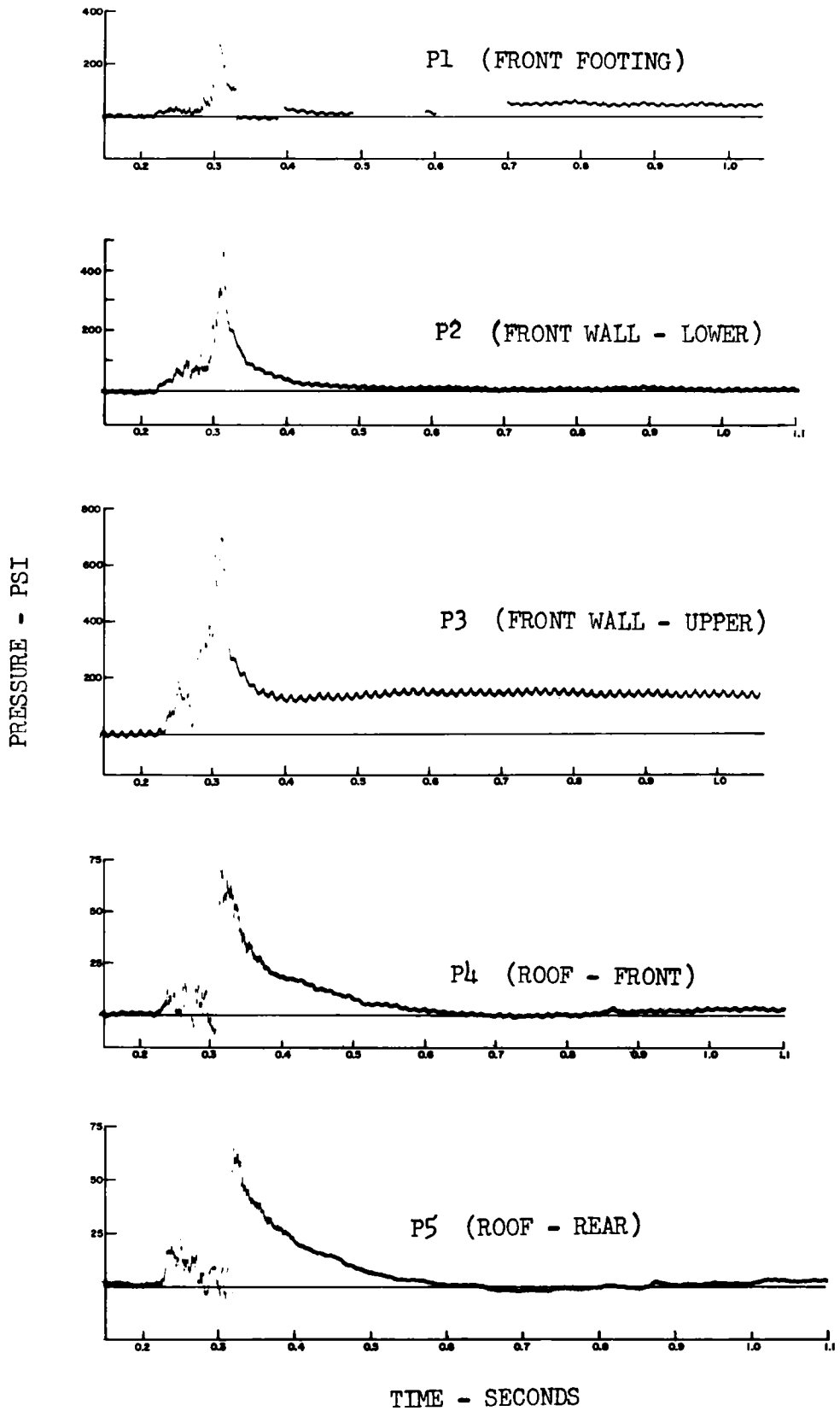

Fig. 3.10— Structure 30.4 pressure–time records.

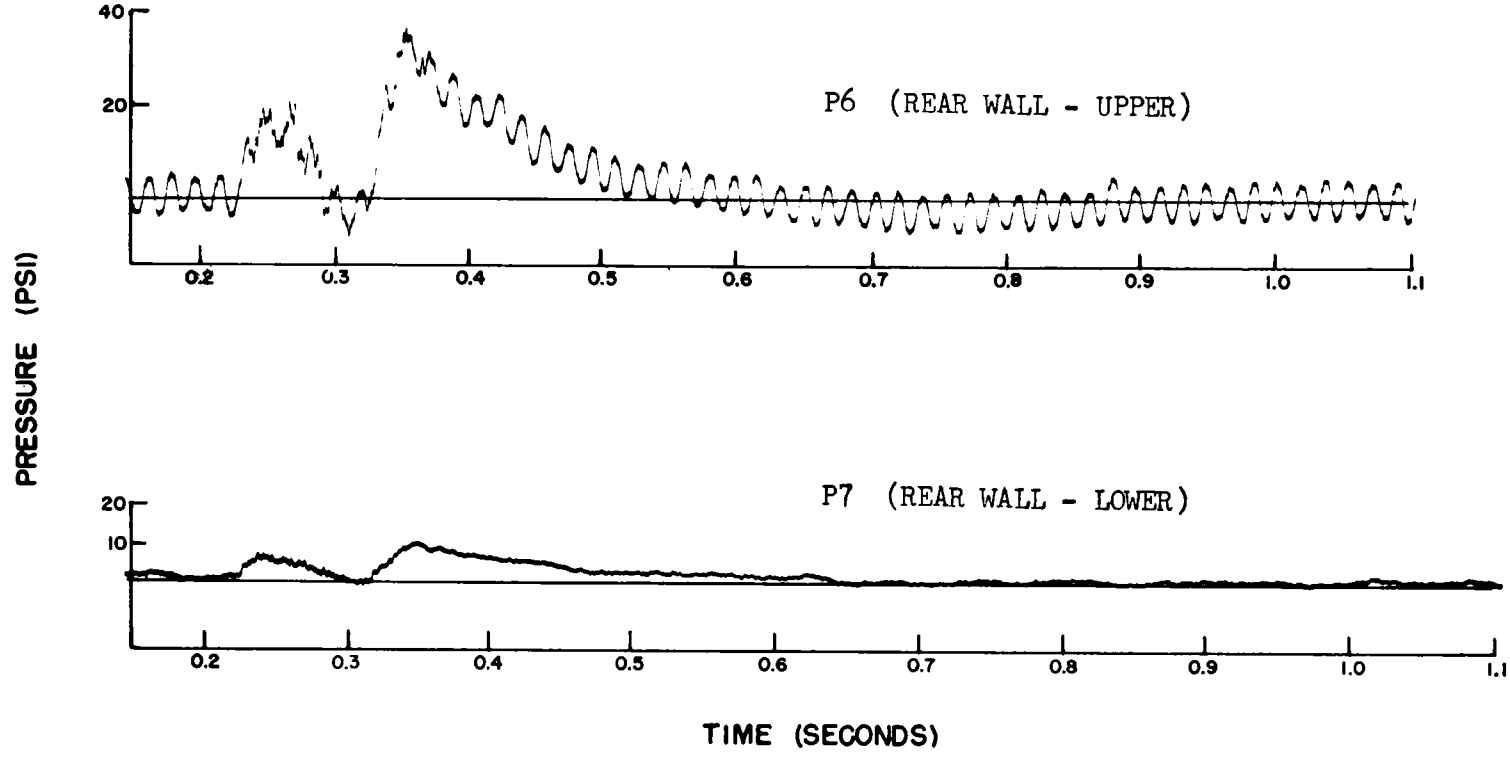

Fig. 3.11—Structure 30.4 pressure–time records (rear wall).

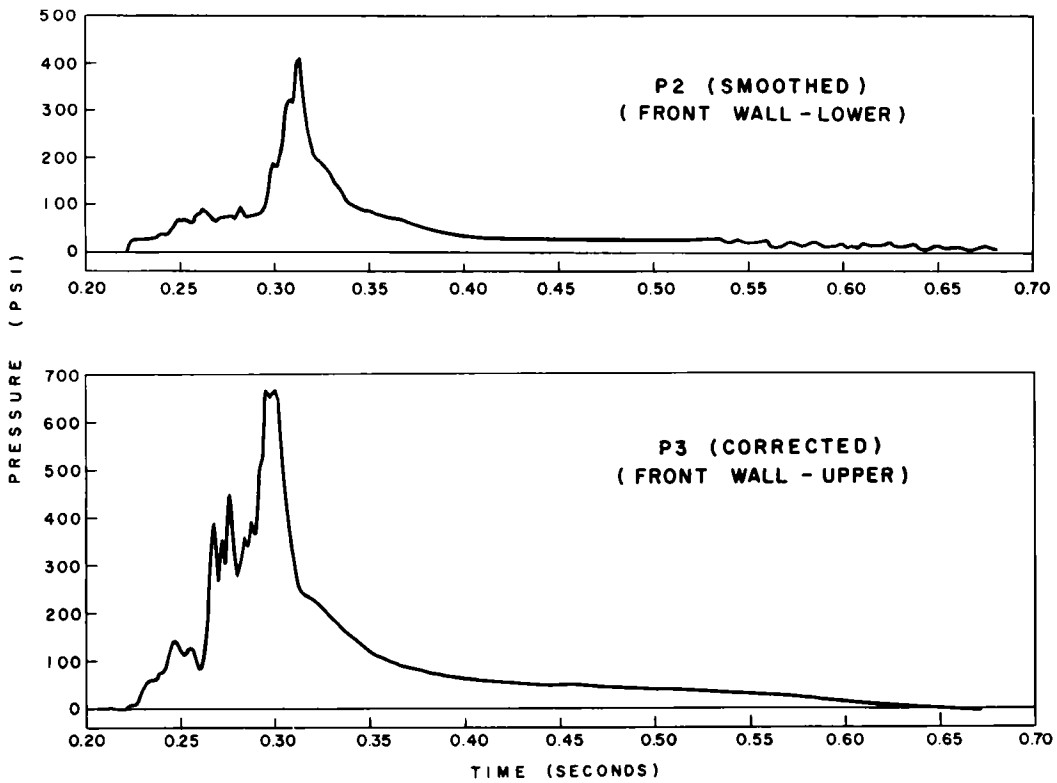

Fig. 3.12— Adjusted front-wall gauge records.

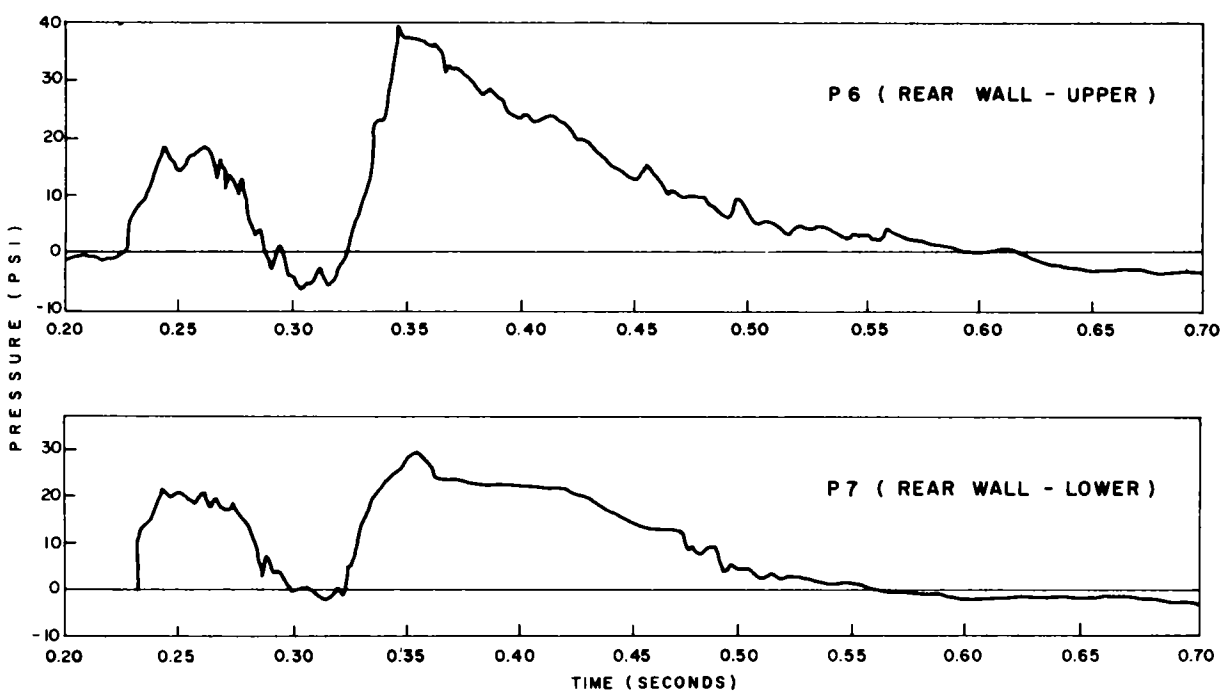

Fig. 3.13— Modified rear-wall gauge records.

without the 60-cycle signal, indicate that, except for amplitude, P7 is a credible record (Fig. 3.13).

Since the records from gauges on the front of the structure indicated that P3 was filled with dust, it is possible that P2 may have been dust-filled also, but to a much less extent. Records from both gauges show wave forms and peaks that are characteristic of those of the incident dynamic-pressure record rather than of the incident-overpressure record.

The wave shapes from gauges on the top and back of the structure agreed with those of the incident-overpressure wave, but they showed a dip below ambient pressure at the end of the precursor just before arrival of the main shock wave, even though the incident-overpressure wave had no such excursion below ambient. No oscillation of the pressure wave was evident.

The single gauge on the forward footing of the structure gave a record which indicated that the gauge was disturbed or damaged by a mechanical blow, probably from a rock, 0.11 sec following shock-wave arrival.

The results of impulse measurements (arithmetic averages of impulses of individual overpressure-time records) are given in Table 3.2.

Tabulated results[2] of the maximum values obtained from the blast-line instrumentation provided by Project 1.1 are given in Tables 3.3 and 3.4. Table 3.3 contains the values for the

TABLE 3.3—P-t GAUGE RESULTS, MAIN BLAST LINE

Station	Ground range, ft	Maximum overpressure, psi	Arrival time, sec	Positive duration, sec	Positive-phase impulse, psi-sec
F1.1-9039.01A	350	No record			
F1.1-9039.01B	350	1030			
F1.1-9039.02A	450	760			
F1.1-9039.02B	450	750		0.175	
F1.1-9039.03A	650	480	0.364	0.095	10.562
F1.1-9039.03B	650	400	0.676	0.162	8.896
F1.1-9040.01A	850	225		0.236	11.957
F1.1-9040.01B	850	206			
F1.1-9040.02A	1050	125		0.233	6.156
F1.1-9040.02B	1050	138		0.195	5.613
F1.1-9041.00A	1350	60.0		0.343	4.503
F1.1-9041.00B	1350	62.0	0.512	0.280	4.501
F1.1-9042.01	1650	31.0		0.467	3.973
F1.1-9042.02	2000	16.3			
F1.1-9042.05	2250	12.4	0.570	0.687	4.039
F1.1-9042.06	2500	9.2	0.523	0.852	4.179
F1.1-9042.07	3000	9.1		0.727	2.849
F1.1-9042.03	3500	9.9			
F1.1-9402.08	4000	8.8	1.729	0.818	2.595
F1.1-9042.04	4500	7.4			
F1.1-9043.01	5000	5.9		0.916	
F1.1-9043.02	6000	No record			

maximum overpressure and arrival time, the positive duration and total impulse for the self-recording pressure–time (P-t) gauges. The maximum values of the total pressure, static overpressure, pressure difference, dynamic pressure, and Mach number for the self-recording dynamic pressure, q, gauges are given in Table 3.4. The curves of maximum overpressure vs. ground distance for the P-t gauges are given in Fig. 3.14. Figure 3.15 is the curve of corrected dynamic pressure vs. ground range for the q gauge maximum values.

It should be noted that the pressure data recorded at the blast line at the 1150-ft range (found by logarithmic interpolation in Tables 3.3 and 3.4) were, except for the incident pressure, substantially different than the data recorded by the gauges adjacent to the vault (gauges approximately 115 ft from the blast line). These data are listed in Table 3.5 for comparison. Similar differences were observed by other projects, as shown in Figs. 3.14 and 3.15.

TABLE 3.4—q GAUGE RESULTS, MAIN BLAST LINE*

Station*	Ground range, ft	Total pressure, psi	Static overpressure, psi	Pressure difference $[(P_p - P_0)^{*\prime}]$, psi	Dynamic pressure (q*), psi	Mach number (u/a)
F1.1-9040.01	850					
F1.1-9040.02	1050	470.0	125.0	445.0	240.0	3.3
F1.1-9041.00	1350	275.0	60.0	255.0	150.0	3.6
F1.1-9041.00Nx	1350					
F1.1-9042.01	1650	143.5	31.0	150.0	80.0	2.3
F1.1-9042.02	2000	58.5	23.0x	44.0	35.0	1.3
F1.1-9042.05N	2250	48.0	12.4	36.0	27.0	1.4
F1.1-9042.06	2500	47.0	9.2	38.0	25.0	1.3
F1.1-9042.06Nx	2500	35.0	9.2	28.0	19.0	1.2
F1.1-9042.07	3000	29.0	9.1	20.0	15.1	1.0
F1.1-9042.07Nx	3000	26.5	9.1	20.5	17.0	1.04
F1.1-9042.02	3500	11.2	8.6x	3.4	2.8	0.45
F1.1-9042.08	4000	10.0	9.0	1.3	1.3	0.29
F1.1-9042.08N	4000					
F1.1-9042.04	4500	7.8	6.5x	1.7	1.2	0.29

* N refers to new q gauge. x values are from q gauge. q* = corrected dynamic pressure (see ITR-1401). $(P_p - P_0)^{*\prime}$ = total head Pitot pressure minus ambient preshock static pressure, uncorrected and containing air and dust components.

3.3 RADIATION INSTRUMENTATION

All radiation-detection instruments were located as shown in Fig. 2.3. The recovery of all interior radiation detectors was accomplished on D+6 day.

The results of the gamma-radiation film dosimeters placed within the structure are given in Table 3.6. No record is available for the single gamma-radiation chemical dosimeter located at point "p" within the structure since the external blast shield and the lithium can were badly damaged and all the vials were broken.

The three film dosimeters that were fastened to the outside face of the vault at points a, h, and q were destroyed.

The goal-post-line dose–distance curve for the initial gamma radiation, obtained with the U. S. Air Force chemical dosimeters (Project 39.1), is shown in Fig. 3.16. These data for various slant ranges from 410 to 1773 yd are given in Table 3.7. The slant range of the vault was approximately 448 yd. Figure 3.17 is a plot of the stake-line dose–distance measurements obtained from the gamma-radiation film dosimetry of Project 39.1a. The data from which this curve was plotted are contained in Table 3.8.

Recovery of the goal-post-line and stake-line dosimetry was accomplished at H+1½ hr H+5 hr, respectively.

A more comprehensive description of the radiation-instrumentation test results can be obtained from the Project 39.1 and 39.1a reports[3,4] ITR-1500 and WT-1466, respectively.

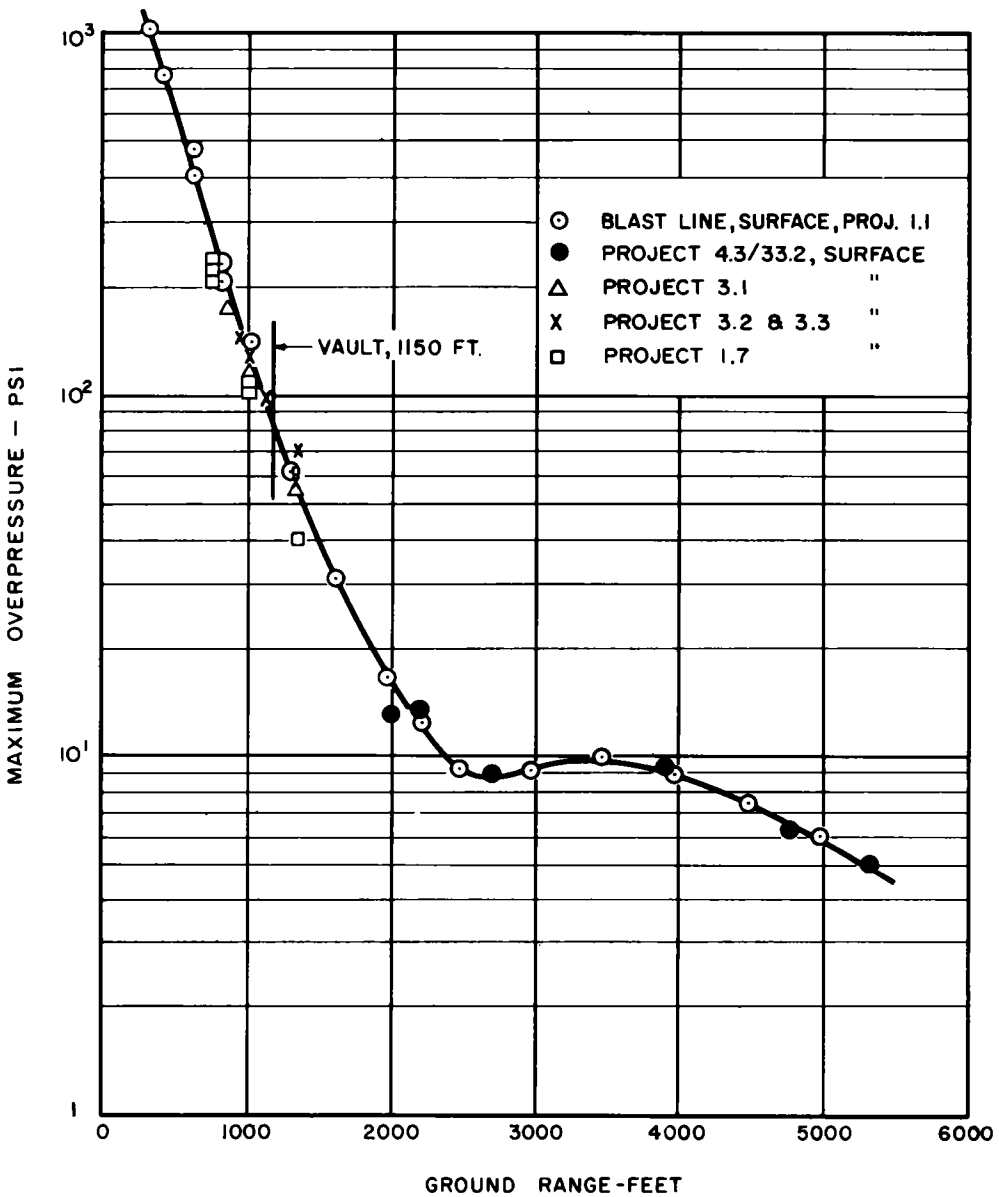

Fig. 3.14— Free-field maximum-overpressure vs. distance curve.

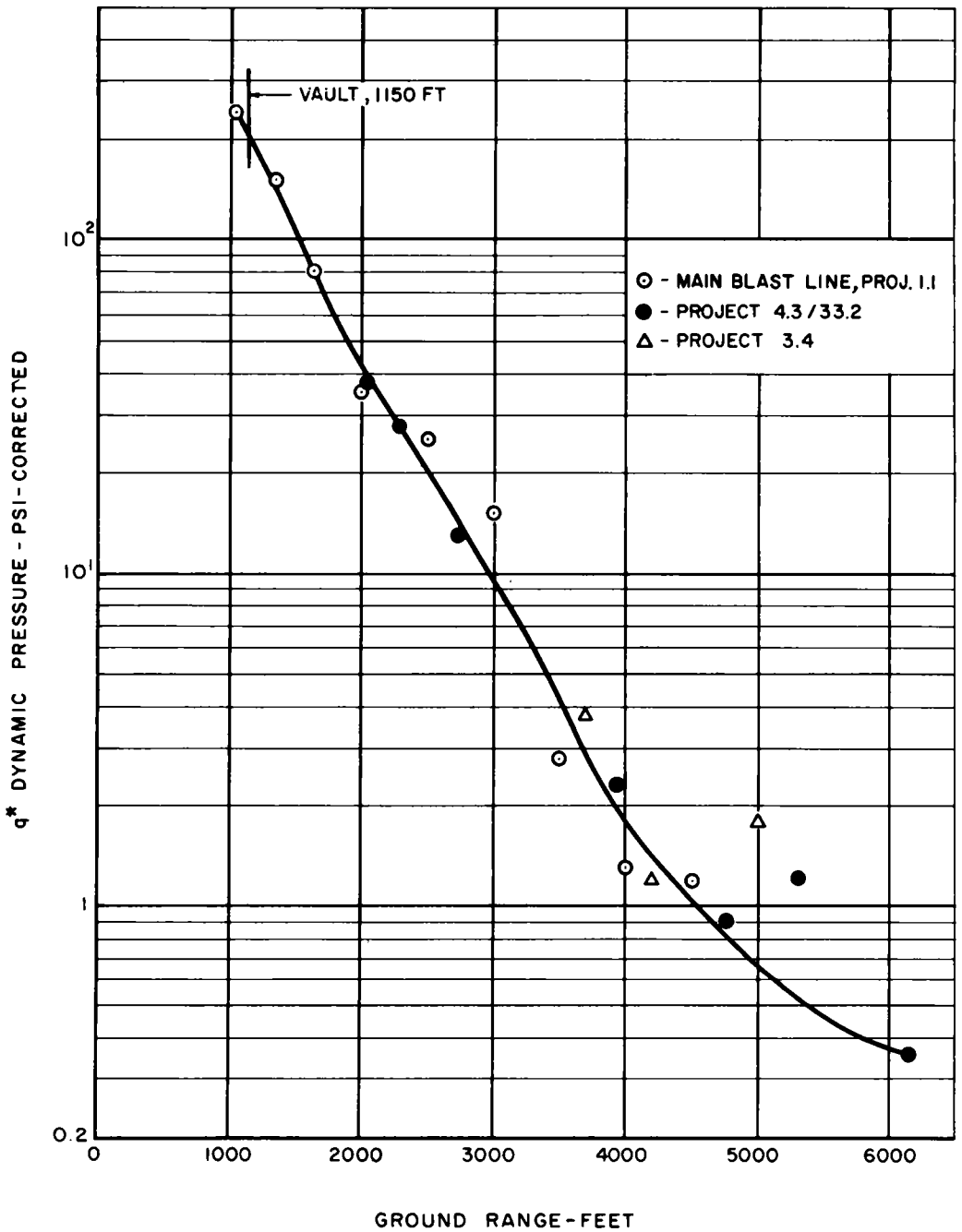

Fig. 3.15— Free-field corrected dynamic-pressure vs. distance curve.

TABLE 3.5— COMPARISON OF FREE-FIELD PRESSURES AT 1150-FT RANGE

	Blast line (Project 1.1)	Vault (Project 34.1)
Peak incident pressure, psi	102	87
Incident-pressure positive-phase impulse, psi-sec	5.4	8.14
Incident-pressure positive-phase duration, sec	0.25	0.46
Peak dynamic pressure, psi	290* (205)†	431*

* As-read value.
† Corrected value.

TABLE 3.6— RESULTS OF GAMMA-RADIATION FILM DOSIMETERS*

Dosimeter	Total dosage, r	Dosimeter	Total dosage, r
a	No recovery	j	4200
b	4300	k	3100
c	4200	l	3800
d	2800	m	3100
e	4400	n	3200
f	4400	o	3800
g	2600	p	Vials broken
h	No recovery	q	No recovery

* All interior dosimeters were 18 in. from the inside wall.

TABLE 3.7— GOAL-POST-LINE GAMMA DATA

Slant range (D), yd	D^2	Dose, r	RD^2
410	1.68×10^5	3×10^5	5.04×10^{10}
470	2.21×10^5	2.05×10^5	4.53×10^{10}
500	2.5×10^5	1.65×10^5	4.13×10^{10}
560	3.14×10^5	1.15×10^5	3.61×10^{10}
650	4.23×10^5	6×10^4	2.54×10^{10}
860	7.40×10^5	1.7×10^4	1.26×10^{10}
1000	1×10^6	7200	7.2×10^9
1383	1.91×10^6	1290	2.46×10^9
1477	2.18×10^6	740	1.61×10^9
1773	3.14×10^6	162	5.09×10^8

3.4 SURVEYS

The pre- and postshot values for the coordinates and elevations of the vault survey points are given in Tables 3.9 and 3.10, respectively. All coordinates are referenced to the Nevada State Grid North, which is neither true nor magnetic.

Subsequent to the postshot survey, it was learned that the triangulation was of second-order accuracy (1 : 10,000 permissible error) and that the average base-line lengths were over 11,000 ft; consequently this survey cannot be relied upon for estimating the absolute movements (Table 3.9) of the structure. Since the survey for the Project 30.2 structure[5] was included in the vault triangulation (350 ft between survey points) and since it can be safely as-

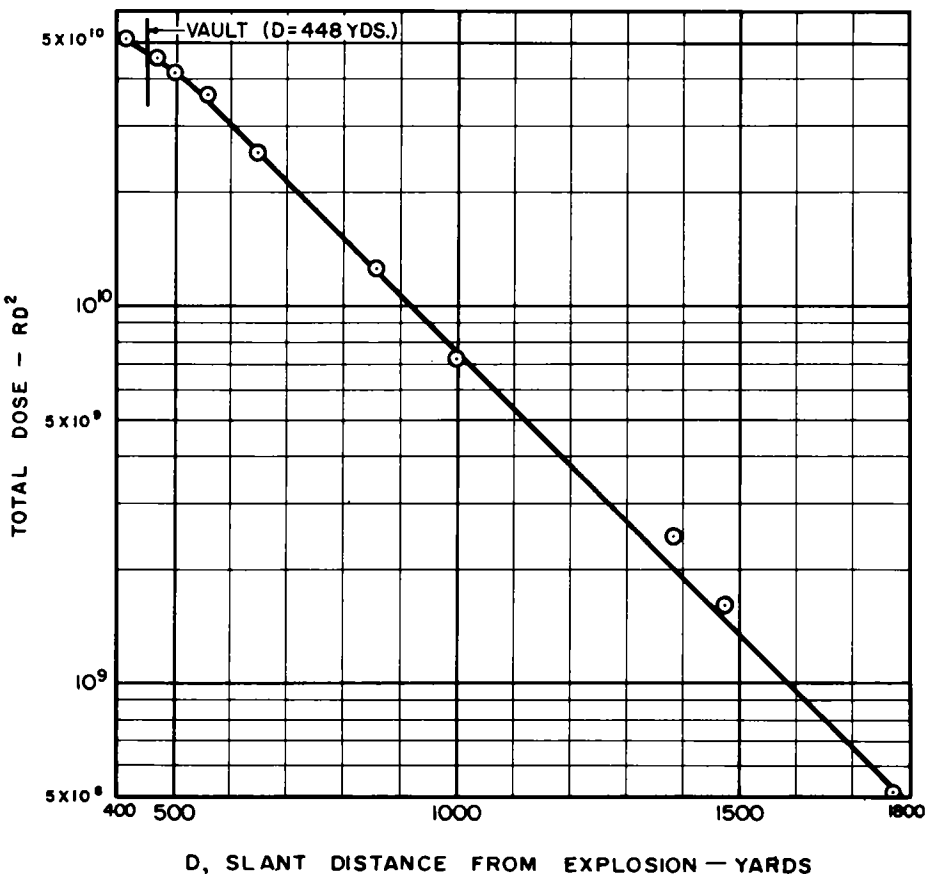

Fig. 3.16—Goal-post-line gamma dose–distance curve.

TABLE 3.8—STAKE-LINE GAMMA DATA*

Slant distance (D), yd	D^2	Dose EG&G container,† r	RD^2	No. of EG&G badges per point	Maximum deviation per point, %	Film types read
410	1.68×10^5	NR				
470	2.21×10^5	NR				
500	2.5×10^5	NR				
560	3.14×10^5	NR				
650	4.23×10^5	NR				
800	7.4×10^5	NR				
1000	1.0×10^6	NR				
1104	1.22×10^6	5.2×10^3	6.34×10^9	2	0.0	1112
1296	1.68×10^6	1.5×10^3	2.52×10^9	2	0.0	1112
1383	1.91×10^6	NR				
1477	2.18×10^6	NR				
1496	2.24×10^6	725.0	1.62×10^9	2	0.69	1112
1694	2.87×10^6	327.5	9.4×10^8	2	0.76	606
1773	3.14×10^6	NR				
1892	3.58×10^6	168.5	6.03×10^8	2	3.86	510
2090	4.37×10^6	122.5	5.35×10^8	2	2.04	510
2289	5.24×10^6	69.0	3.61×10^8	2	1.45	510

*Dose vs. distance: RD^2 vs. D.
†NR, not recovered.

TABLE 3.9—PRE- AND POSTSHOT COORDINATES

Point	Preshot	Postshot	Absolute movement, ft	Relative movement, ft*
1	N 746,414.04	N 746,414.58	0.54 N	0.03 N
	E 714,866.99	E 714,866.93	0.06 W	0.17 W
2	N 746,422.20	N 746,422.75	0.55 N	0.04 N
	E 714,856.83	E 714,856.79	0.04 W	0.15 W
3	N 746,417.26	N 746,417.78	0.52 N	0.01 N
	E 714,844.93	E 714,844.90	0.03 W	0.14 W

*Relative movement was obtained by deducting absolute movement of 0.51 ft N and 0.11 ft E of reference survey point on Project 30.2 structure.[5]

TABLE 3.10—PRE- AND POSTSHOT ELEVATIONS

Corner	Preshot	Postshot	Movement, ft
NE	77.48	77.47	0.01 downward
SE	77.48	77.45	0.03 downward
SW	77.49	77.50	0.01 upward
NW	77.50	77.50	0.00

sumed that the Project 30.2 structure had negligible permanent movement, the permanent horizontal movement of the vault can be reasonably estimated by the differences between the survey points of these two structures. These values are included in Table 3.9 in the column listing the relative movements.

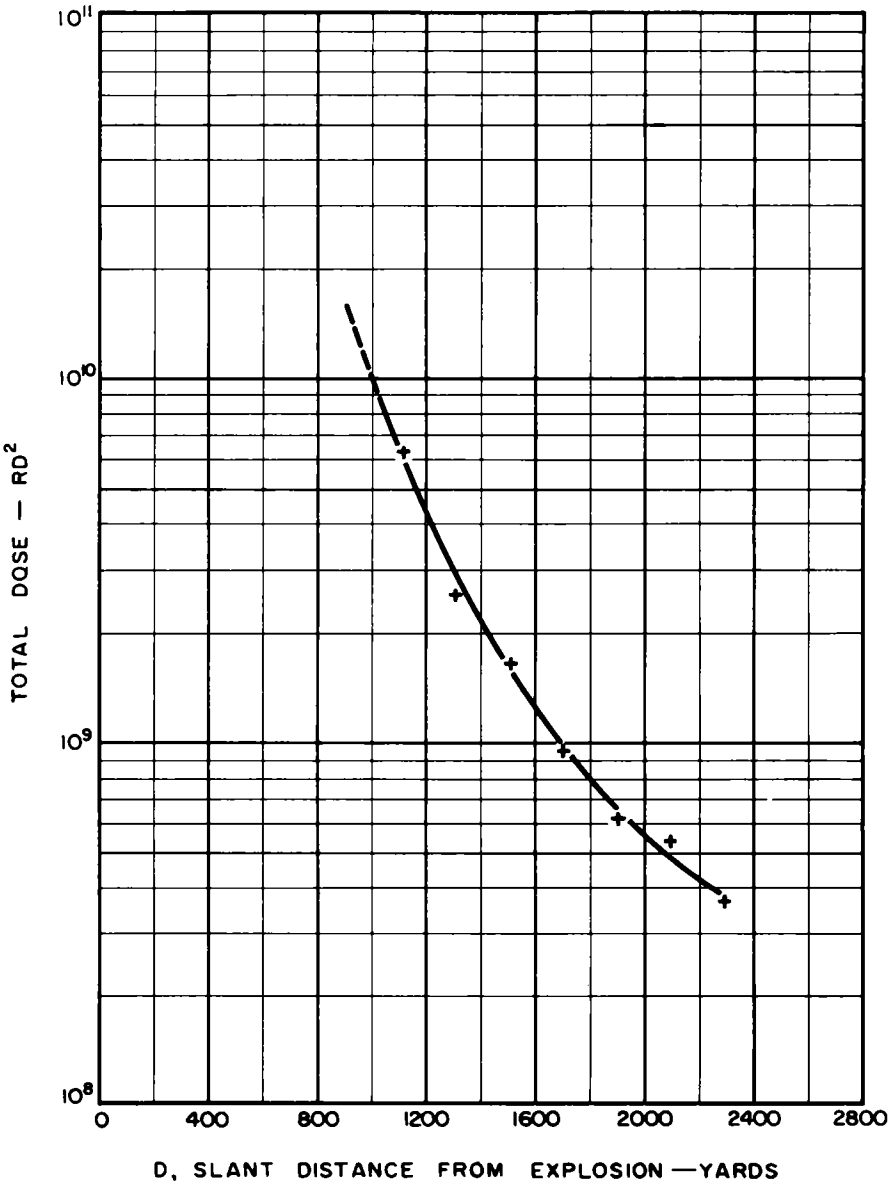

Fig. 3.17—Stake-line gamma dose–distance curve.

3.5 FREE-FIELD GROUND-MOTION DATA

During shot Priscilla free-field ground motions were recorded at various depths below the ground surface and at various ground ranges in the general vicinity of the shot Priscilla test structures. These records included ground-acceleration and -displacement measurements recorded at approximately 100 ft radially from the vault by gauges located 1050 ft from GZ at the approximate 100-psi overpressure range during Project 1.4 (Ref. 6) and Project 1.5 (Ref. 7). The recorded peak surface overpressure for Project 1.4 was 104 psi, and the recorded peak surface overpressure for Project 1.5 was 120 psi.

The results of the pertinent available free-field data in the proximity of the vault location are summarized in the following paragraphs. These data consist of surface and near-surface acceleration vs. time and displacement vs. time measurements. Also included are velocity vs. time, displacement vs. time, and shock-spectra ground-motion data computed from the acceleration vs. time records. Although these measurements were not recorded at the exact ground range of the vault, they are presumed to be representative of the range of values of free-field ground motions in the vicinity of the vault, consistent with the accuracy of the test records. It should be noted that certain inconsistencies exist, and in some cases the reliability of the test data is uncertain.

TABLE 3.11—MEASURED PEAK FREE-FIELD GROUND ACCELERATION

Project 1.4			Project 1.5		
Depth, ft	Vertical acceleration, g	Horizontal acceleration, g	Depth, ft	Vertical acceleration, g	Horizontal acceleration, g
1	21.7	No record	Surface	27.0	8.5
5	16.8	No record	10	8.8	No record
10	No record	2.8			

TABLE 3.12—COMPUTED PEAK FREE-FIELD GROUND VELOCITY

Project 1.4			Project 1.5		
Depth, ft	Vertical velocity, ft/sec	Horizontal velocity, ft/sec	Depth, ft	Vertical velocity, ft/sec	Horizontal velocity, ft/sec
1	6.55	No record	Surface	5.86	No record
5	6.18	No record	10	5.66	No record
10	No record	0.40			

The free-field acceleration vs. time ground motions in the horizontal and vertical direction were recorded by accelerometers enclosed in protective canisters that were buried at various depths below the ground surface. Listed in Table 3.11 are the peak accelerations in the vertical and horizontal directions recorded near the ground surface.

As shown on the near-surface acceleration vs. time records plotted in Refs. 6 and 7, the vertical-acceleration curves are characterized mainly by a single sharp peak of acceleration in the downward direction, preceded and followed by minor disturbances. The horizontal-acceleration curves show a somewhat similar wave form; however, the first major positive (outward from GZ) peak acceleration is followed by a pronounced negative peak.

The acceleration vs. time records of Projects 1.4 and 1.5 were numerically integrated to obtain the particle-velocity vs. time curves. The peak values in the vertical and horizontal directions are tabulated in Table 3.12. These curves, plotted in Refs. 6 and 7, indicate that the wave form is similar to the air pressure, falling off somewhat more rapidly than the pressure and becoming zero before the end of the positive phase of the air pressure. The peak velocities are downward and outward from GZ for the vertical and horizontal directions, respectively.

Displacement vs. time plots were also computed from the double integration of the acceleration records of Project 1.4 (Ref. 6) and Project 1.5 (Ref. 7). In addition, vertical ground displacements were directly measured by Project 1.5 by the use of relative-displacement gauges. The displacement gauges recorded the displacement vs. time relative to the ground-surface motion at various depths below the ground surface. Relative displacements were converted to absolute displacements of the surface and gauge anchors on the assumption that the deepest anchors (200 ft below the surface) were not displaced.[7] The wave forms of the displacement plots [6,7] exhibit a somewhat gradual time of rise to the peak value, which occurs at approximately the end of the positive phase of the air pressure. The computed and measured peak and permanent displacements are tabulated in Tables 3.13 and 3.14, respectively. These peak values are downward and outward from GZ for the vertical and horizontal directions, respectively.

TABLE 3.13— COMPUTED PEAK TRANSIENT FREE-FIELD GROUND DISPLACEMENT

Project 1.4			Project 1.5		
Depth, ft	Vertical displacement, in.	Horizontal displacement, in.	Depth, ft	Vertical displacement, in.	Horizontal displacement, in.
1	3.59	No record	Surface	6.13	No record
5	3.68	No record	10	6.55	No record
10	No record	0.096			

TABLE 3.14— MEASURED VERTICAL PEAK FREE-FIELD GROUND DISPLACEMENT (PROJECT 1.5)

Depth, ft	Peak downward displacement, in.	Permanent downward displacement, in.
Surface	2.8	0.3
10	2.0	0.2

As shown in Tables 3.13 and 3.14, the computed displacements are considerably higher than the measured displacements for Project 1.5. However, the measured-displacement records are considered more reliable since a good deal of judgment is involved in obtaining meaningful results in the acceleration integration computations. The calculated peak horizontal displacement at the 10-ft depth (0.096 in.) is unreasonably low and is a result of the apparently low peak-acceleration gauge reading of 2.8 g, based on a study of other test records at various pressure levels and depths below the ground surface.[6–9] It is more reasonable to expect peak horizontal displacements to be in the range of $\frac{1}{3}$ to $\frac{2}{3}$ of the vertical component and perhaps equal to the vertical component at certain pressure levels and with certain geological conditions.

Response spectra of ground motion were computed for the input ground-motion data recorded during Project 1.4 (Ref. 6). A response spectrum is defined as the maximum response of a linear single-degree-of-freedom spring mass system relative to the motion of the ground.[9,10] Figure 3.18 shows the vertical-displacement-spectrum curve for the 1- and 5-ft depths and the horizontal-spectrum curve for the 10-ft depth for the 100-psi overpressure range.[6] These response spectra correspond to the input ground-motion data presented above for Project 1.4. Corresponding velocity- and acceleration-spectrum curves can be determined easily from the shock-spectra theory:[10]

$$\text{Velocity spectra} = \omega\, |X|_{max.}$$

$$\text{Acceleration spectra} = \omega^2\, |X|_{max.}$$

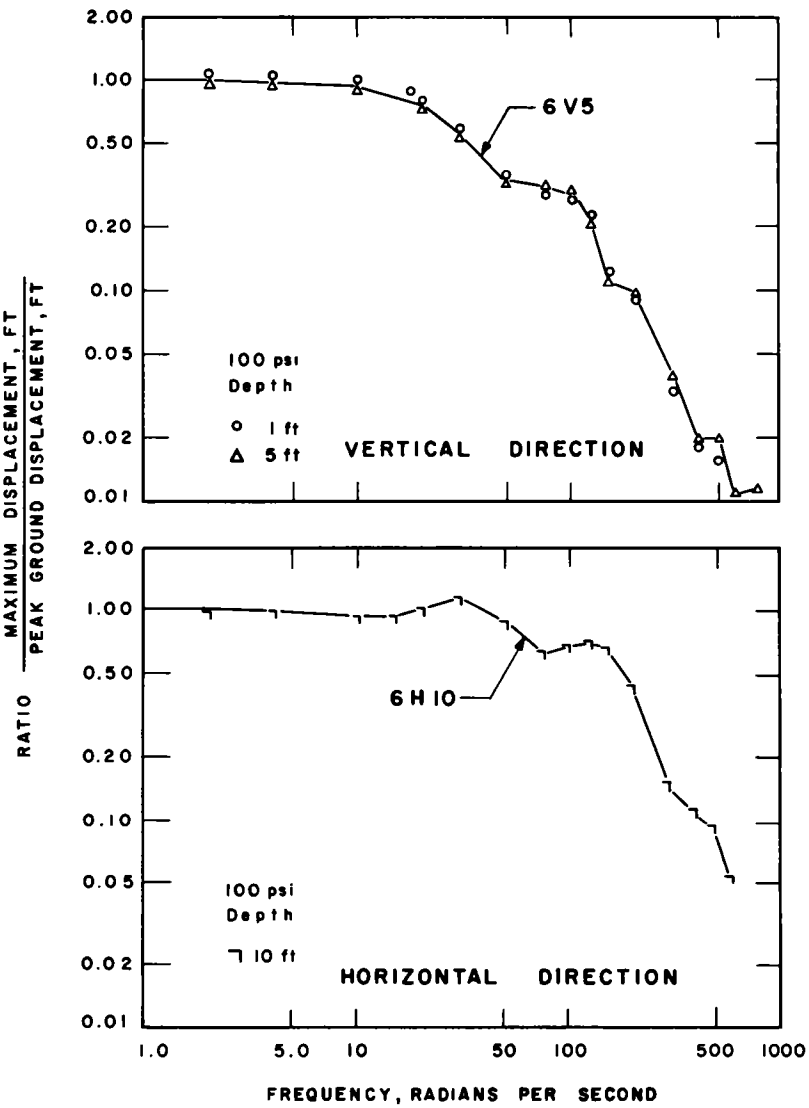

Fig. 3.18—Displacement-response spectra.

where X is the displacement spectra value at the frequency ω in radians per second. The velocity and acceleration units are consistent with the unit of displacement.

It should be noted that the horizontal-spectrum curve for the 10-ft depth has low response values, as previously discussed, with regard to the unusually low values of the horizontal input data.

3.6 THERMAL AND MISCELLANEOUS INSTRUMENTATION

The vault contents were only slightly disturbed by the blast. The sandbags against the front wall were shifted a few inches toward the rear of the vault. The movie camera, mounted

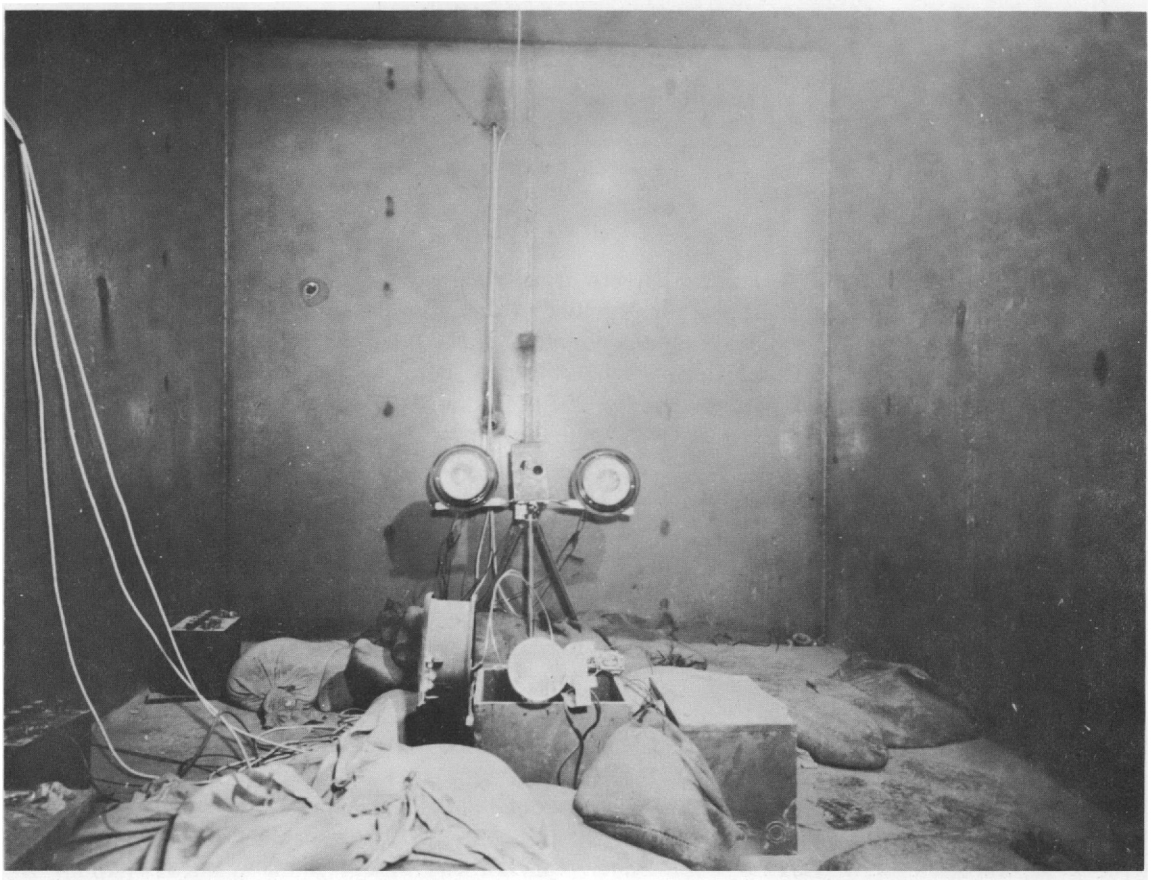

Fig. 3.19— Postshot, view looking toward rear showing camera tilt.

on a tripod attached to the floor lining by three machine screws, was tilted upward approximately 10 deg (Fig. 3.19) from its original position. The camera operated as planned, running 40 ft of film. The developed film, however, was completely fogged. The two clinical type thermometers registered 88°F, and the 24-hr American stylus temperature recorder showed no variation in temperature from H−6 hr through H+18 hr, remaining constant at 88°F. The Leeds & Northrup thermocouple recorder ran 20 min; however, the bulb connection at the exterior front face of the vault was blown off, and the temperature recorded on the chart dropped from 100 to 0°F and remained at 0°F for the duration of its run. The lag in the mechanical equipment was too large to record the temperature in the time interval between the arrival of the thermal wave and the arrival of the shock wave. Figure B.16 shows the vault interior before preshot sandbagging of the instrumentation.

3.7 POSTSHOT AIR TEST

Several days after the door had been opened, all conduits leading from the vault were sealed off for the postshot air test. During this time the door seal suffered minute cuts and nicks from wind-blown sand and dust. Although the seal was wiped with a nonhardening gasket shellac (Permatex), it is doubtful whether the postshot air test of the vault is indicative of the airtightness prior to the initial postshot opening of the door.

The results of the postshot air test are shown in Table 3.15.

TABLE 3.15—POSTSHOT AIR TEST OF VAULT

Pressure, psi	Time, hr
3	0
1	1/2
1/8 to 1/10	14 or more

REFERENCES

1. J. R. Banister and L. J. Vortman, Effects of a Precursor Shock Wave on Blast Loading of a Structure, Project 34.1, Operation Plumbbob Report, WT-1472, August 1961.
2. E. J. Bryant et al., Basic Air-blast Phenomena, Part I, Project 1.1, Operation Plumbbob Report, October 1957. (Classified)
3. S. Sigoloff et al., Gamma Measurements Utilizing the USAF Chemical Dosimeter, Project 39.1, Operation Plumbbob Report, WT-1500, January 1960. (Classified)
4. Nucleonics Department, Edgerton, Germeshausen & Grier, Inc., Gamma Dosimetry by Film-badge Techniques, Project 39.1a, Operation Plumbbob Report, WT-1466, July 1959. (Classified)
5. E. Cohen et al., Response of Dual-purpose Reinforced-concrete Mass Shelter, Project 30.2, Operation Plumbbob Report, WT-1449, in preparation.
6. L. M. Swift et al., Ground Acceleration, Stress, and Strain at High Incident Overpressures, Project 1.4, Operation Plumbbob Report, WT-1404, May 1960. (Classified)
7. Wm. R. Perret, Ground-motion Studies at High Incident Overpressure, Project 1.5, Operation Plumbbob Report, WT-1405, June 1960.
8. L. M. Swift and D. C. Sachs, Ground Motion Produced by Nuclear Detonations, Operation Hardtack Report, Project 1.8, ITR-1613, August 1958. (Classified)
9. J. F. Halsey and M. V. Barton, Spectra of Ground Shocks Produced by Nuclear Detonations, Operation Plumbbob Report, Project 1.9, WT-1487, August 1959. (Classified)
10. Y. C. Fung and M. V. Barton, Some Shock-spectra Characteristics and Uses, J. Appl. Mechanics, 25: 365-372(1958).

Chapter 4

DISCUSSION

The vault door was designed to remain elastic for the theoretical reflected-pressure loading consistent with an ideal (zero rise time) 100-psi incident overpressure. In the test, however, the ratio of rise time to natural period was approximately 3.8, and consequently the response factor was probably only slightly greater than unity.

The main vault behind the door and steel box frame was a $\frac{1}{2}$-in.-thick rectangular steel box enclosed in, and anchored to, an 18-in.-thick reinforced-concrete box. The steel-plate door box frame was designed to transmit the blast load on the door and door frame directly to the roof slab and foundation. An extension of the 18-in.-thick concrete side walls was continued toward the front of the structure. This was poured and anchored to the interior steel box and finished flush with the front wall. Anchorage of the 18-in.-thick concrete side-wall extensions to the steel door frame was by $\frac{3}{8}$-in. form ties only (Figs. 3.4, 3.5, and 3.6). Also the extensions were not connected to the concrete roof as were the side walls. Under these conditions it is probable that the high front pressures seeped into the joint at the interface of the concrete wall and steel box frame, causing the joint to widen with explosive force, tearing the concrete away from the steel box, and causing major damage to the side walls.

The separation of the reinforcing steel bars from the concrete, the separation of the concrete along the planes of the reinforcing bars, and the reduction of the concrete to debris with few breaks through the aggregate also indicated the poor adhesive qualities of the concrete in place. The damage might have been avoided completely had the front face joints been completely sealed to prevent the entrance of the high positive pressures.

The extensive damage to the concrete side walls demonstrated the value of the interior steel box in providing added protection to the interior of the vault. The instruments and movie camera in the vault were undamaged by the shock.

The roof slab and rear wall adequately resisted the blast load. The crack in the top surface of the foundation at the face of the vault indicated that a substantial part of the stabilizing effect of the front toe was developed.

Use of the latest design criteria rather than the methods available at the time of design of the test structure would not have significantly changed the structure design. The only addition necessary would have been the placement of a blast seal across the intersection of the door frame and the cantilevered extension of the side wall.

In view of the high prestress and the state of over-consolidation encountered in the soil survey, the probable natural static in-place stress-strain relations, failure strength, and shearing strength cannot be less than would be obtained under a lateral stress, P3, of 40 psi (Table 2.1). The residual lateral pressure of a soil is commonly taken to be 0.3 to 0.7 times the prestress. For the soils encountered here, the residual lateral pressure was in excess of 0.4 of the prestress. Theoretical studies and correlations of load-settlement relations from plate-bearing tests and from full-scale footings with triaxial test stress-strain relations obtained from undisturbed soil samples have shown that the estimated static failure stress under a footing can be at least 2.5 times the comparable laboratory triaxial failure stress.[1] This re-

sults from the natural confinement and restraint conditions afforded to lateral displacements by the natural soil mass surrounding a footing, which cannot be duplicated by a simple stress restraint of the lateral stress in a triaxial test. In addition, the confining and restraining influences of the surrounding earth surcharge above the level of the base may increase this value to 3.0 or more. When triaxial data were used for a lateral stress of 40 psi (2.88 tsf), the static failure stress on the footing was computed as 16 tsf × 2.5 = 40 tsf (see Appendix C). These postconstruction analyses indicated that the footing size could have been reduced.

Although foundation movements were not apparent on visual observation, comparison of the preshot and postshot surveys (Tables 3.9 and 3.10) indicates permanent vertical and horizontal displacements. The measured average permanent horizontal displacement of the vault (Table 3.9) was 0.152 ft (1.8 in.). A dynamic sliding and overturning analysis (Appendix D) based on the recorded pressures acting on the vault indicated a permanent horizontal displacement, relative to the ground, of 2.26 in. and a peak transient rotation of 0.00328 radians. This rotation corresponds to a relative vertical movement of 1.33 in. between the front and rear edges of the footing. The peak stress developed in the soil at the rear edge was computed as 150 psi.

Based on the free-field ground-shock environment data in the vicinity of the vault and the blast pressures acting directly on the above-ground portion of the structure in conjunction with the dynamic sliding and overturning analysis, it may be possible to roughly estimate the range of magnitude of absolute peak motions which the vault experienced. In the vertical direction the peak transient displacement of the vault was estimated to be equal to the peak free-field ground displacement at a depth corresponding to the bottom of the vault foundation, i.e., on the order of 2 to 3 in. downward. The permanent downward displacement was estimated as 0.2 to 0.3 in.

In the horizontal direction the upper bound of the peak transient displacement would be equal to the summation of the peak horizontal free-field ground displacement and the relative horizontal displacement of the vault with respect to the ground. It should be noted that relative motion of the vault caused by blast pressures acting directly on the structure and the motion due to the surrounding soil are not necessarily in phase, and therefore the actual peak absolute horizontal displacement would be less than the summation of these motions. A more rigorous dynamic sliding and overturning analysis could be accomplished, if needed, by considering the motion of the surrounding soil during the analysis.[2–4] Although the horizontal free-field displacement test data are limited, a reasonable estimate of the peak free-field horizontal displacement component is ½ of the peak vertical component, i.e., on the order of 1 to 1.5 in. outward from GZ. Thus the upper bound of the peak horizontal transient absolute displacement of the vault would be equal to this value added to the relative displacement of approximately 2 in. and would result in a total displacement of 3 to 3.5 in. Since the permanent free-field horizontal displacement can be estimated on the order of 10 per cent of the peak transient value, i.e., about 0.1 to 0.15 in., it is reasonable that the postshot survey, the dynamic sliding, and the overturning analysis would be of the same order of magnitude, the permanent free-field displacement being negligible compared to the 2 in. of vault motion relative to the ground. Thus the main permanent displacement of the vault was due to the vault sliding with respect to the ground.

Previous test data[5,6] have indicated that the peak accelerations for structures are generally attenuated from the free-field accelerations depending on the configuration and mass of the structure and on the stiffness of the structural components. The peak vertical acceleration of the vault foundation was estimated as the free-field acceleration of the soil under the foundation, which would be on the order of 10 g. In the horizontal direction the peak acceleration of the vault foundation may be estimated also at 10 g (although the horizontal component of acceleration is usually less than the vertical component for buried structures) since the high reflected and dynamic blast pressures acting directly on the vault reinforce the horizontal ground acceleration.

The gamma dosage at the vault obtained by interpolating the Project 39.1 chemical-dosimeter data (Table 3.7) was estimated at 194,000 r. Since the film dosimeters on the exterior of the vault were destroyed and the Project 39.1a film-dosimetry data between 410 and

1000 yd (slant distance) were not recovered, a second estimate is not available. It should be noted, however, that the gamma dosages recorded by the film badges (Fig. 3.17) were always greater than those measured by the chemical dosimeters (Fig. 3.16). The attenuation factor was computed as 0.0188, using 194,000 r as an exterior dose and 3650 r as the average interior dose (Table 3.6). For document storage an interior radiation level of the magnitude recorded would not be detrimental. However, if materials affected by radiation are included in the contents or if personnel protection were desired, additional shielding would have to be provided.

REFERENCES

1. D. M. Burmister, The Importance of Natural Controlling Conditions Upon Triaxial Compression Test Conditions, Am. Soc. Testing Materials Spec. Tech. Publ. No. 106, pp. 248-266, 1951.
2. E. Cohen and S. Weissman, Underground Shock Environment Data and Application to the Design of Underground Structures, in Proceedings of the 28th Symposium on Shock, Vibration, and Associated Environments, Bulletin No. 28, Part III, Office of the Secretary of Defense, Washington, D. C., September 1960.
3. E. Cohen and W. Weissman, Nuclear Ground Shock Effects in Relation to Hardened Design, in Symposium on Scientific Research in Protective Construction, Ernst-Mach Institut, Freiburg i. Br., Eckerstrasse 4, West Germany, September 1960.
4. S. Weissman et al., Nuclear Weapon Blast and Ground Shock Effects on Dynamic Response of Interior Components and Equipment in Underground Structures, in Proceedings of the 29th Symposium on Shock, Vibration, and Associated Environments, Bulletin No. 29, Part III, Office of the Secretary of Defense, Washington, D. C., July 1961.
5. J. F. Halsey and M. V. Barton, Spectra of Ground Shocks Produced by Nuclear Detonations, Operation Plumbbob Report, Project 1.9, WT-1487, August 1959. (Classified)
6. W. J. Flathau et al., Blast Loading and Response of Underground Concrete-arch Protective Structure, Project 3.1, Operation Plumbbob Report, WT-1420, June 1959. (Classified)

Chapter 5

CONCLUSIONS

Above-ground structures can be designed and constructed to survive the pressure levels experienced by this structure. The vault provided adequate blast and thermal protection for normal usage at the test peak incident-pressure level of approximately 87 psi, and the door withstood a peak pressure of 668 psi. The test vault resisted overturning and excessive sliding under the conditions of the test.

Although the concrete cover stripped, the steel box lining remained intact, and the test vault survived without damage to seals or welds, which demonstrated the additional safety afforded by the liner.

It is probable that the concrete stripped from the side walls because of the combined effects of the low pressure at the front-side portion of the walls and the high front-face pressure seeping into the joint between the concrete wall and the steel box frame of the door. The stripping effect can be overcome by sealing the joint.

The door is structurally and mechanically adequate for an equivalent static overpressure of at least 750 psi, and there is no reason to believe that it would not be adequate for an equivalent static load of 1000 psi. Although the exterior hardware was destroyed, the door was easily opened by a person familiar with its operation. It is recommended that the auxiliary dial housing be modified to make it blast resistant.

With the addition of a blast seal at the joint between the side walls and the door frame box, the vault should be structurally adequate for at least a 100-psi peak incident ideal or nonideal loading, regardless of weapon yield.

There was no apparent temperature rise in the vault.

Radiation measurements indicated that additional shielding would have to be provided if the vault were to be used to protect objects affected by radiation.

The peak transient motions of the vault due to ground shock and blast pressures were about equal. The permanent motions, however, were mainly the result of the blast pressure on the vault.

In connection with the blast loading, the following should be noted:

(1) There was a pronounced asymmetry in the blast wave between the various structures and the nearby free-field gauges.

(2) According to WT-1472, the high dust concentration close to the ground is a symptom rather than a cause of high dynamic pressure, which results from high mass velocity. This is justified by the high dynamic pressures, caused largely by air, which were observed at the 10-ft-level gauges. This high air velocity was transmitted later and incompletely to heavily dust-laden layers below.

(3) The spacial extent of the reflected pressure forward of the front of the structure is not adequately described by the dimensions of the structure. Mach number of the flow must also affect the distance to which reflected pressures will exert force on the footing.

For a more detailed description of the pressure phenomena on the vault and other above-ground structures, the reader is referred to WT-1472 (Ref. 1).

REFERENCE

1. J. R. Banister and L. J. Vortman, Effects of a Precursor Shock Wave on Blast Loading of a Structure, Report 34.1, Operation Plumbbob Report, WT-1472, August 1961.

Appendix A

AS-BUILT DRAWINGS

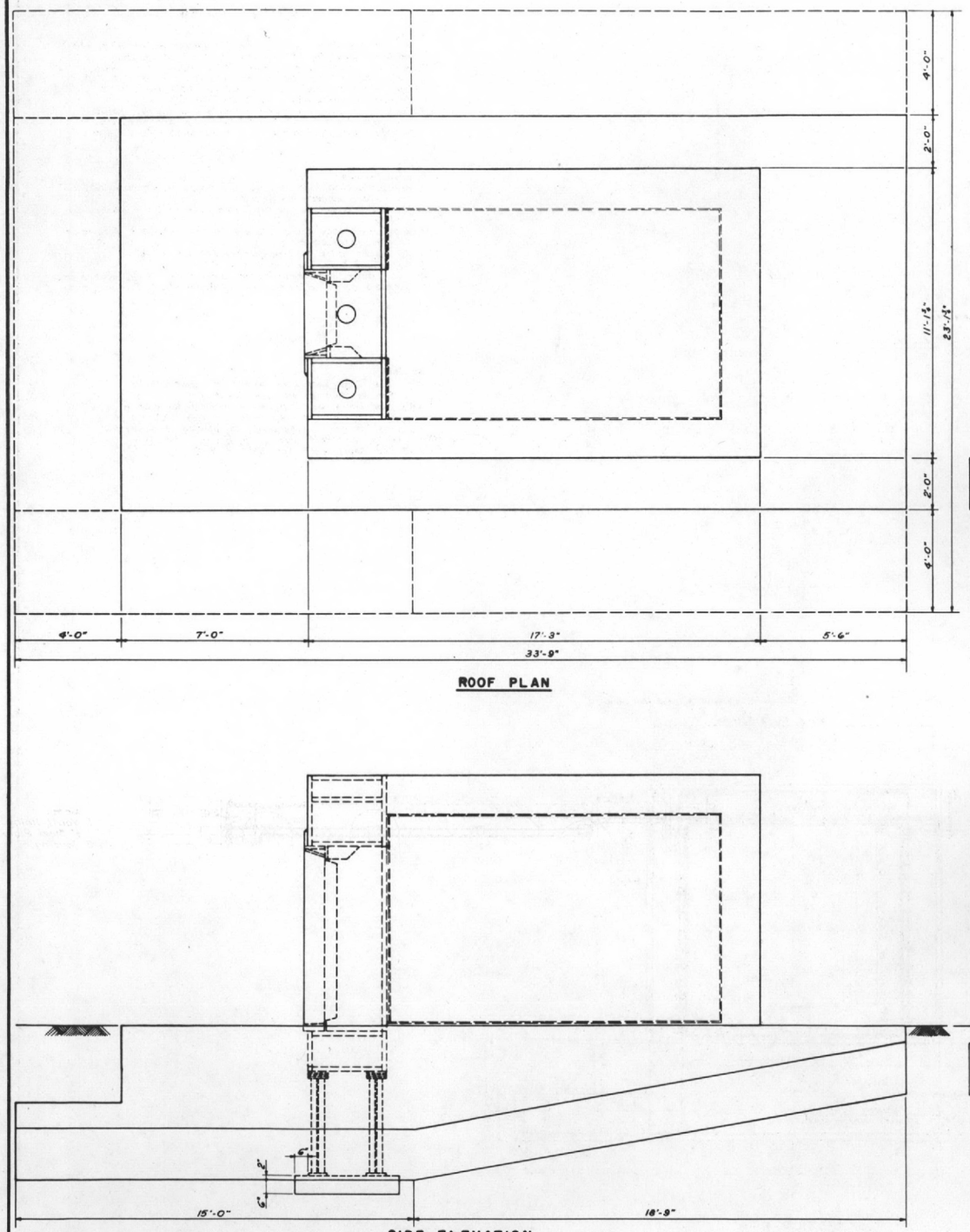

ROOF PLAN

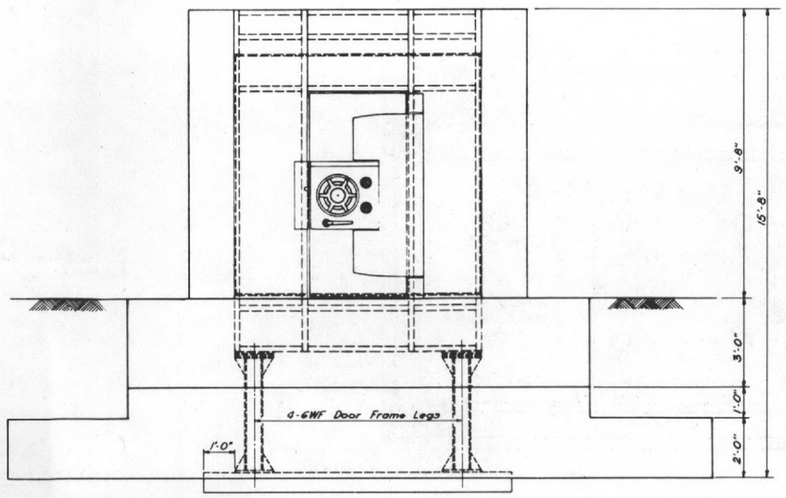

FRONT ELEVATION

SIDE ELEVATION

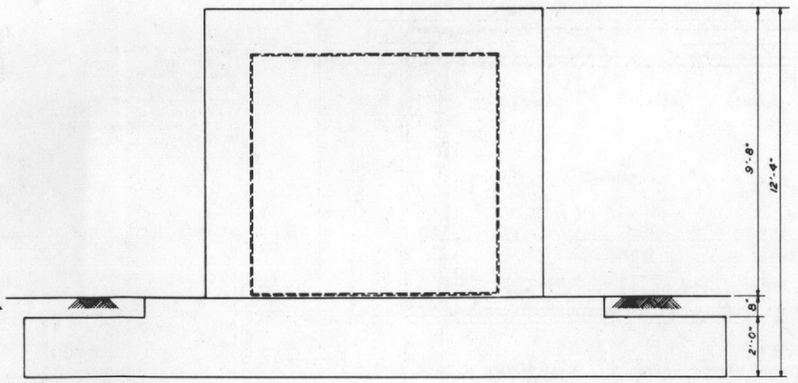

REAR ELEVATION

Fig. A.1—Roof plan and elevations.

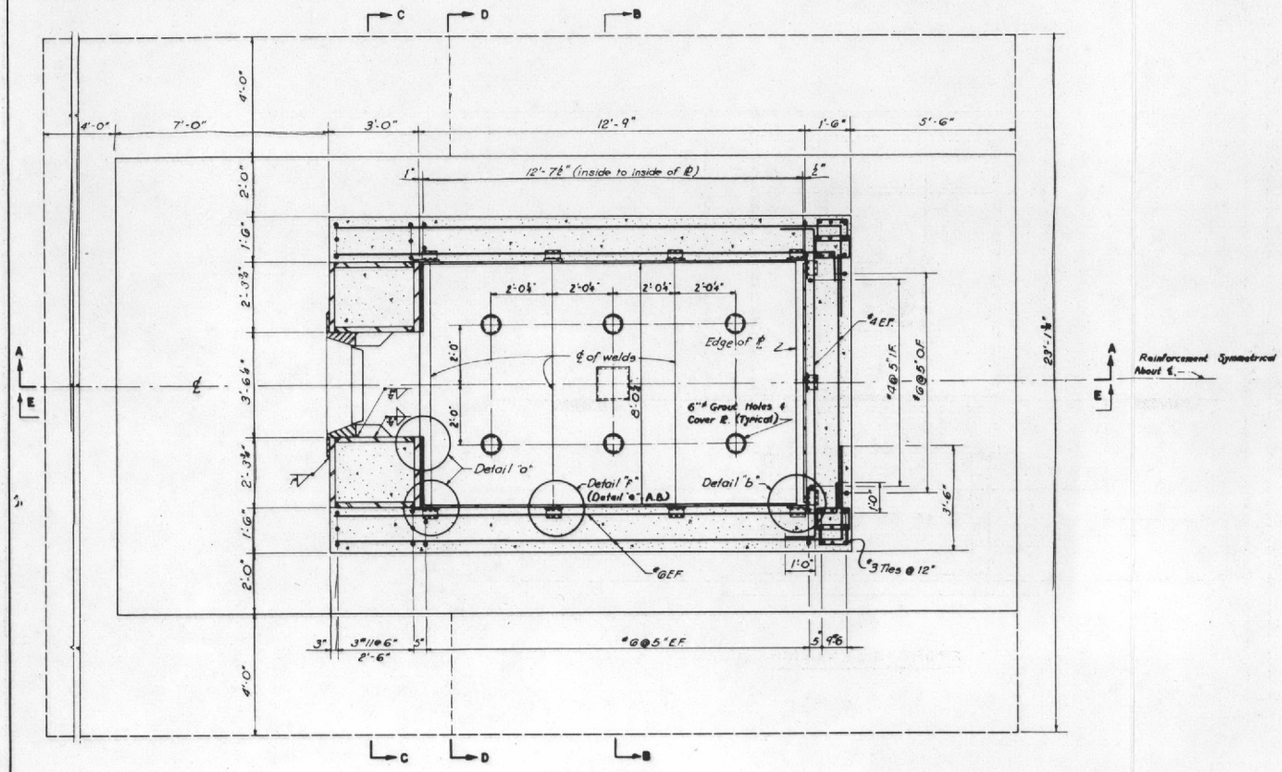

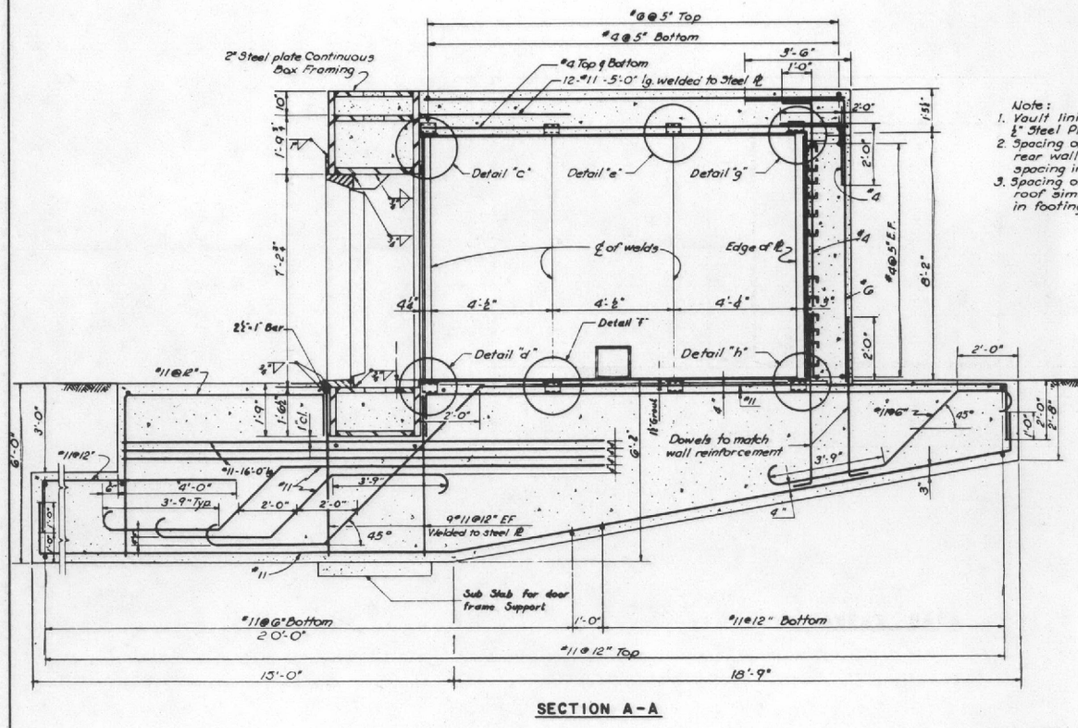

Note:
1. Vault lining to be ½" Steel Plate
2. Spacing of U clips in rear wall similar to spacing in side walls.
3. Spacing of U clips in roof similar to spacing in footing.

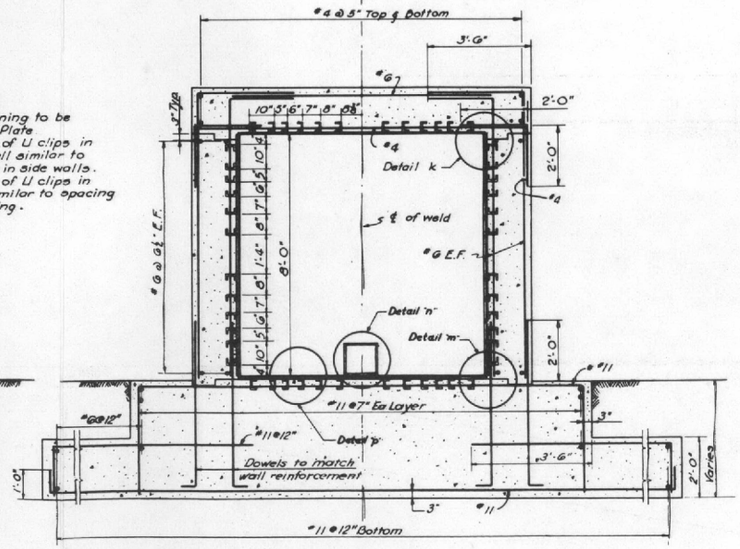

GENERAL NOTES

Material:
1. All concrete shall have a minimum compressive strength of 4,000 pounds per square inch at 28 days.
2. All reinforcing steel shall be intermediate grade. Deformation shall be in accordance with A.S.T.M. specification designation A305-53T and with Federal specification QQ-S-71a(3).
3. Structural steel, (including welds and bolts), shall conform to A.S.T.M. specifications designation A7-53T and to Federal specifications QQ-S-741a.

Miscellaneous:
1. All reinforcing laps and splices to be a minimum of 30 diameters except as noted.
2. Minimum cover for reinforcement is to be 2" except as noted.
3. Wall and Floor Slab Plates to be installed subsequent to concrete pouring.
4. All welds to be continuous except as noted.
5. See sheet 3 for Sections C-C & D-D
6. Vault door, door box frame, steel plate lining, lockers and accessories to be fabricated by Mosler Safe Company.

As Built:
A.B.1 Zee Clips were used instead of Channel Clips. For As Built Details see Sheet 7 of 7.
A.B.2 Door Frame was installed subsequent to pouring of concrete foundation. Wall and floor slab plates was installed subsequent to pouring of concrete walls and roof slab.
A.B.3 See Sheet 4 of 7 for Section E-E.

Fig. A.2—Floor plan and sections.

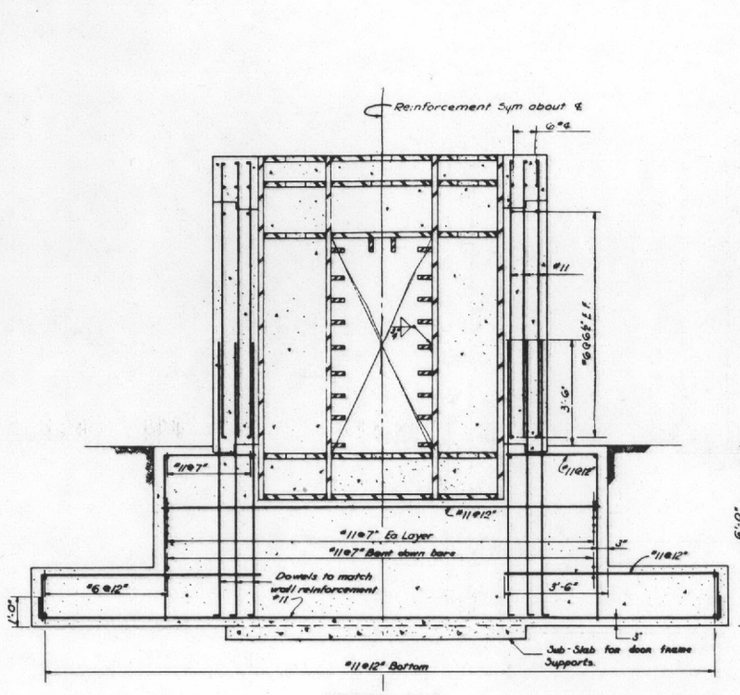

SECTION C-C

SCALE: $\frac{1}{2}$"=1'-0"

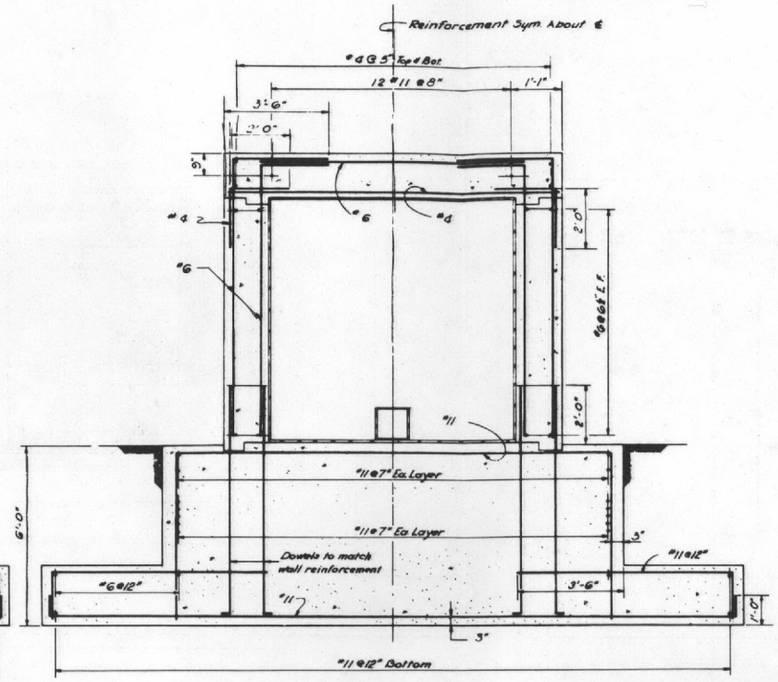

SECTION D-D

SCALE: $\frac{1}{2}$"=1'-0"

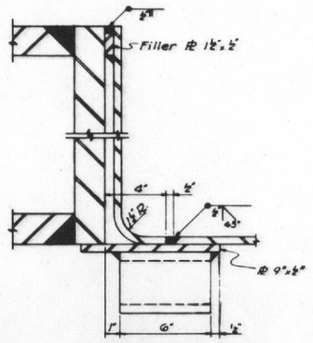

DETAIL "a"

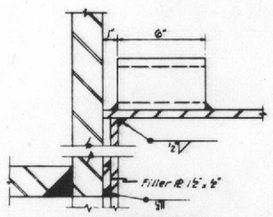

DETAIL "c"

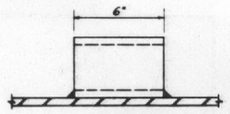

DETAIL "e"

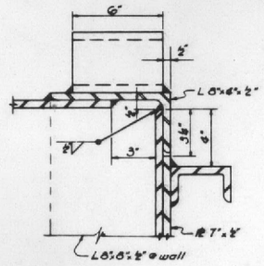

DETAIL "g"

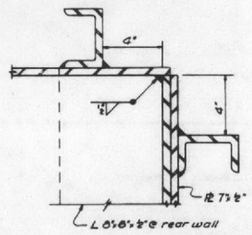

DETAIL "k"

SCALE: 3"=1'-0"

NOTE:
1. All channels 6"x2" @ 13.8
2. All welding of channels to plates are ¼" Fillet shop welds.

As Builts:
A.B.I. Tee Clips were used instead of Channel Clips. for As Built Details See Sheet 7 of 7

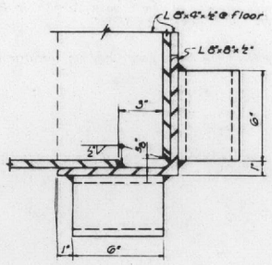

DETAIL "b"

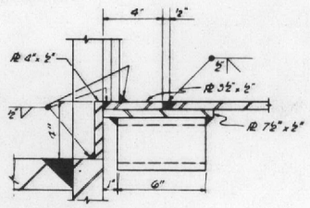

DETAIL "d"

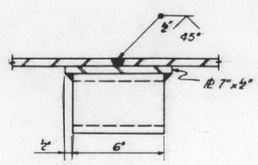

DETAIL "f"

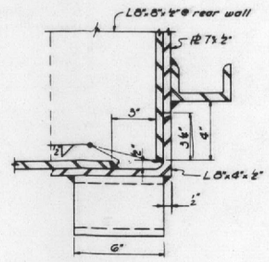

DETAIL "h"

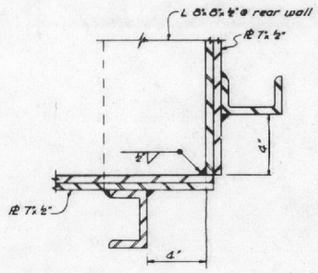

DETAIL "m"

SCALE: 3"=1'-0"

Fig. A.3— Sections and details.

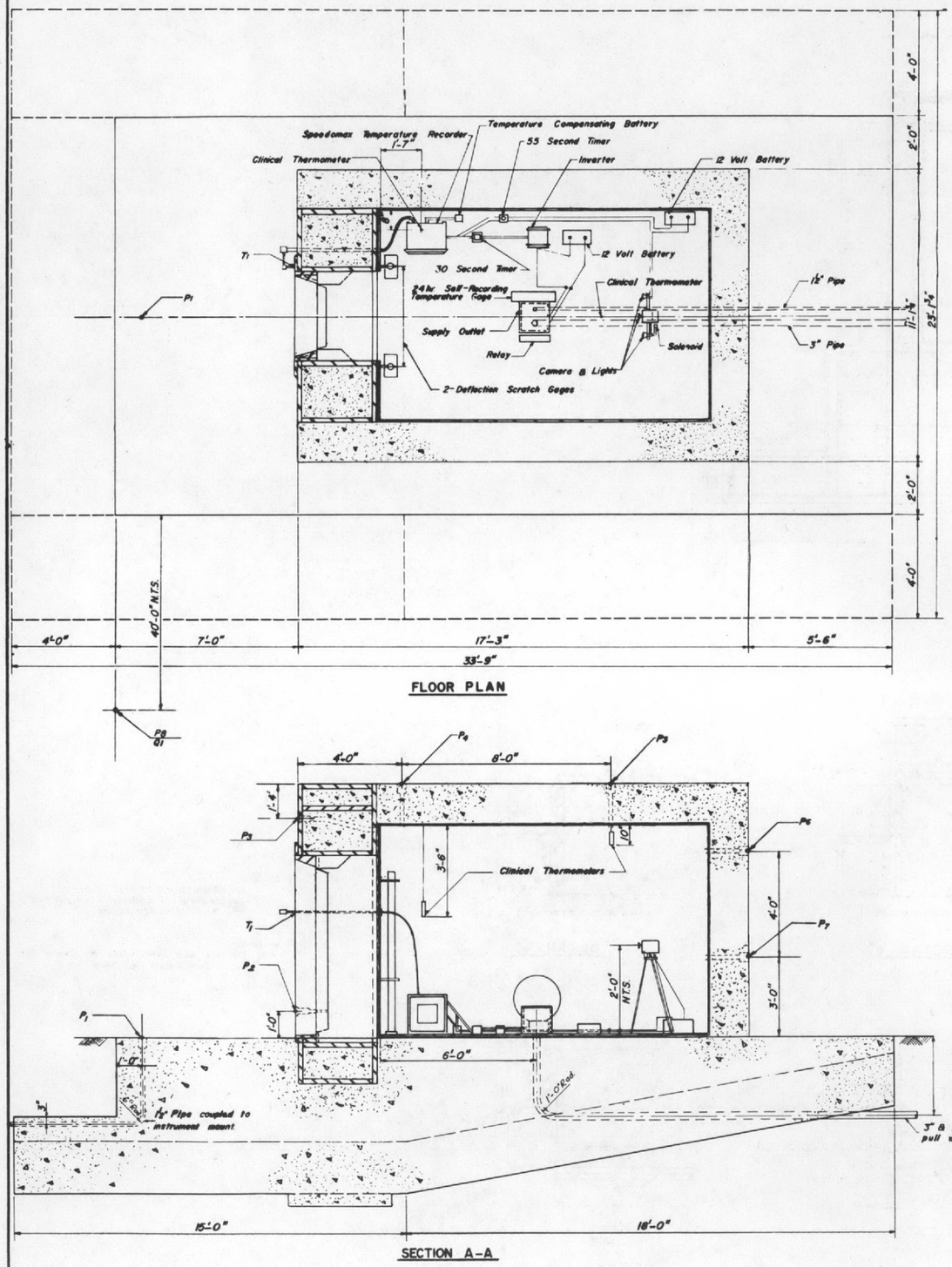

FLOOR PLAN

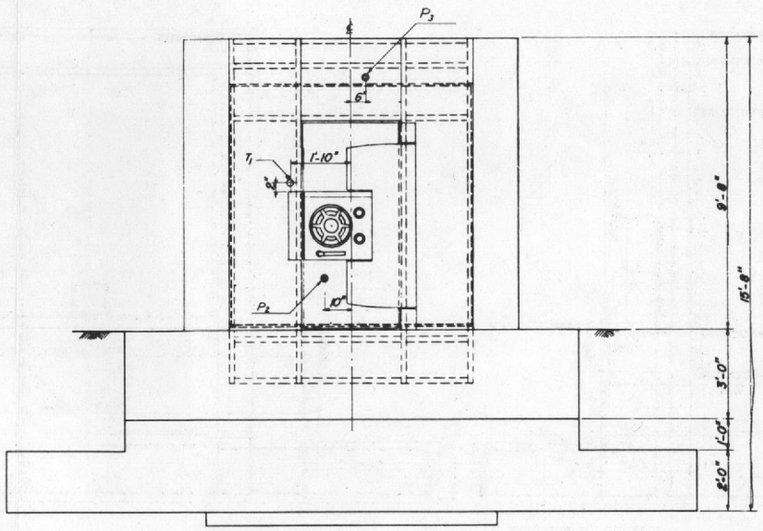

FRONT ELEVATION

SECTION A-A

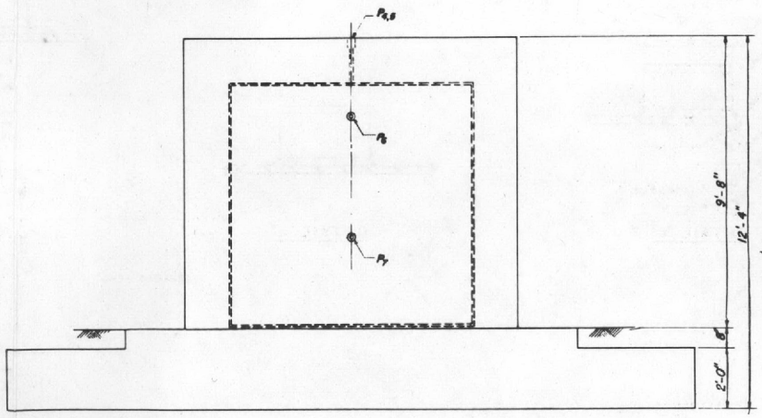

REAR ELEVATION

NOTES

1. Pressure gages are indicated (P).
2. Dynamic pressure gages are indicated (Q).
3. Thermocouples are indicated (T).
4. All pressure gages to be Wacko electronic gages.
5. Gages P8 & Q1 may be omitted if equivalent free field gages are to be installed by other projects.
6. Pressure gage mount at each gage location to be of the type used by Sandia Corporation.

AS BUILT:

A.B.I. All instrumentation as shown were used in construction.

Fig. A.4—Instrumentation.

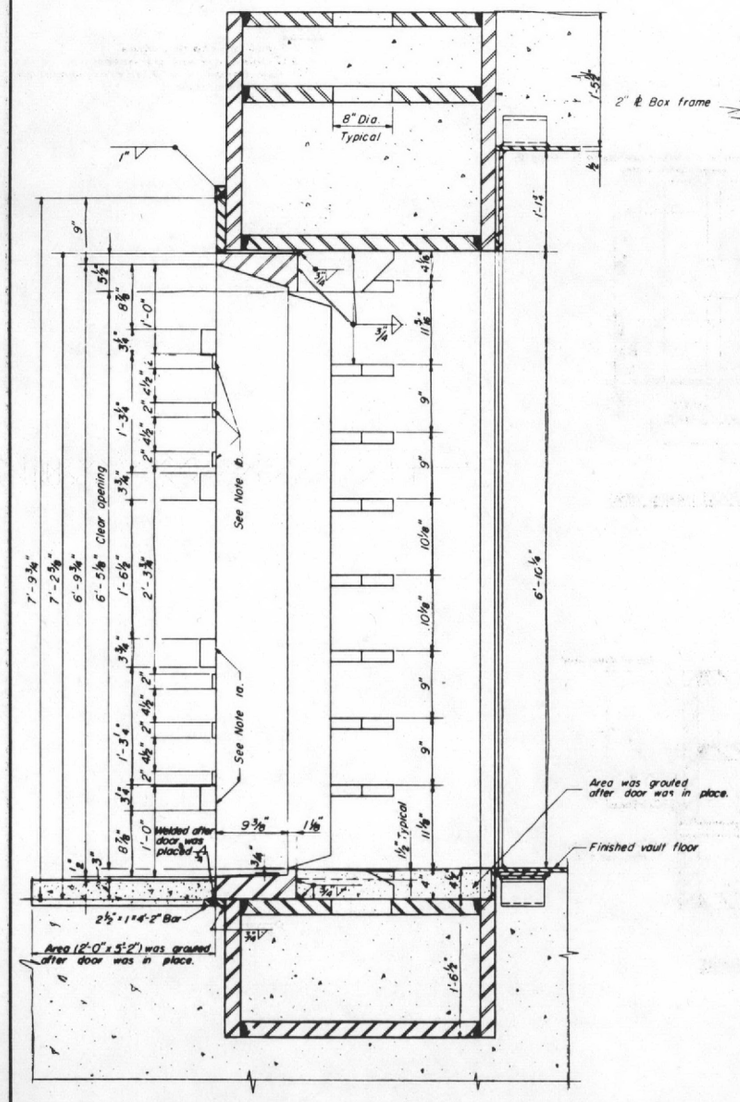

VERTICAL SECTION THROUGH DOOR FRAME

SCALE: 1½" = 1'-0"

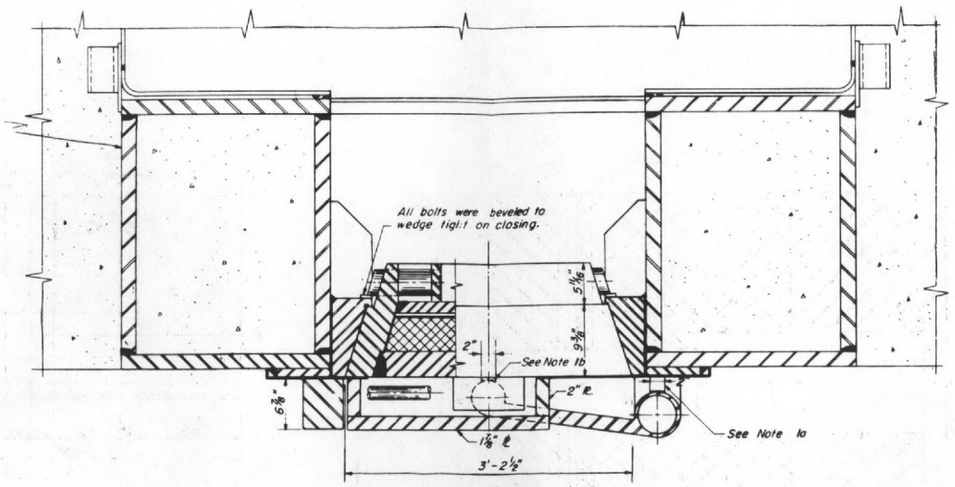

HORIZONTAL SECTION THROUGH DOOR & FRAME

SCALE: 1½" = 1'-0"

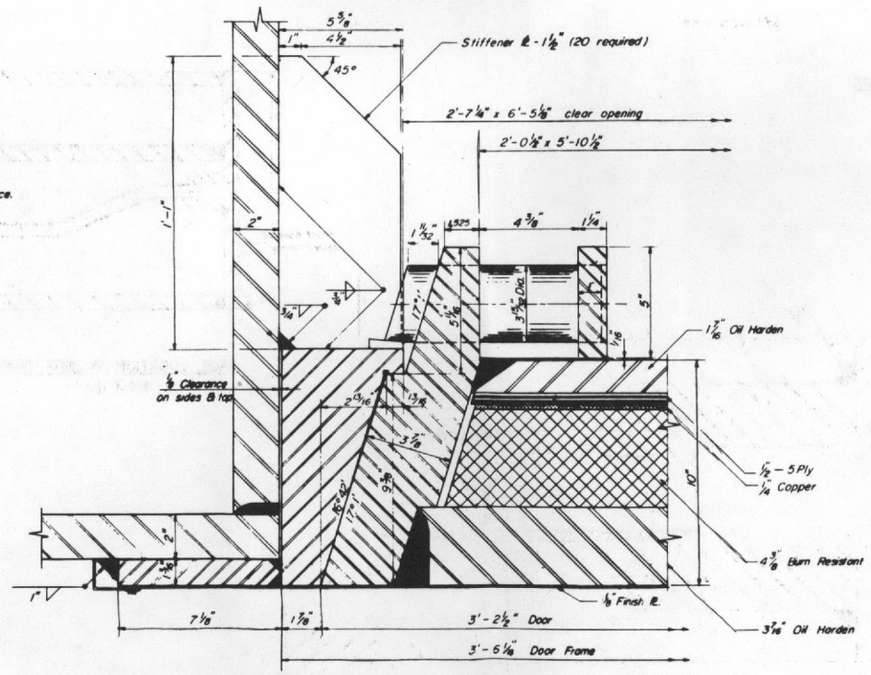

TYPICAL SECTION THROUGH TOP & SIDES

SCALE: 1" = 1"

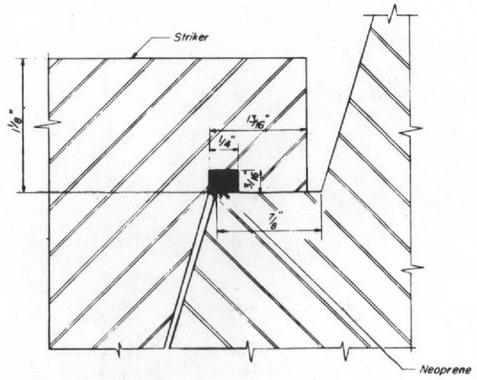

TOP & SIDE STRIKERS

SCALE: 2" = 1"

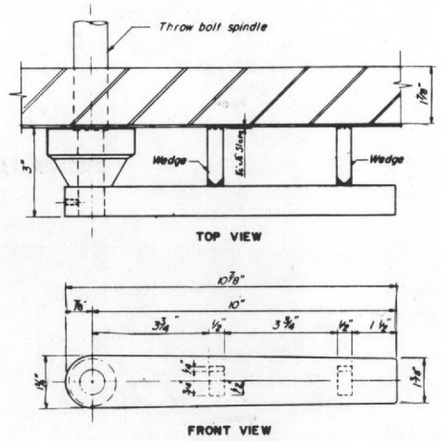

LATCHING HANDLE WITH STIFFENERS

SCALE: 1" = 1"

NOTES

1. Hinge Assembly Stiffeners:
   (a) Jamb hinge tube: 4 Stiffeners required, spacing as shown. Stiffeners at jamb blocks: 2" x 1¼" or equivalent bearing area. Intermediate stiffeners: 2" x 3⅜" or equivalent bearing area. Clearance — 0.1" maximum.
   (b) Door hinge tubes: 6 Stiffeners required, 3 each hinge, spaced at ends and center of hinge, (Spacing shown in Vertical Section Thru Door & Frame
   All stiffeners 2" x 2" or equivalent bearing area.
2. All door and frame welds full penetration except as noted.
3. All welds were continuous shop welds except as noted.

Fig. A.5—Modified details for a standard C-10 door.

NOTES:
1. Break all sharp edges.
2. ▽ Finish except as noted.
3. See Sheet 4 of 7 "Instrumentation" for gage locations.

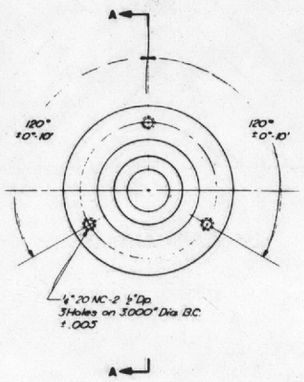

PLAN

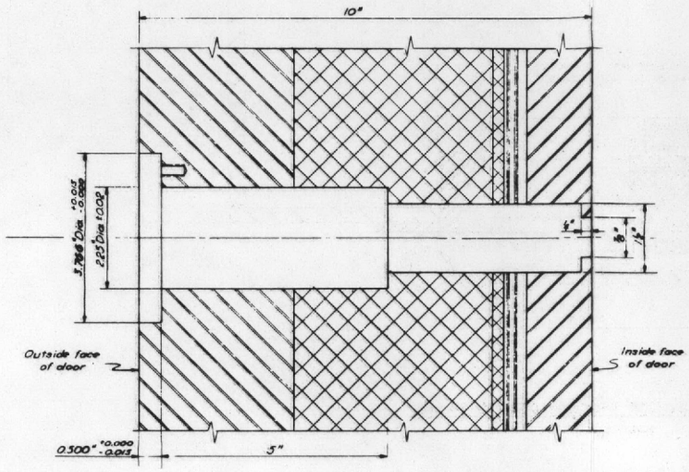

SECTION A-A

PRESSURE GAGE MOUNT IN VAULT DOOR
SCALE: $\frac{3}{4}$" = 1"

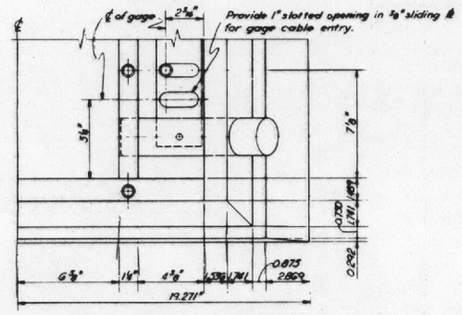

GAGE LOCATION IN VAULT DOOR (INSIDE VIEW)
SCALE: 3" = 1"

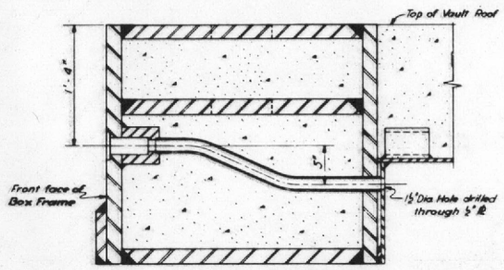

GAGE LOCATION IN BOX FRAME
SCALE: 1½" = 1"

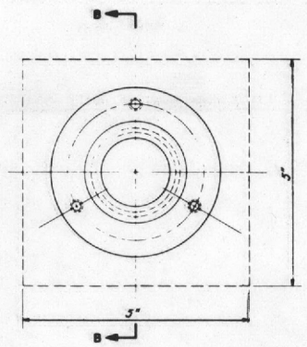

PLAN

(Similar to Plan at Vault Door except as noted)

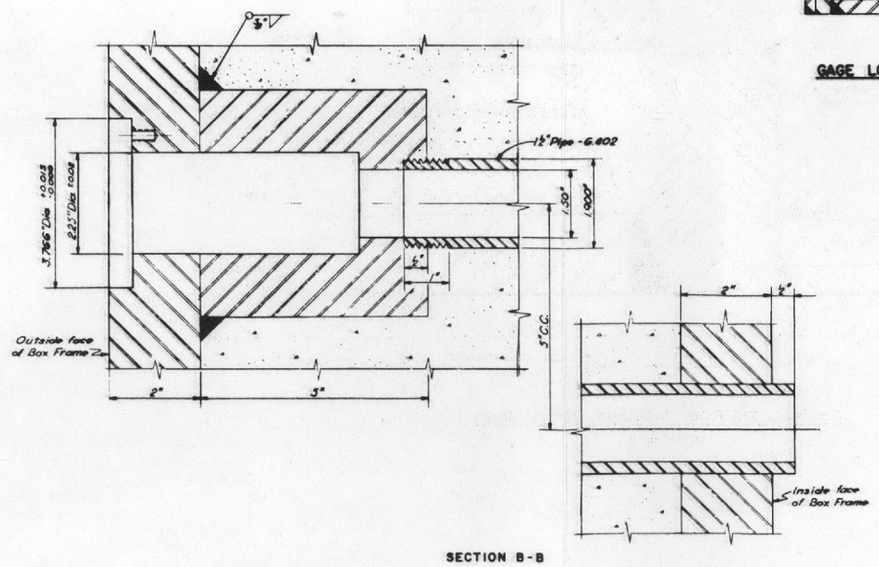

SECTION B-B

PRESSURE GAGE MOUNT IN BOX FRAME ABOVE VAULT DOOR
SCALE: $\frac{3}{4}$" = 1"

Fig. A.6—Modified details for a standard C-10 door.

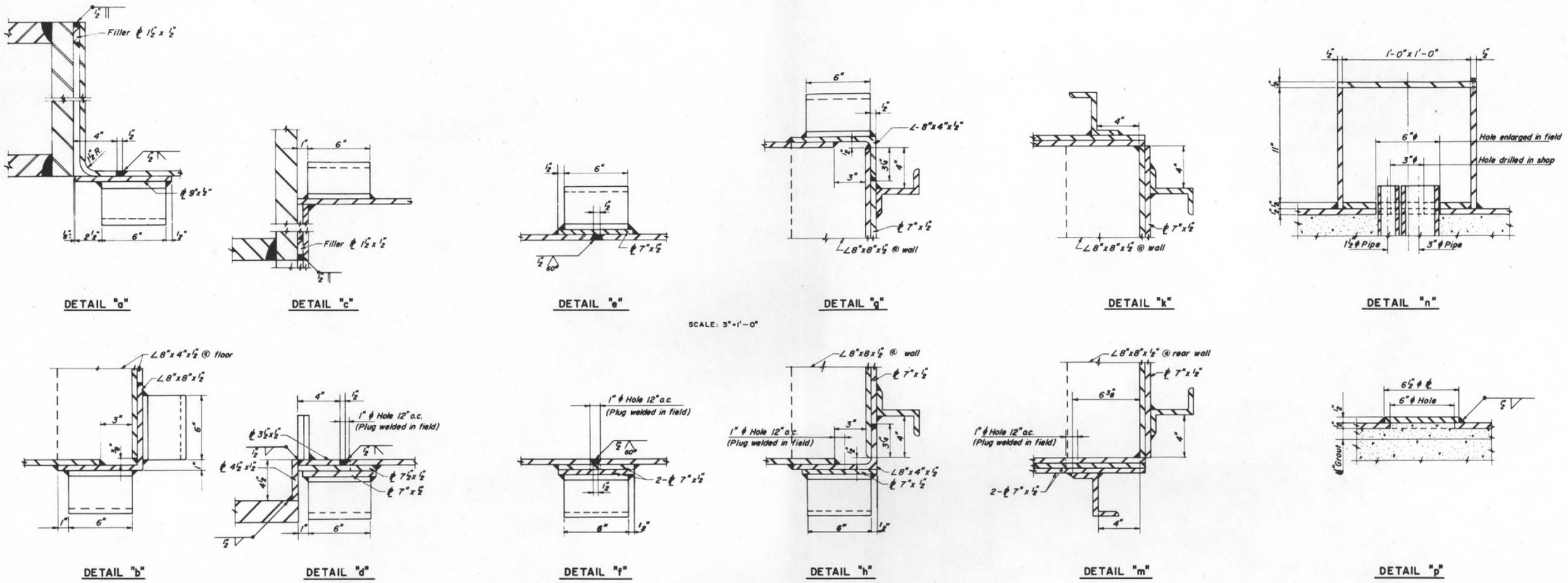

NOTE:
1. All zee clips are 4 ⌐ 15.9
2. All welds are ¼" fillet shop welds except as noted.

Fig. A.7—As-built details.

Appendix B

CONSTRUCTION

B.1 GENERAL

All work was done under contract to the U. S. Atomic Energy Commission. The contractor for the construction of the reinforced-concrete vault and for the installation of the steel vault door was the Sierra Construction Co. of Las Vegas, Nev. Reynolds Electrical and Engineering Co., Inc. (REECO) supplied the concrete aggregate and miscellaneous work required to make the structure ready for the test. Holmes and Narver, Inc., provided over-all supervision and coordination as field representatives of the AEC.

The OCDM, under whose sponsorship the test structure was built, was continuously represented at the site by an Ammann & Whitney field representative and by an erector from the Mosler Safe Co. These field representatives provided inspection and advisory services for the construction groups. This service was supplemented by visits to the site at critical times by the Project Officer.

Construction, in general, was geared to a very rapid time schedule. The schedule called for a maximum of 75 calendar days from Feb. 22, 1957, for the completion of the structure. Excavation was started on February 27, and the backfilling was scheduled to be completed on May 7. This schedule was adhered to even though problems developed during construction. These problems are more fully defined in Secs. B.3.1 through B.3.7 of this report.

Figures B.1 through B.19 are photographs of the reinforced-concrete vault at various stages of construction. These photographs show the progress made on this rather unusual test structure. Deviations from the drawings and specifications are recorded in Appendix A, As-built Drawings. Table B.1 indicates the schedule adhered to during the construction phase of the operation.

B.2 MATERIALS

B.2.1 Concrete

Concrete was mixed at a central mixing plant operated by REECO. The plant was a permanent batch type installation and was located approximately 5 miles from the structure. The concrete was trucked to the structure by conventional transit-mix trucks. During transportation the concrete was in a dry state, and, after it arrived at the construction site, the mixing water, as predetermined by the concrete design, was added to the dry mix. The concrete was placed by one and/or both of the following methods: (1) by dumping it into a $\frac{3}{4}$-cu yd bucket and placing by crane or (2) by placing it directly with concrete chutes. Hunt's paraffin-base curing compound was used for curing the concrete.

A total of six standard 6- by 12-in.-cylinders were taken from the structure for the 7- and 28-day tests.

TABLE B.1—SCHEDULE OF CONSTRUCTION

Item	Concrete pours		Exterior forms		Steel
	Date	Quantity, cu yd	Placed	Stripped	placed
Foundation	4/12/57	108	3/11/57	4/18/57	4/10/57
Walls	4/25/57	29	4/20/57	4/30/58	4/19/57
Roof slab	4/25/57	60		4/30/57	4/19/57
2-in. door frame					4/4/57
½-in. steel lining					4/15/57
10-in. steel door					5/7/57

TABLE B.2—LABORATORY CYLINDER-TEST RESULTS

Member	Test results, psi	
	After 7 days	After 28 days
Foundation slab	3160	4230
		4210
Walls and roof slab		4520
		4270
		3840
Av.	3160	4214

The results of the concrete-strength tests are contained in Table B.2, and Table B.3 gives the typical concrete-mix design used during construction.

B.2.2 Concrete Components

(a) *Cement.* The cement used for the construction of the reinforced-concrete vault was type II Portland cement. Batching was by bulk.

(b) *Coarse Aggregate.* The coarse aggregate, 1½-in. graded aggregate, was stock-piled at the batching plant. Owing to the handling procedure and transportation methods employed in moving the aggregate from the crusher to the batch plant stock pile, segregation of the aggregate was evident in the stock pile and batched concrete. Site conditions and limited time allowed for construction were the major causes of the poor handling and segregation.

(c) *Fine Aggregate.* The fine aggregate had additional wind-blown fines not indicated in Table B.3. These fines were caused primarily by adverse weather conditions at the Nevada Test Site (NTS).

B.2.3 Concrete Forms

Exterior-wall and roof-slab forms consisted of plywood panels from ⅝- and ¾-in.-stock. Dimension stock for studs was 2 by 4 in. The interior forms consisted of the steel-plate lining referred to in Sec. B.3.4. The exterior forms were held in place by welding ⅜-in. threaded tie rods to the plate lining at a spacing of approximately 3 ft on centers and then connecting the wood forms to the ties.

B.2.4 Reinforcing Steel

Reinforcing steel used in the structure was of intermediate grade. The fabrication of the steel was subcontracted by Sierra to Fontana Steel Co. Specimens of the bars were kept for future tests. The specific location of the bars from which the specimens were taken was noted.

TABLE B.3—TYPICAL CONCRETE-MIX DESIGN

Sieve size	Per cent passing U. S. standard sieve: Fine aggregate	Coarse aggregate	Combined
1.5 in.		100.0	100.0
¾ in.		59.0	76.4
⅜ in.		11.6	49.2
4	100.0	1.4	43.3
8	78.8		33.5
16	57.0		24.2
30	32.9		14.0
50	17.9		7.8
100	4.3		1.8
F. M.	3.091	7.280	5.498
Specific gravity (S. and S.D.)	2.47	2.665	

Mix design for one cubic yard of concrete is 4500 psi.
Absolute volume of aggregate in one cubic yard of concrete—19.22 cu ft.
Weight of one cubic yard batch of aggregate—3243 lb.

	Per cent	Batch wt., lb		Absolute vol., cu ft
Gravel			2100	12.11
Sand, dry	38	1095		7.11
Free water in sand, 5.76 gal	4.35	48		0.77
		1143	1143	
Water, added 27.4 gal			228	3.66
Cement, 7.0 sacks			658	3.35
			Total	27.00

Maximum slump = 5 in.

TABLE B.4—RESULTS OF LABORATORY REINFORCEMENT TEST

Nominal size	Deformation	Yield stress,* psi	Ultimate stress, psi	Elongation,† %
No. 4	Kaiser	53,316	80,612	19.5
No. 6	Kaiser	47,510	78,732	18.8
No. 8	Kaiser	50,829	81,007	18.8
No. 11	Kaiser	51,184	82,867	21.1

* Average yield = 50,710 psi.
† Percentage of elongation is based on an 8-in.-specimen.

These specimens, totaling four in all, were tested by the Los Angeles Testing Laboratory, Los Angeles, Calif.

All reinforcing steel was cut and bent in the shop and then transported by flat-bed trucks to the structure. On the whole, the bending operation was adequate. Placement of the reinforcement in the field compared favorably with the reinforcing details shown on the drawings.

The yield and ultimate stresses and the percentage of elongation of the 8-in. reinforcement specimens tested by the Los Angeles Testing Laboratory are given in Table B.4.

B.2.5 Structural Steel

Structural steel was fabricated by the Mosler Safe Co. of Hamilton, Ohio. The structural steel was transported from the fabrication shop in Ohio by rail to Las Vegas, where it was transferred to flat-bed trucks and shipped to NTS. The structural steel consisted essentially of the ½-in.-thick plate lining; the door frame which was made up of 2-in.-thick plates; one 10-in.-thick vault door; and miscellaneous erection items. All the above items arrived at NTS in good condition. Figures B.20 and B.21 are photographs of the structural steel on a low-boy trailer prior to, and during, the unloading operation at NTS, respectively.

B.3 CONSTRUCTION OF THE STRUCTURE THROUGH ITS COMPONENT ITEMS

B.3.1 General

The following sections deal with the procedures used in the construction of the component items of the structure and with the resulting conditions at the completion of the construction phase of the operation. Also included in this section are all deviations from the drawings and specifications and any additions that were deemed necessary to complete the structure in a satisfactory manner.

B.3.2 Excavation

The soil condition at the forward site was a clayey silt material. A full description of the soil is given in Appendix C. The predominant characteristic of the soil in relation to the excavation was its ability to maintain a vertical cut without shoring. This characteristic of the soil made it possible to excavate a minimum working area using conventional back-hoeing equipment. All excavation proceeded as scheduled.

B.3.3 Foundation

When approximately one-half of the steel for the foundation had been placed, a change order was received outlining the revised fabrication and installation of the door frame and vault lining. The revised details indicated a base slab to be placed under four I-beam legs of the door frame. (See Fig. A.1 for the location of the slab.) It was therefore necessary to move and/or remove some of the reinforcement that had been placed so that an area of approximately 10 ft by 3 ft by 8 in. deep could be excavated under the center portion of the steel frame. Once the reinforcement was in place, the door frame was placed in position, and the main footing was poured.

B.3.4 Door Frame and Steel Lining

The 14-ton steel door frame was placed and shimmed to the correct elevation prior to the placement of the foundation concrete. The door frame as originally contracted for construction was to be welded in the field (Fig. A.3). Because of the more favorable working conditions, it was decided to weld it in the shop and ship it as a unit. Four I beams, as described in Sec. B.3.3 and shown in Fig. A.1, were used as construction supports until the foundation could be poured. When the I beams arrived at NTS, it was found that they were of such a length that the frame would be located at a height less than the elevation required by the drawings. Shims were therefore placed between the legs and the frame and welded into position. The frame was braced for wind loading prior to the placement of the footing. Two No. 11 reinforcing bars, one on each side of the structure, were welded at one end to the top of the frame and at the other end to the reinforcement at the rear of the foundation. Figure B.4 is a photograph of the wind bracing for the frame. The reinforcement, as indicated on the drawings, was welded to the frame.

The 7-ton ½-in.-thick plate lining was placed in two operations. The first operation consisted in placing the Z-shear connectors, as shown in Detail F, Fig. A.7, and in Fig. B.6, prior to pouring the foundation. The additional portion of the lining was placed after the base slab

was completed and all required field welding was accomplished. Just prior to placing the lining, it was found necessary to enlarge the hole in the center of the floor plate to provide access for a 1½-in. instrumentation conduit. Under the lining there remained a 1½-in. space that was to be grouted at a later date.

Figure B.8 is a photograph of the plate lining being placed, and Fig. B.22 shows sections through the door and the door frame.

B.3.5 Concrete Walls and Roof

When the frame and lining had been set, the reinforcement and forms were placed for the walls and roof. All reinforcement sizes and placements conformed with the details shown in Appendix A.

B.3.6 Vault Door

The 10-in. vault door was the last major item installed in the structure. The secondary door frame was welded to the stiffener plates, as shown in Fig. A.5. Before the foundation concrete was placed, it was necessary to box out a 2-ft 0-in. by 5-ft 2-in. by 2½-in. section of the foundation in front of the door proper. At this time a 2½-in. by 1-in. by 4-ft 2-in. steel bar was welded to the main door frame. This bar facilitated the installation of the door at a later date.

B.3.7 Miscellaneous Items

After the door had been installed, the areas in front of, and behind, the door and under the steel lining were grouted. A wooden frame was constructed around the steel door to protect it from the wind and construction personnel before the test operation. A 3-psi air test was performed on the interior of the vault to check the plate-lining welds for leakage. All leaks that were found during the air test were rewelded. Instrumentation mounts and conduits were placed prior to concrete placement.

B.4 SUMMARY

When the backfilling had been completed, the instrumentation as described in Sec. 2.3 was installed. All mechanical parts and the door as a whole were placed in good working condition. All construction debris was removed from the site. The wooden frame around the door was removed before the test operation.

Fig. B.1—Placement of base-slab reinforcement.

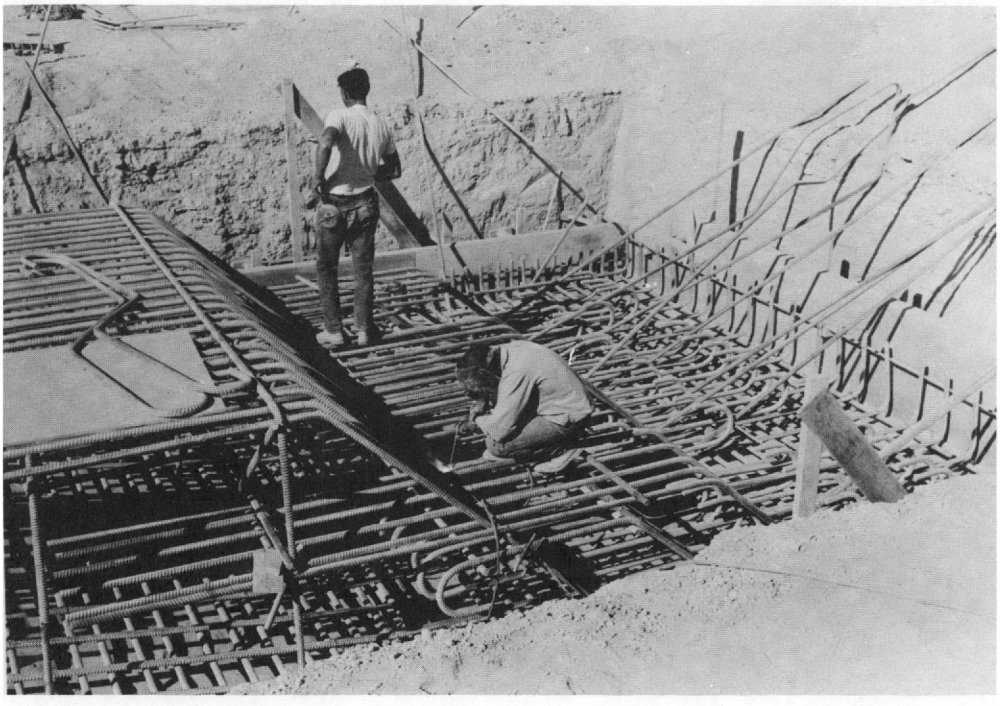

Fig. B.2—Placement of base-slab reinforcement.

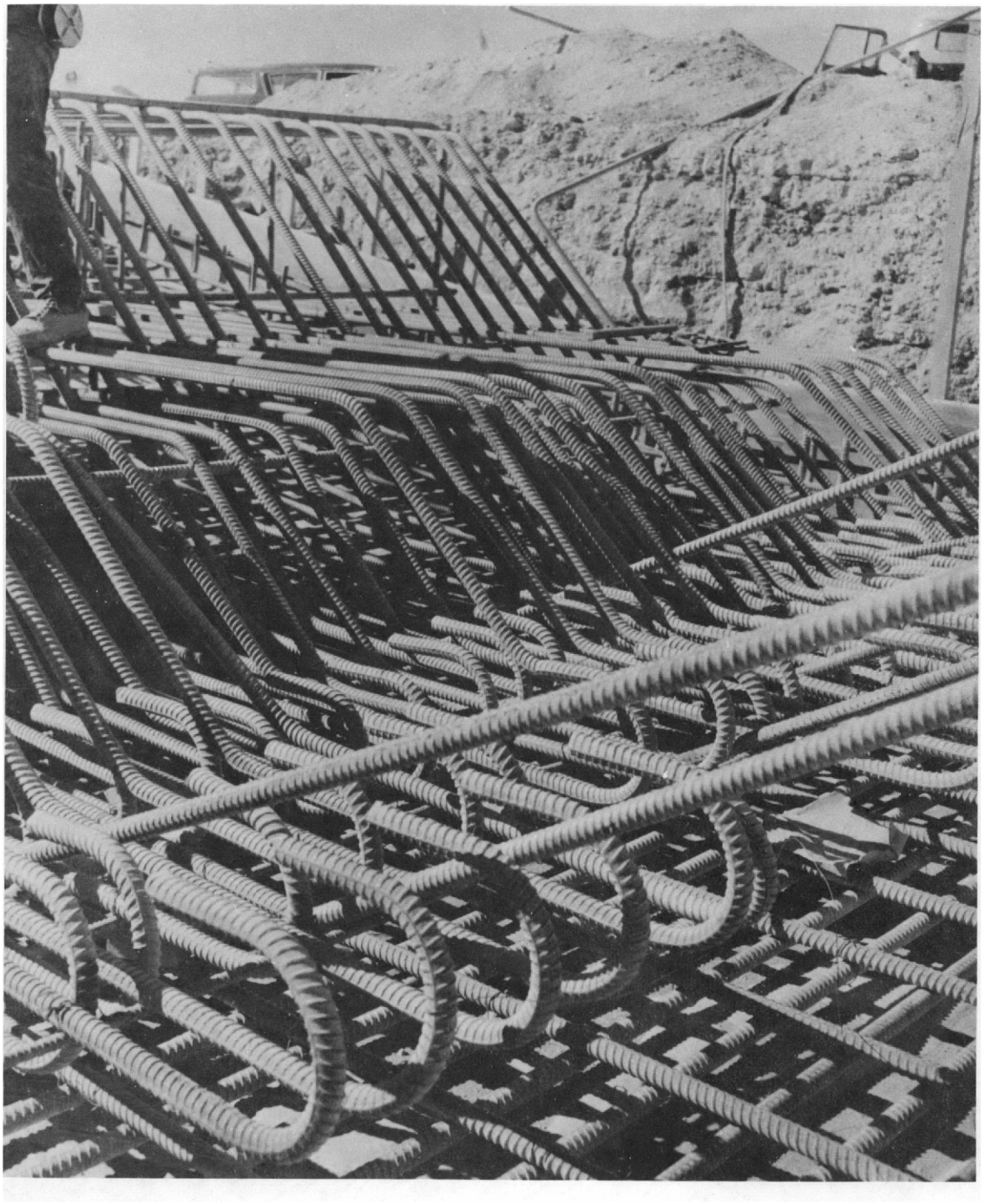

Fig. B.3—Detail of base-slab reinforcement.

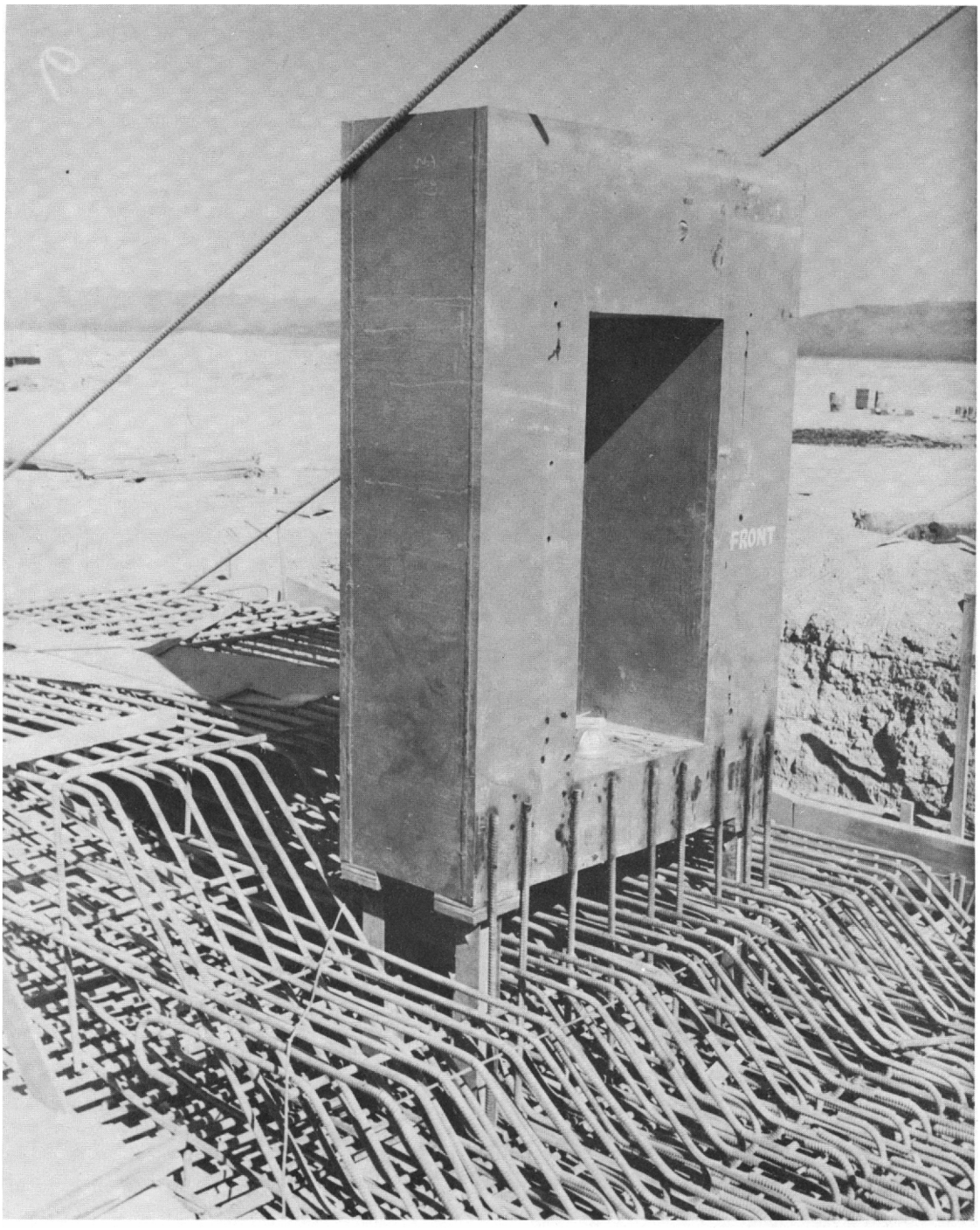

Fig. B.4—Base slab with door frame in place. Note wind bracing.

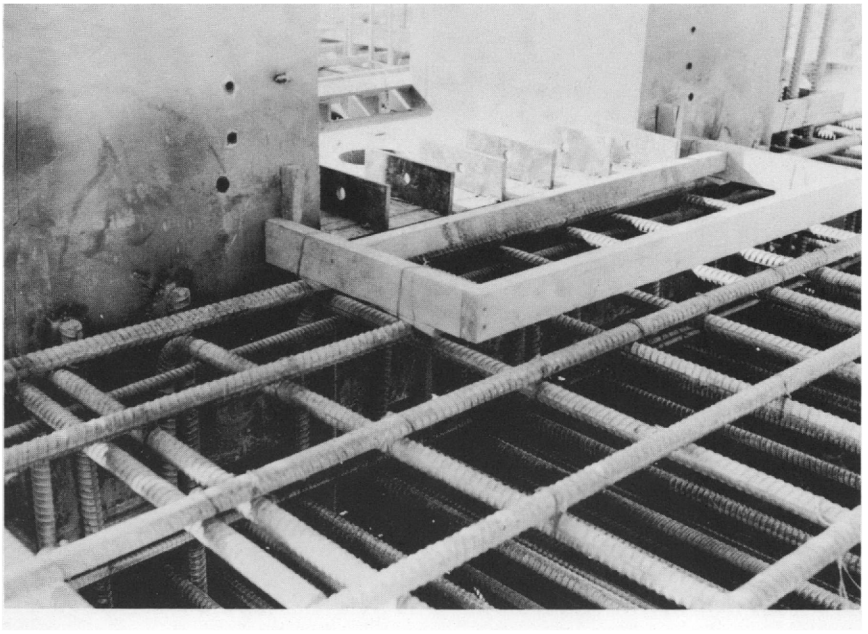

Fig. B.5—Detail in front of door frame.

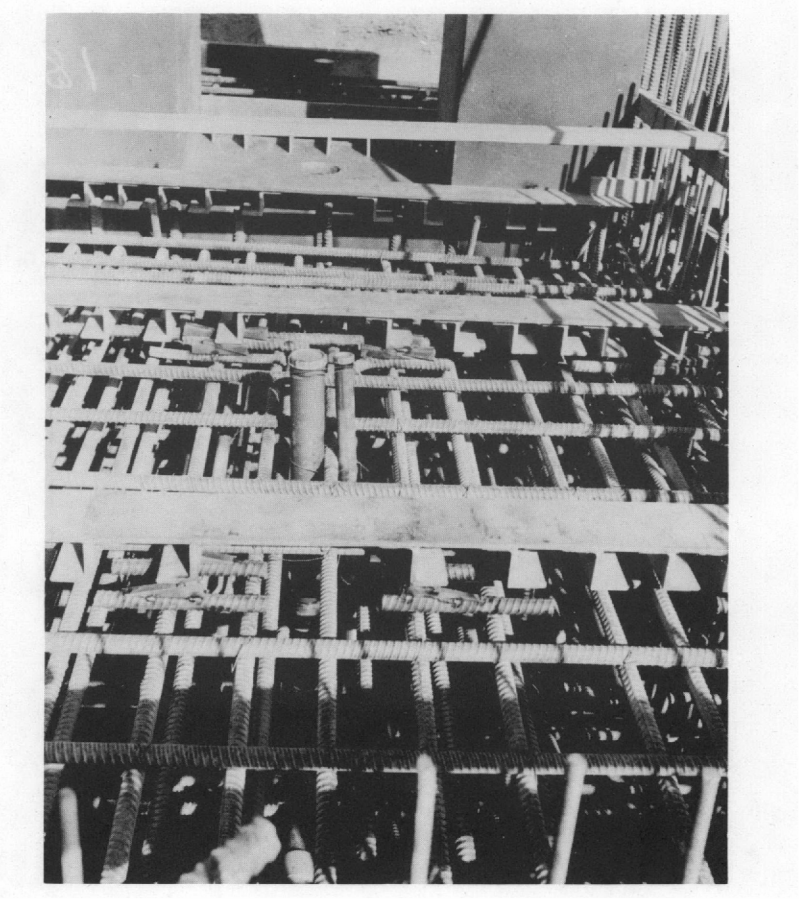

Fig. B.6—Base-slab reinforcement inside vault area. Note Z shear connectors.

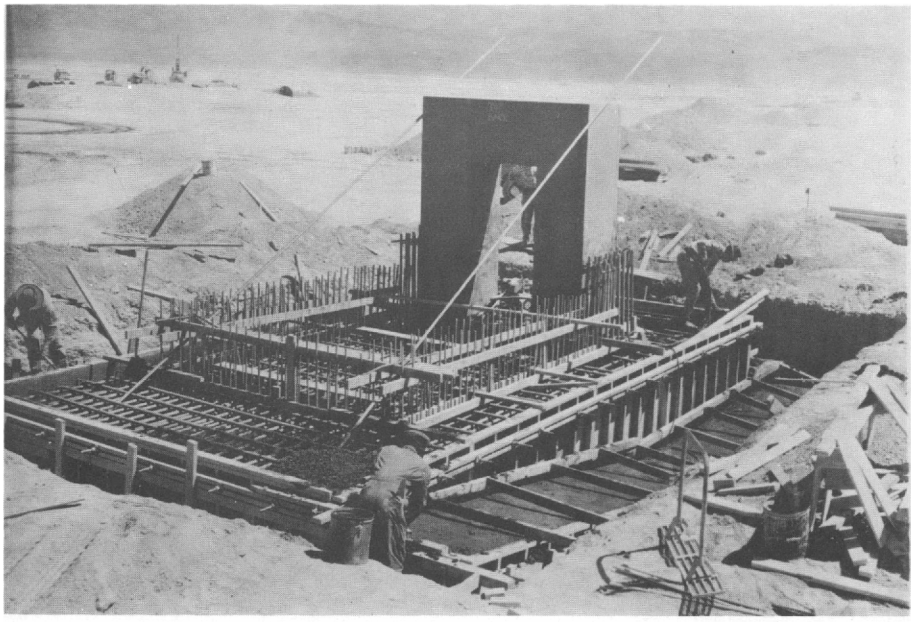

Fig. B.7—Base slab during placement of concrete

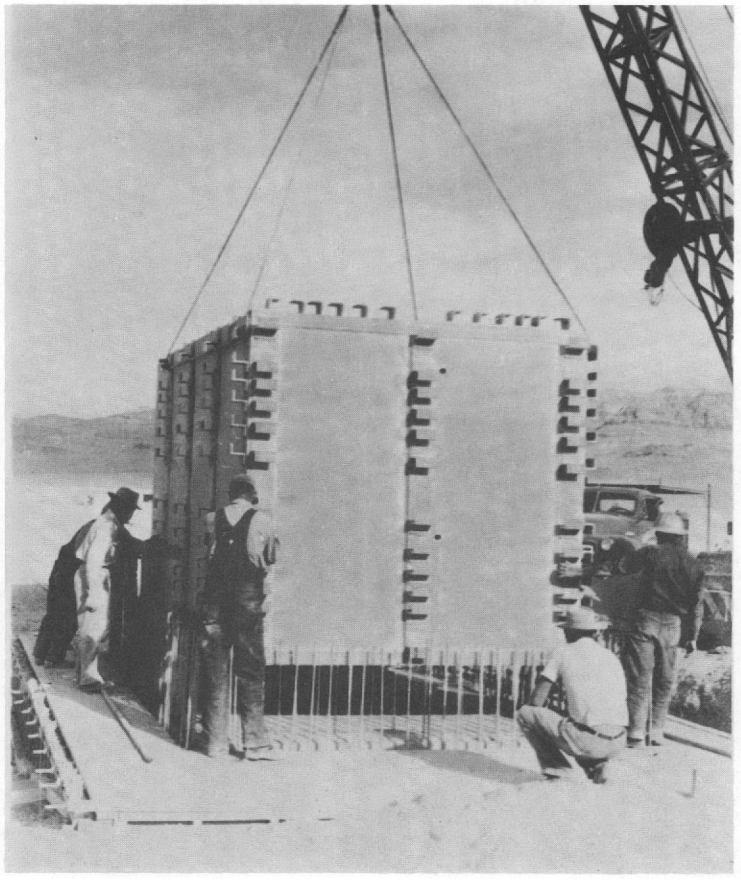

Fig. B.8—Placement of plate liner.

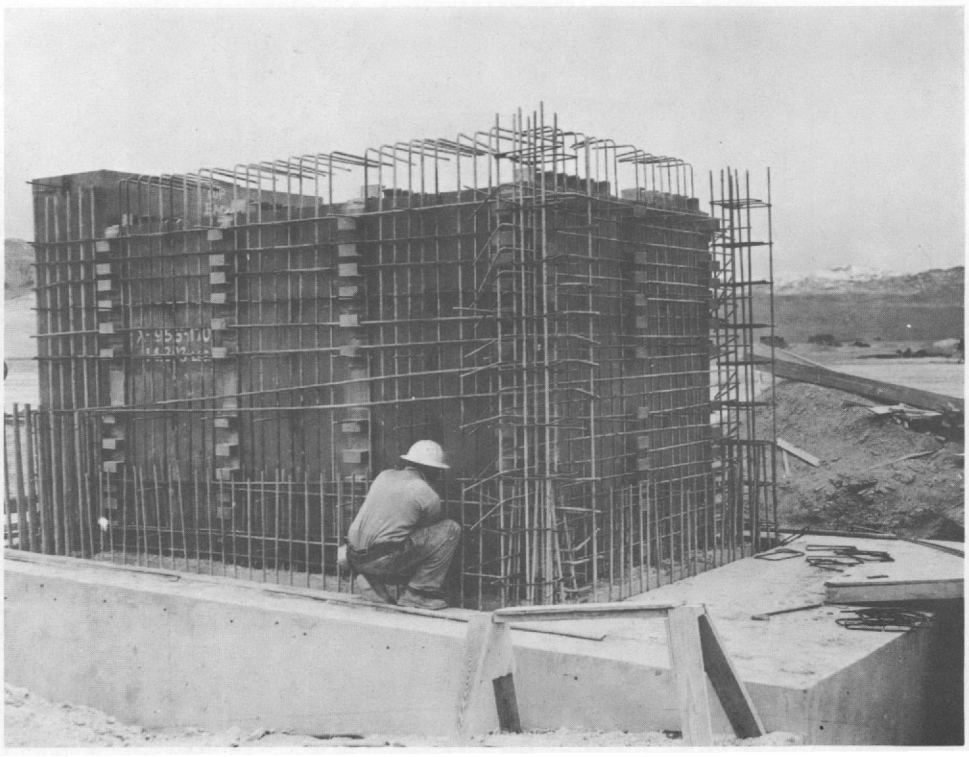

Fig. B.9—Placement of wall reinforcement.

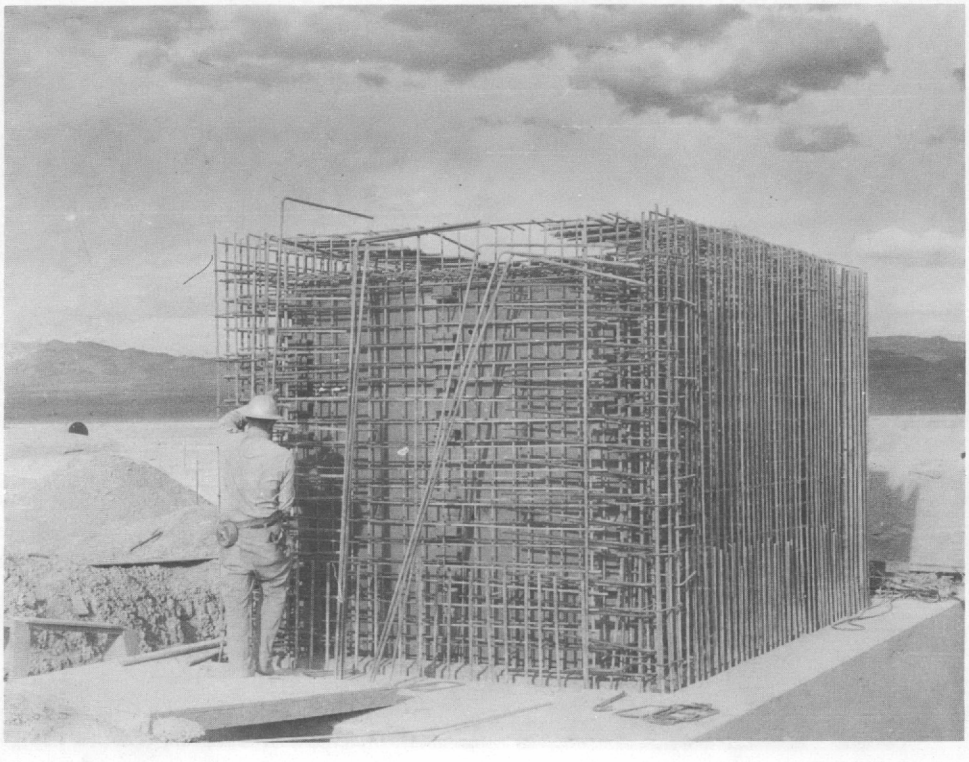

Fig. B.10—Placement of wall reinforcement.

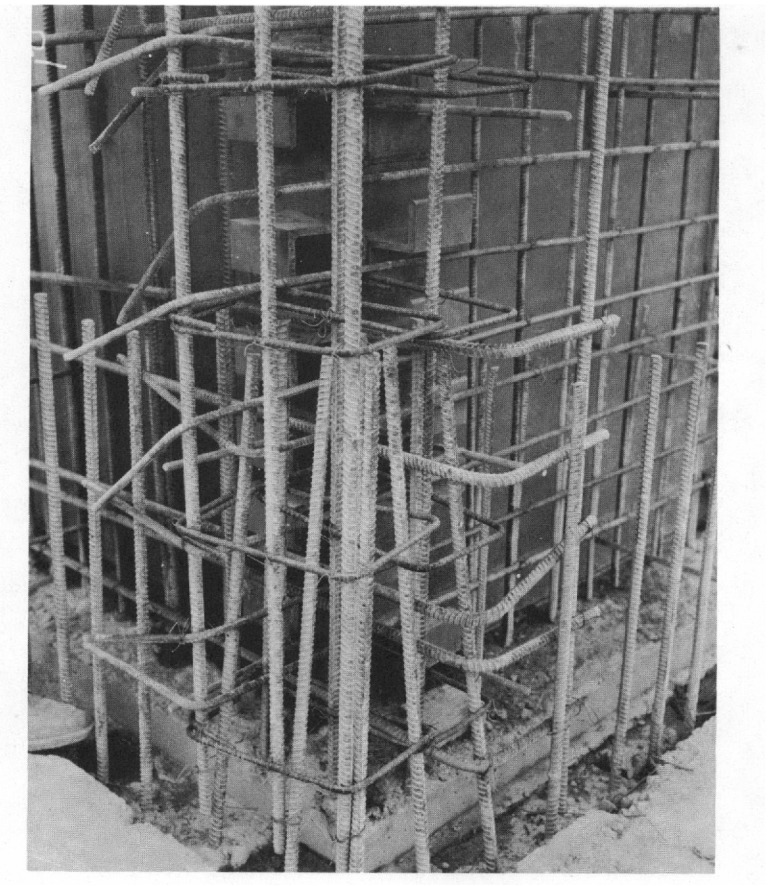

Fig. B.11—Detail of wall reinforcement at rear corner.

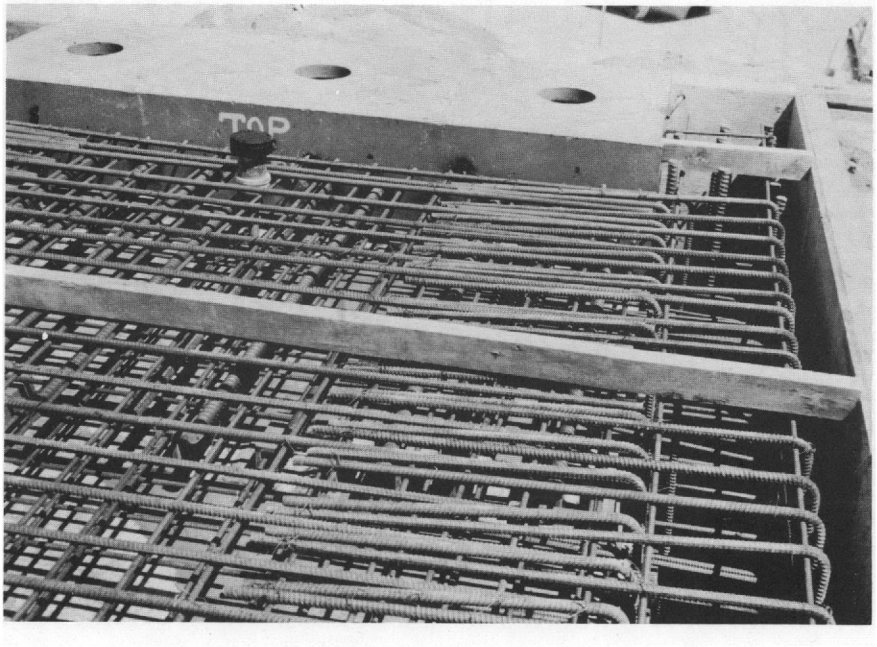

Fig. B.12—Wall and roof-slab reinforcement with forms in place.

Fig. B.13—Door before placement.

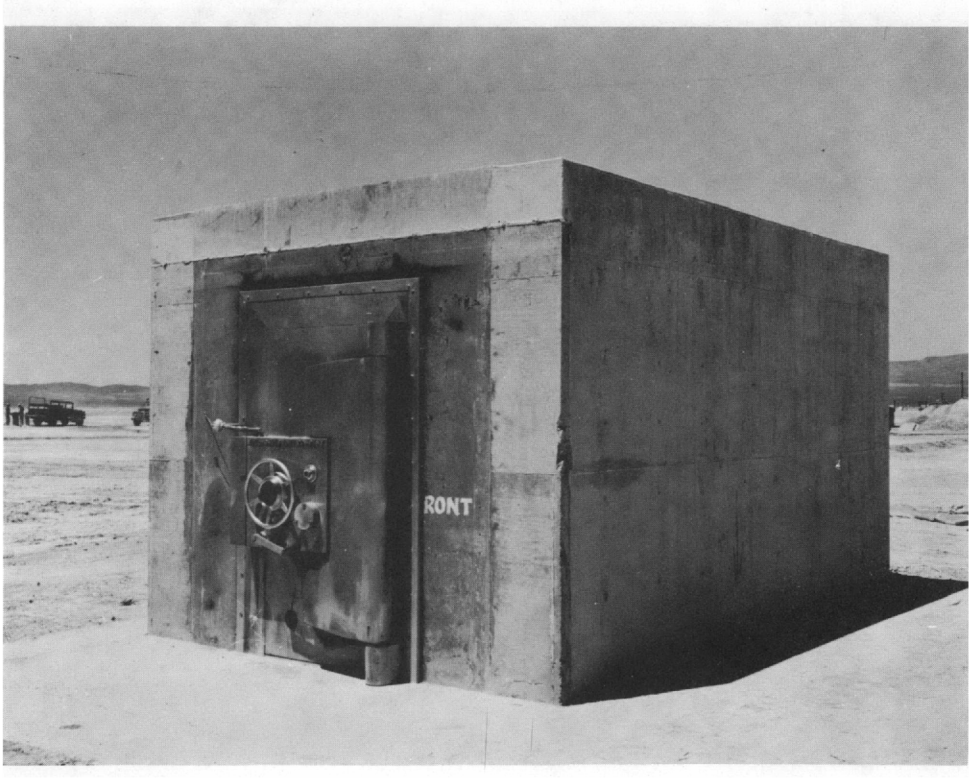

Fig. B.14—Perspective of northeast corner of vault.

Fig. B.15—Perspective of southeast corner of vault.

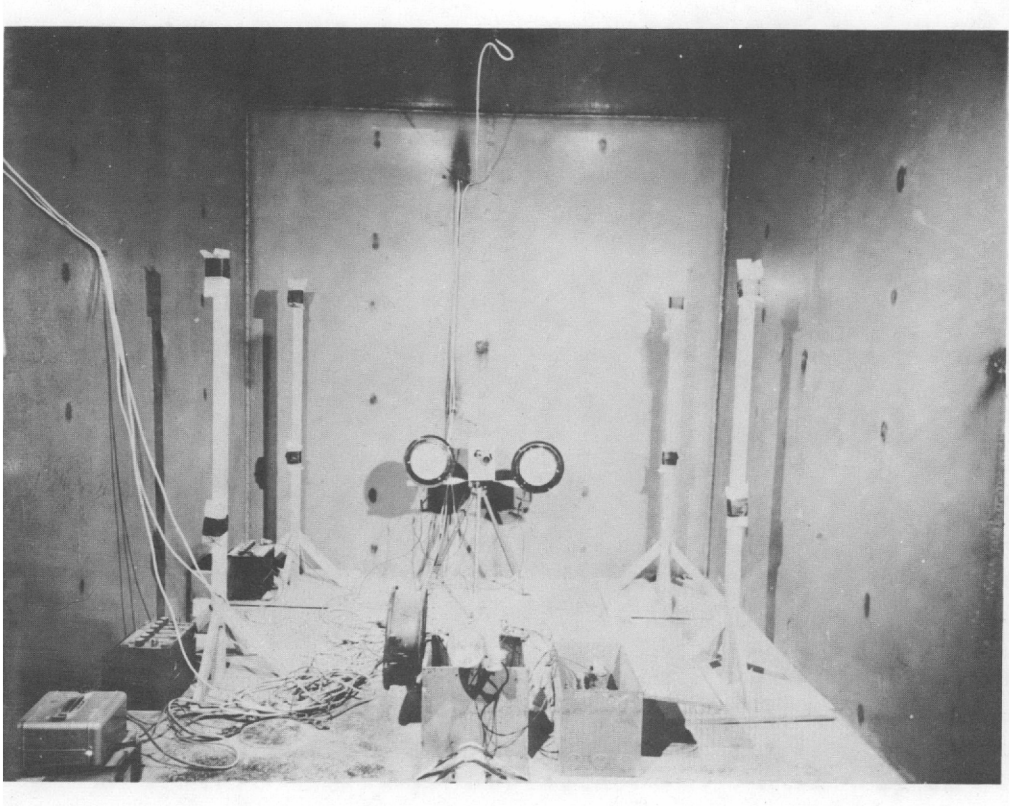

Fig. B.16—Vault interior completely instrumented.

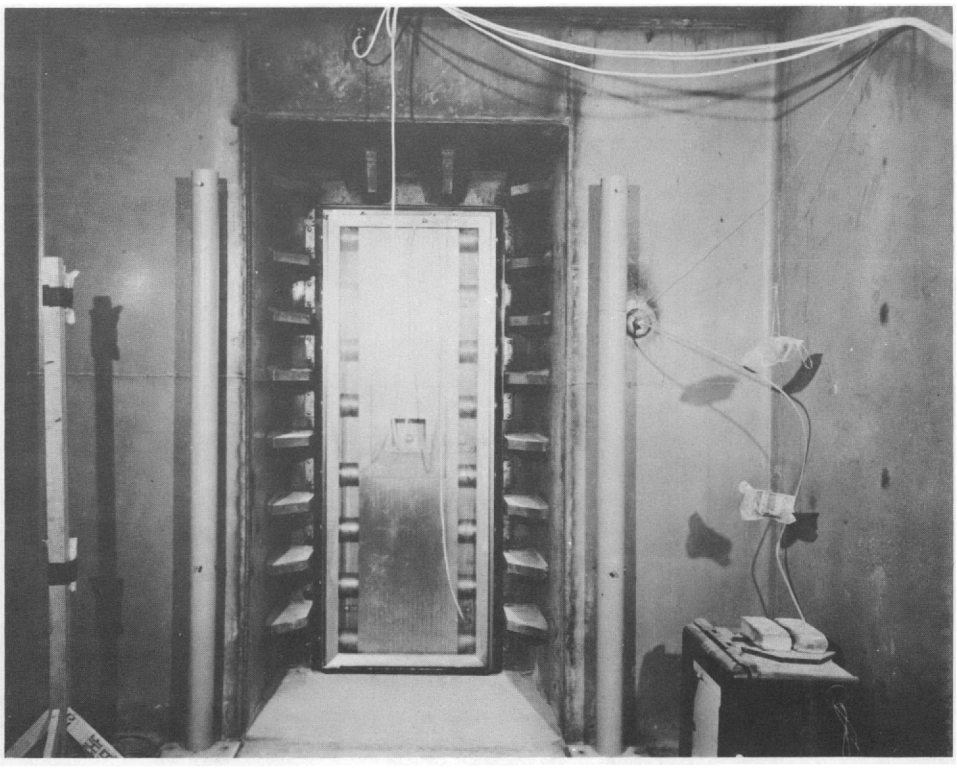

Fig. B.17 — Interior of vault with door closed.

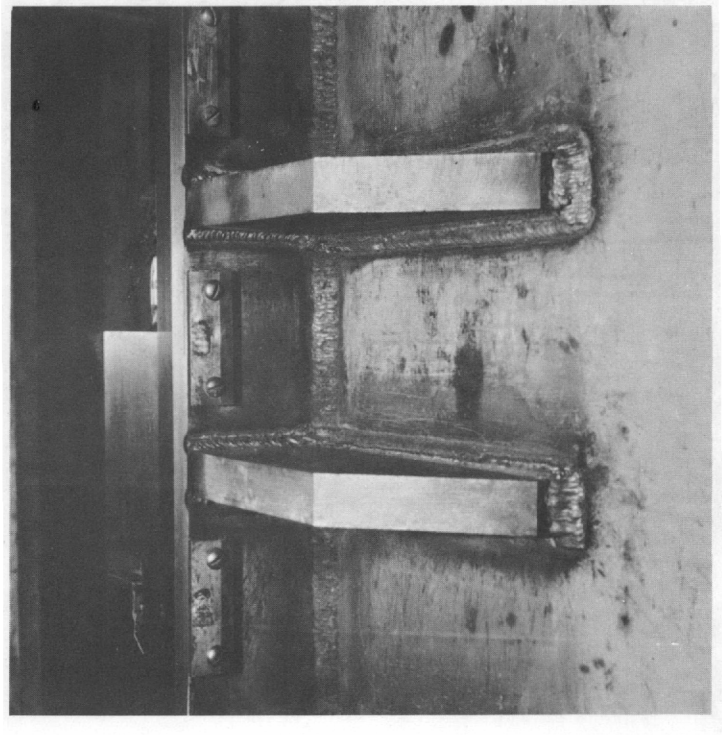

Fig. B.18 — Detail of stiffener plates and welds.

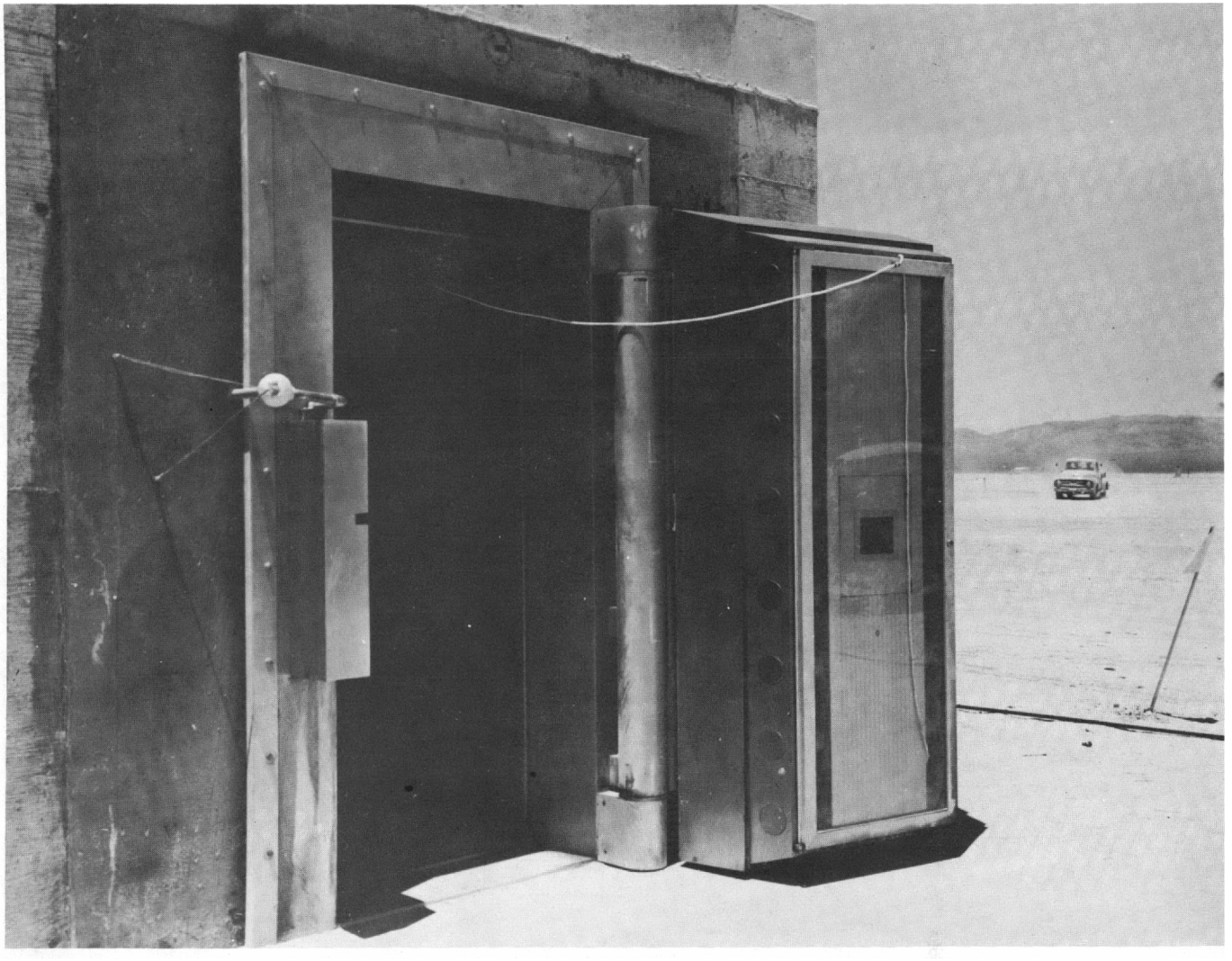

Fig. B.19—Front face of vault.

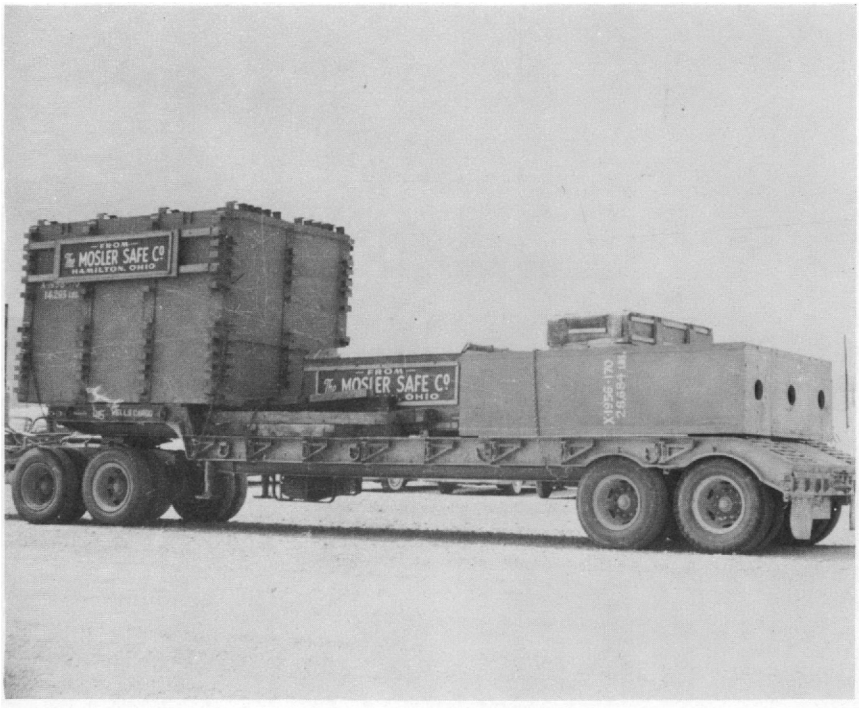

Fig. B.20—Plate liner, door, and door frame prior to unloading at NTS.

Fig. B.21—Unloading of vault door at construction site.

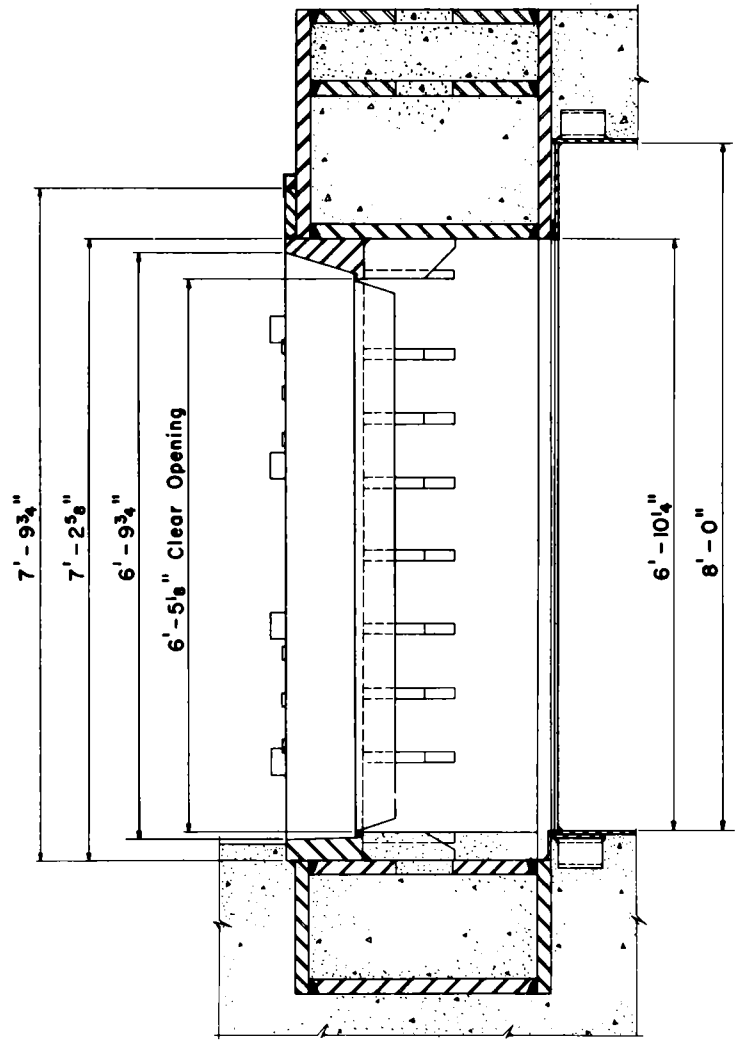

VERTICAL SECTION THROUGH DOOR FRAME

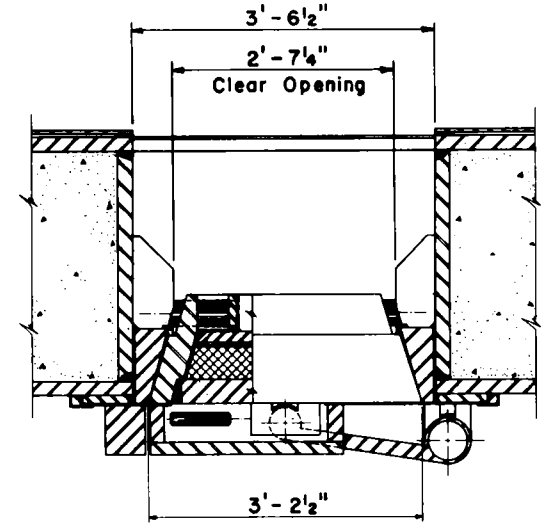

HORIZONTAL SECTION THROUGH DOOR & FRAME

Fig. B.22— Sections through door and door frame.

Appendix C

SOIL INVESTIGATIONS

C.1 TEST BORINGS

Two test borings were drilled: a 16-in.-diameter hole 66 ft deep and a 48-in.-diameter hole 42 ft deep. The boring locations are shown in Fig. 2.1.

C.2 SOIL SAMPLES

A rotary bucket rig was used to drill the 16-in. and 48-in. borings. Disturbed samples were recovered at 2-ft intervals from the 16-in. boring. Undisturbed samples were obtained from the 48-in. boring.

Three types of samples were taken. Disturbed bag samples were obtained from the rotary bucket; driven samples were taken in thin-wall brass liners with a split-spoon sampler; and undisturbed block samples were cut by hand in the borings and sealed in paraffin.

The driven samples were found to be badly disturbed owing to the heavy driving necessary to obtain them. Because of the high resistance of the soil to driving, driven samples could be taken only within a few feet of the surface. Recovery was poor, and the thinly stratified material could not be extracted from the brass tubes without further disturbance of the material. Cutting the tube to release the samples was only partially successful and did not eliminate further disturbance of the sample. The driven samples were therefore set aside.

Difficulty was also encountered in preparing test specimens from the block samples owing to the friable nature of the soil.

C.3 TEST PROCEDURE

C.3.1 Liquid Limit and Plastic Limit

Liquid-limit tests were performed in accordance with the requirements of the American Association of State Highway Officials (A.A.S.H.O.) Designation T-89, "Standard Method of Determining the Liquid Limit of Soils," mechanical method. Plastic-limit tests were performed in accordance with the requirements of A.A.S.H.O. Designation T-90, "Standard Method of Determining the Plastic Limit of Soils." No unusual difficulties were experienced in the liquid- and plastic-limit testing program.

C.3.2 Sieve Analysis

The sieve analyses were performed in accordance with requirements of the American Society for Testing Materials (ASTM) Designation D-1140, "Standard Method of Test for Amount of Material in Soils Finer than the No. 200 Sieve," with two exceptions, No. 270 and No. 400 sieves were used and the No. 40 sieve was not. The small amount of material which

was occasionally retained on the No. 8 sieve was an angular chiplike light-gray material, probably largely calcium carbonate.

Soaking the samples did not produce the normally expected results, and even after prolonged soaking and vigorous agitation with the mechanical stirring apparatus, the quantity and size of clumps was not greatly reduced. The clumps were finally broken down by very lightly rubbing the material under running water on the No. 200 sieve.

C.3.3 Field Density

(a) *Wax Method* The field density of undisturbed samples was determined in accordance with the method described in A.A.S.H.O. Designation T-147, "Standard Method of Test for the Field Density of Soil In-Place," except that, when samples of proper size were waxed in the field, the weight of the soil and the weight of the paraffin were determined after the sample had been immersed in the volumetric apparatus. This was accomplished by carefully separating the paraffin and the soil into containers and weighing each material.

(b) *Consolidometer Ring Method* After consolidation testing, samples removed from the consolidometers were weighed, dried in the rings, and reweighed; then the dry density was computed.

C.3.4 Consolidation

Consolidation samples 2.37 in. in diameter by 1-in. deep were cut from block samples with the stratification horizontal. The samples were tested at field moisture content. Some slight loss of moisture from the specimens probably took place during the test, but the effect of this loss, if any, is considered negligible.

The samples were tested on fixed-ring beam-loading consolidometers. A sample was loaded by progressively doubling the previous load over the range 575 to 36,800 psf, with an intermediate loading at 27,600 psf. The next load was applied when two successive consolidation dial readings at half-hour intervals showed less than 0.01 per cent consolidation. The loading procedure included an unload–reload cycle in accordance with the method described in the article "Importance of Natural Controlling Conditions Upon Triaxial Compression Test Conditions" by Prof. D. M. Burmister published in the American Society for Testing Materials Special Technical Publication No. 106. The duration of the consolidation tests with the unload–reload cycle varied from 33 to 114 hr, with an average length of 71 hr.

C.3.5 Triaxial Shear

Triaxial-shear test specimens were carved from block samples with the axis of the sample normal to the bedding planes. The specimens were approximately $2\frac{1}{2}$ in. in diameter and varied in length from 4 to $4\frac{5}{8}$ in. The ends of the specimens were trimmed as nearly square as possible and were capped with either plaster of paris or a stiff water–soil mixture.

The samples were preconsolidated at 0.6 p_n chamber pressure for approximately 1 hr or until no further change in length of the specimen was observed. After preconsolidation the samples were tested at chamber pressures varying from 10 to 80 psi. In at least one instance, the higher chamber pressure resulted in an axial load approaching the capacity of the 1500-lb axial-load proving ring. During the testing the rate of axial strain on the proving ring was 0.05 in. per min. Except for the extreme care required in handling the samples, no unusual difficulties were experienced in the triaxial testing program.

C.3.6 Unconfined Compression

Samples for unconfined-compression tests were prepared in the same manner as those for triaxial-shear tests. The size of the samples varied from approximately $1\frac{1}{2}$ in. to $2\frac{1}{2}$ in. in diameter, with an approximate height of two diameters. During the testing the rate of axial strain was approximately 0.05 in. per min. In several instances unconfined-compression specimens shattered at failure.

C.4 TEST RESULTS

C.4.1 Description and Classification of Material

Throughout the area there was little variation in the material samples. In the 48-in. boring the material was a clayey silt having a plasticity index ranging from 0 to 7. The soil in general is thinly stratified, there being, in places, as many as twenty horizontal beds to an inch of depth with variation in density from bed to bed of the same type material. Variation in material is more marked from one bed to the next than it is over a depth of several feet. Pronounced horizontal planes of weakness exist in places, with only slight cohesion across the faces.

Pockets and layers of soil of high void ratio are frequent and were the cause of the loss of many specimens during carving. Most of the pockets encountered were small and of the order of 1 cu. in. in volume. The pockets are thought to account for some of the low densities meas-

TABLE C.1—SUMMARY OF SOIL-CLASSIFICATION TESTS*
(16-in.-diameter Boring, Disturbed Samples)

Depth, ft	Moisture content, %	Material passing sieve, %	
		Sieve No. 8	Sieve No. 200
2	8.1	100	78
4	8.7	100	80
6	11.1	100	98
8	11.7	100	90
10	14.9	100	98
12	14.3	100	98
14	7.0	100	99
16	13.6	100	96
18	17.0	100	100
20	16.3	100	100
22	16.3	100	100
24	25.0	100	99
26	16.3	100	99
28	13.0	100	98
30	8.1	100	100
32	11.1	100	99
34	15.6	100	98
36	15.6	100	98
38	8.1	100	92
40	7.0	100	98
42	7.0	100	96
44	7.5	100	93
46	6.4	100	94
48	7.0	100	93
50	13.0	100	89
52	14.3	100	90
54	17.0	100	96
56	18.3	100	95
58	17.0	100	99
60	18.3	100	99
62	20.5	100	99
64	18.3	100	96
66	20.5	100	99

* Soil tested was stratified and fissured silty clay and clayey silt.

ured by the waxed-sample method. The soil breaks up rapidly in water. The cementing agent is thought to be calcium carbonate, which also exists in some beds in pieces about 8-mesh size.

The results of the liquid- and plastic-limit tests, the sieve analyses, and the field-density and moisture-content tests are shown in Tables C.1 and C.2.

C.4.2 Consolidation Characteristics

The results of the consolidation tests are shown in Table C.3. It should be pointed out that the consolidation tests were run for the sole purpose of establishing a value of the natural prestress p_n and that the results reflect the consolidation characteristics of the material only at the field moisture content. It is believed that the higher moisture content in test C-2 was responsible for the greater consolidation of that specimen. The consolidation characteristics are thought to be more typical of the denser strata because of the difficulty in cutting test specimens from the more friable low-density materials. A typical consolidation stress-strain relation is illustrated in Fig. C.1.

C.4.3 Strength Characteristics

The results of the triaxial and unconfined-compression tests are given in Tables C.4 and C.5.

TABLE C.2—SUMMARY OF SOIL-CLASSIFICATION TESTS*
(48-in.-diameter Boring, Undisturbed Samples)

Depth, ft	Dry-unit weight, lb/cu ft	Moisture content, %	Material passing sieve, %		Liquid limit	Plastic limit	Plasticity index
			Sieve No. 8	Sieve No. 270			
2							
4	72	11.7	100	99	35.9	27.7	8.2
5	71	9.2					
6	73	9.5	100	97	31.1	26.2	4.9
7	73	8.4					
8	68	12.6					
10							
12							
14							
15							
16	77	20.3					
17	85	15.3	99	97	33.9	25.8	8.1
18							
20							
22							
24							
25	86	15.8					
26	84	23.8					
27	91	13.6	100	96	34.4	26.1	8.3
28	87	14.8					
30							
32							
34							
35							
36	90	10.1	100	98	33.6	27.1	6.5
38							
40							
	76	14.9					
42	89	12.6	100	95	34.6	26.5	8.1
	80	14.9					

* Soil tested was stratified and fissured silty clay and clayey silt.

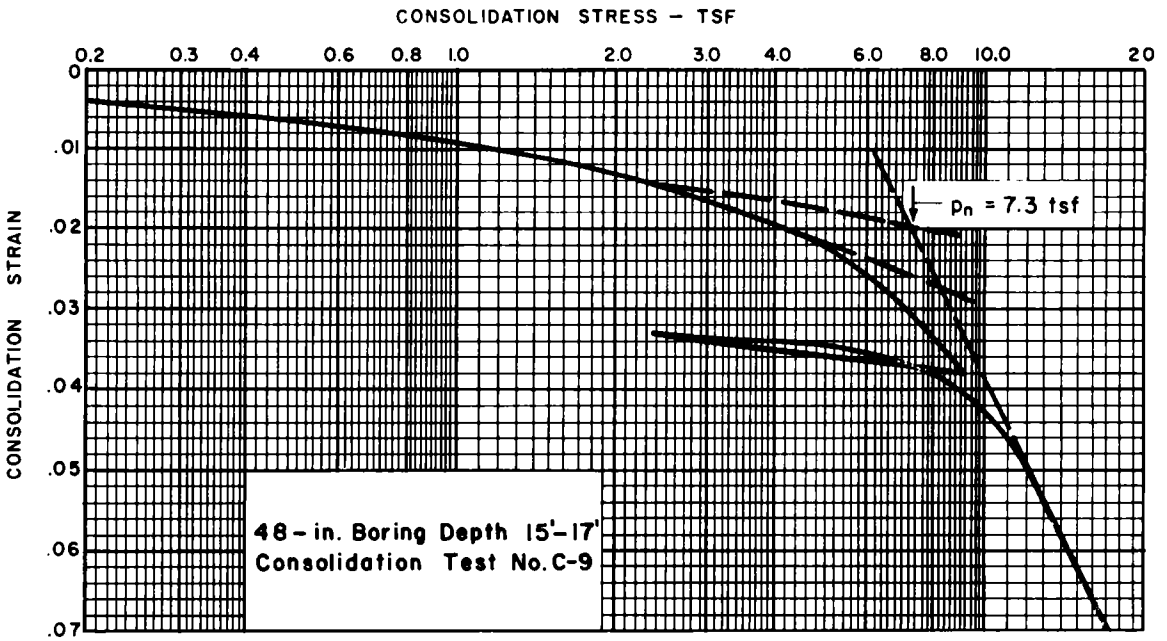

Fig. C.1—Typical consolidation-test stress–strain relation.

TABLE C.3—SUMMARY OF CONSOLIDATION TEST RESULTS
(48-in.-diameter Boring, Undisturbed Samples)

Test no.	Depth, ft	Prestress (p_n), tsf
C-5	5 to 7	6.2
C-15	5 to 7	6.2
C-9	15 to 17	7.3
C-2	25 to 27	2.6*
C-3	25 to 27	4.6
C-13	25 to 27	8.4
C-1	35 to 36	9.8
C-8	40 to 42	8.0

* Specimen believed to have absorbed moisture during test.

The Mohr circles for peak shear strengths at various depths in the 48-in. boring have been plotted, and a suggested peak shear envelope has been developed. The suggested peak shear envelope is shown in Fig. C.2.

It should be noted that the suggested soil-strength values on Fig. C.2 are likely to be higher than actual strengths for several reasons:

1. The specimens are loaded at right angles to the planes of weakness of the material.
2. Samples could be taken only of the stronger materials in the field, and specimens could be cut only from the stronger portion of these.
3. Peak shear strengths are used in the plotting of the Mohr circles. The applicable shear-strength value depends on the type, duration, and direction of loading anticipated in the field, and the shear envelopes are therefore recorded as "suggested shear envelopes."

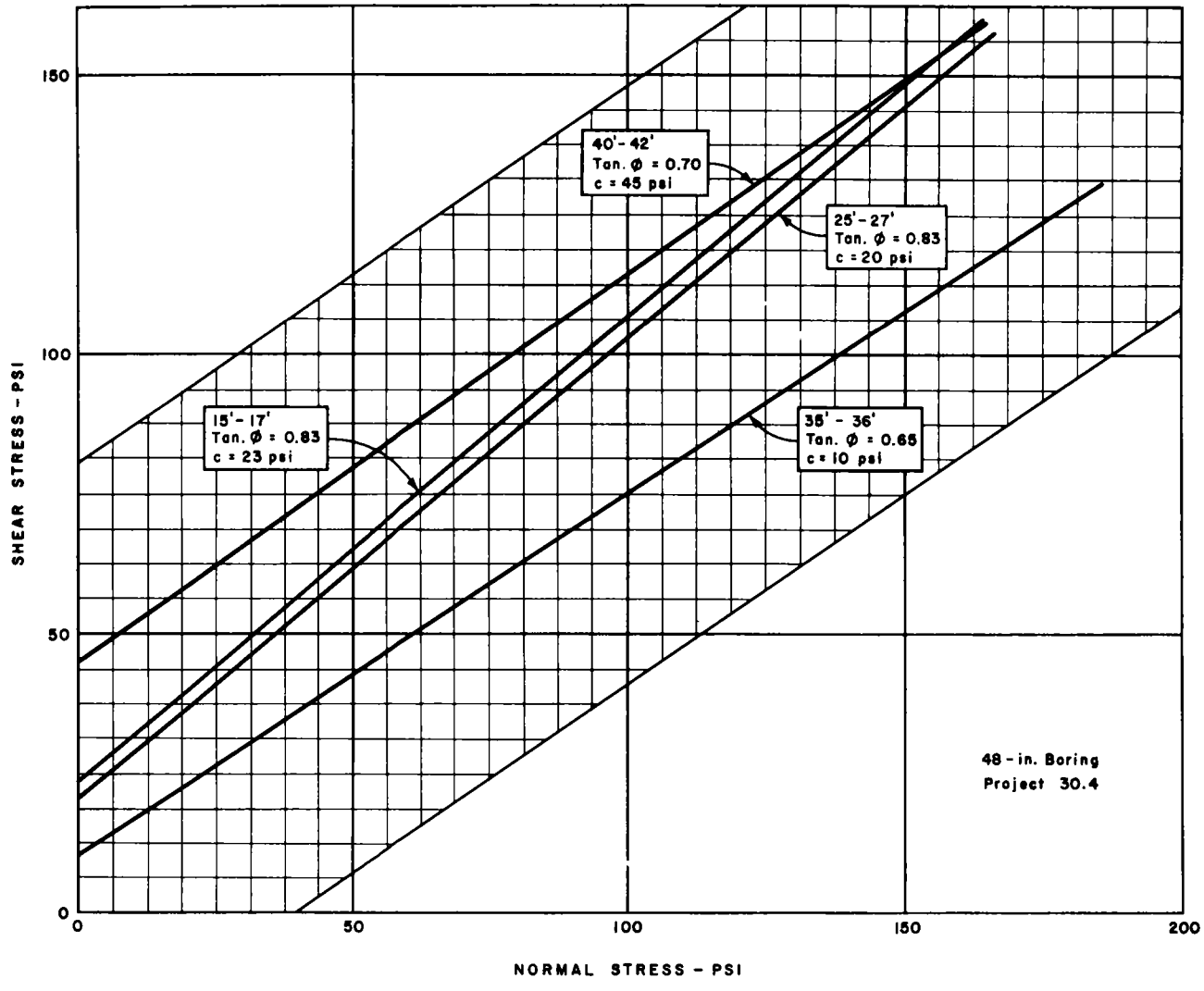

Fig. C.2—Suggested peak shear envelope.

TABLE C.4—SUMMARY OF TRIAXIAL TESTS
(48-in.-diameter Boring, Project 30.4)

Test no.	Depth, ft	0.6 p_n,* psi	Restraint stress (σ_3), psi	Maximum triaxial stress ($\sigma_1 - \sigma_3$), psi	Remarks
T-5	15 to 17	61	61	197	
T-6	40 to 42	67	20	217	
T-7	35 to 36	82	82	233	Incomplete failure
T-8	40 to 42	67	67	302	No failure
T-9	40 to 42	67	10	222	Retest of T-8
T-10	15 to 17	61	20	154	
T-11	15 to 17	61	80	303	No failure
T-12	15 to 17	61	40	217	Retest of T-11
T-13	15 to 17	61	20	170	
T-14	15 to 17	61	40	238	
T-15	15 to 17	61	50	276	
T-16	25 to 27	40	40	229	
T-17	Sample run as unconfined compression U-10				
T-18	40 to 42	67	10	204	
T-19	40 to 42	67	40	280	

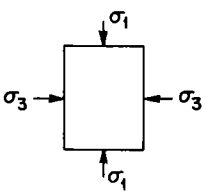

* p_n = natural prestress on soil.

TABLE C.5—SUMMARY OF UNCONFINED-COMPRESSION TESTS
(48-in.-diameter Boring, Project 30.4)

Test no.	Depth, ft	Maximum triaxial stress ($\sigma_1 - \sigma_3$), psi
U-2	35 to 36	37
U-3	25 to 27	80
U-4	15 to 17	50
U-5	15 to 17	45
U-6*	35 to 36	101
U-7	5 to 7	35
U-8	25 to 27	95
U-9	40 to 42	172
U-10	15 to 17	38

* Retest of T-7.

4. Tests were performed on the specimens at field moisture content. At increased moisture content the shear strengths of the materials tested would be greatly reduced.

For additional soil-test data see Chaps. 2 and 3. Appendix C, as well as the information presented in Chaps. 2 and 3, has been based on the report "Soil Test Data, Frenchman Flat, Nevada Test Site, Mercury, Nevada," prepared by Nevada Testing Laboratories, Ltd., Las Vegas, Nev., and International Testing Corporation, Long Beach, Calif.

Appendix D

POSTSHOT DYNAMIC ANALYSIS OF TEST VAULT

For the postshot analysis the blast loadings on the exposed surfaces of the vault were taken as those recorded by the pressure–time gauges described in Sec. 3.2.

The loads acting on the vault are shown in Fig. D.1. The corresponding equations of motion are as listed below:

$$\sum F_H - \mu\left(\sum F_V + m\bar{r}\ddot{\theta}\sin\alpha\right) - m\bar{r}\ddot{\theta}\cos\alpha = m\ddot{x}_0 \tag{D.1}$$

$$\sum M_0 - EI\theta - I_0\ddot{\theta} = m\ddot{x}_0\bar{y} \tag{D.2}$$

where ΣF_H = sum of all forces in the horizontal direction
ΣF_V = sum of all forces in the vertical direction
ΣM_0 = the externally applied couple (due to F_H and F_V forces)
μ = coefficient of sliding friction
m = mass of structure including overburden above foundation projections
$\bar{r}$ = distance between center of gravity of mass and assumed point of rotation
$\bar{y}$ = lever arm between point of rotation and line of application of $\ddot{x}_0$
α = angle formed by $\bar{r}$ and a vertical line passing through the point of rotation
θ = angular rotation at time t
$\ddot{\theta}$ = angular acceleration at time t
$\ddot{x}_0$ = horizontal acceleration of structure at time t
I = moment of inertia of the base slab about its center line
I_0 = polar moment of inertia of the structure about the center line of the foundation

The simultaneous solution of Eqs. D.1 and D.2 yields the acceleration, velocity, translation, and rotation at any time t. The soil parameters used in the dynamic analysis are E = 100 psi per inch of deflection and $\mu = 0.5$. Earth pressure on the rear face of the footing was: active pressure, $P_a = -5.13\ P'_{s0}$; passive pressure, $P_p = -108.9\ P'_{s0}$ (fx), where P'_{s0} is the free-field side-on pressure with a time lag of 0.01 sec and fx is a function of the horizontal displacement of the vault as estimated from recent criteria.[1,2]

The passive-pressure–displacement relation used is shown in Fig. D.2. The results of the dynamic analysis are presented in Fig. D.3.

REFERENCES

1. J. E. Smith, Tests of Concrete Deadman Anchorages in Sand, Symposium on Soils, Am. Soc. Testing Materials Tech. Publ. No. 206, pp. 115-132, 1957.
2. J. E. Smith, Passive Resistance of Earth Anchors in Sand, Part 2, U. S. Naval Civil Engineering Laboratory, Port Hueneme, Calif., Mar. 8, 1960.

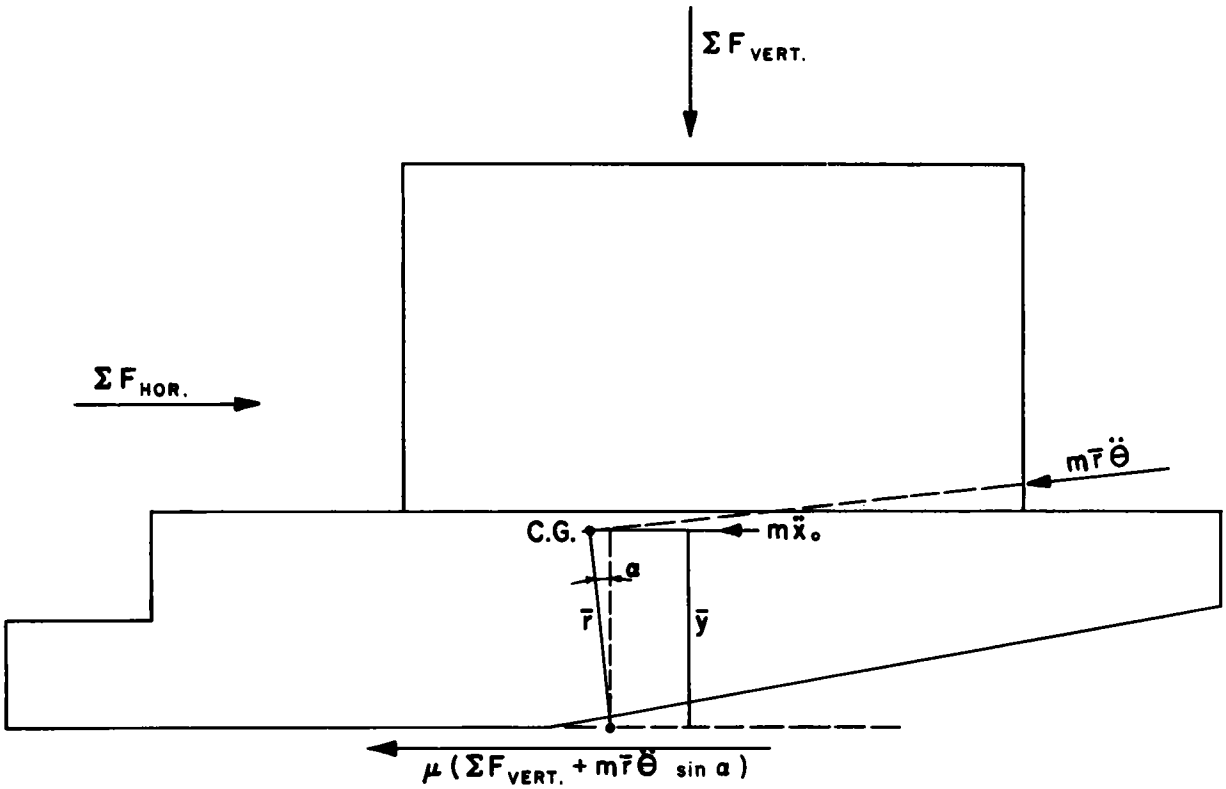

Fig. D.1—Diagram of forces.

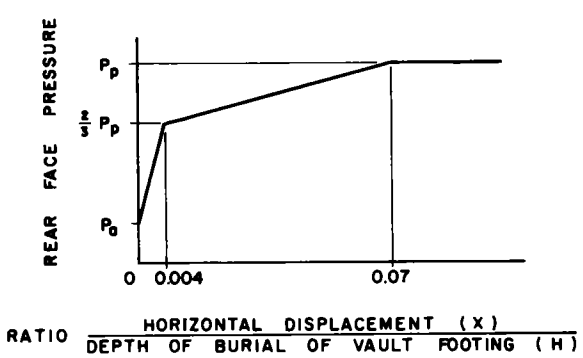

Fig. D.2—Passive-pressure–displacement relation.

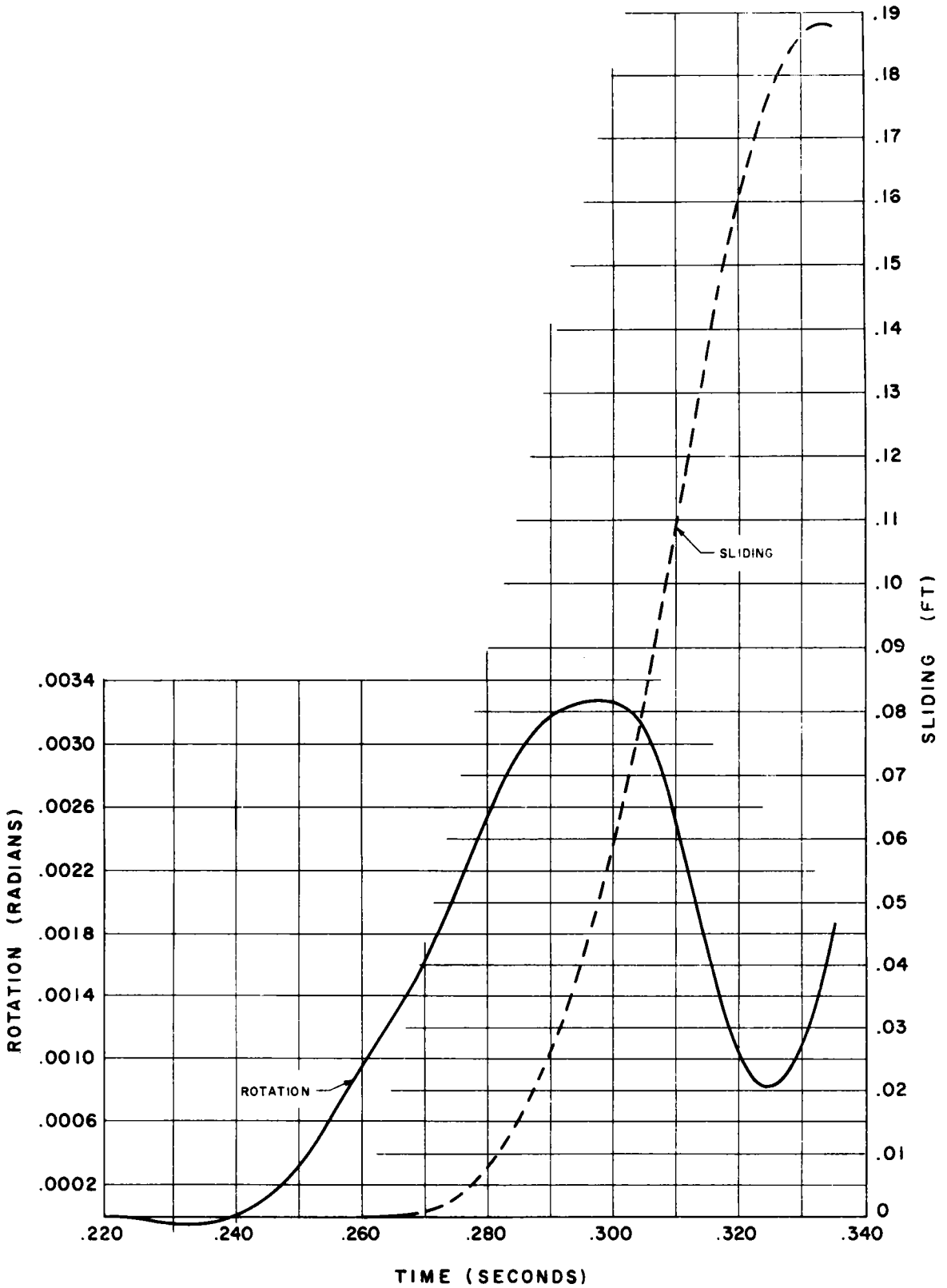

Fig. D.3—Postshot dynamic-analysis results.